Solid- and liquid-like polyelectrolyte complexes : interfacial tension, local structure and complexation strength

Hongwei Li

université de BORDEAUX

THÈSE PRÉSENTÉE

POUR OBTENIR LE GRADE DE

DOCTEUR DE

L'UNIVERSITÉ DE BORDEAUX

ÉCOLE DOCTORALE DES SCIENCES CHIMIQUES

SPÉCIALITÉ Polymères

Par

Hongwei LI

Solid- and liquid-like polyelectrolyte complexes: interfacial tension, local structure and complexation strength

Sous la direction de : Jean-Paul CHAPEL et Christophe SCHATZ

Soutenance prévue le 16 mars 2022

Membres du jury :

Mme BANC Amélie	Maître de conférences, Université de Montpellier	Examinateur
Mme ZAKRI Cécile	Professeur, CNRS/Université de Bordeaux	Président
M. CHAPEL Jean-Paul	Directeur de recherche, CNRS	Directeur de thèse
M. SCHATZ Christophe	Maître de conférences, Bordeaux INP	Co-directeur de thèse
M. COUSIN Fabrice	Ingénieur de recherche, CEA-CNRS /Saclay	Rapporteur
M. FRESNAIS Jérôme	Chargé de recherche, Sorbonne Université	Rapporteur

Titre: Complexes polyélectrolytes solides et liquides : tension interfaciale, structure locale et intensité de complexation

Résumé:

Les complexes de polyélectrolytes (PEC) sont formés par association de polyélectrolytes (PE) de charge opposée, principalement par interaction électrostatique. Les PECs ont de nombreuses applications dans différents domaines technologiques et industriels, comme la cosmétique, la biomédecine, les biotechnologies, l'assainissement de l'eau et bien d'autres. Dans ce travail de recherche, la complexation entre deux PEs a été étudiée en utilisant deux systèmes modèles dont l'intensité de complexation est très différente : le système poly(chlorure de diallyldiméthylammonium)/poly (acrylate de sodium) (PDADMAC/PANa) interagissant faiblement et le système poly(chlorure de diallyldiméthylammonium)/poly (4-styrènesulfonate de sodium) (PDADMAC/PSSNa) interagissant fortement. A la stœchiométrie en charges, le premier montre une transition de phase liquide-liquide conduisant à la formation de microgouttelettes de coacervat liquide en équilibre avec la phase continue, tandis que le second se caractérise par une séparation de phase liquide-solide conduisant à un précipité solide hors équilibre. Dans une première partie, nous nous sommes intéressés à l'influence de la force de complexation sur la tension interfaciale des complexes en étudiant systématiquement l'activité de surface des deux types de suspension de PECs en fonction du rapport de charge molaire Z (= [-]/[+]). Ceci a permis de montrer que de simples mesures de tension de surface sont suffisamment sensibles pour caractériser, discriminer et mieux comprendre les mécanismes de formation des PECs. Dans une seconde partie, nous avons focalisé notre travail sur la phase coacervat du système PDADMAC/PANa obtenue à Z=1 c'est-à-dire à la neutralité. En particulier, nous avons étudié l'influence de l'intensité de complexation sur la tension interfaciale, la fraction volumique en polymère et la structure locale de cette phase riche en polymère en équilibre avec le surnageant. Pour ce faire nous avons étudié de manière exhaustive et systématique l'effet de la concentration des solutions de PE, de la température, de la force ionique et de la teneur en éthanol sur la structure en réseau du coacervat à l'aide de techniques complémentaires telles que la TGA, la DLS, la SANS et les mesures de tension interfaciale. Il s'agit d'une approche globale qui a montré une variation de la longueur de corrélation du réseau avec la force de complexation pouvant aller jusqu'à la disparition de la phase coacervat lorsque la concentration en polymère est suffisamment élevée. Une transition de type 'température inférieure critique de démixtion' (LCST) de la phase coacervat a également pu être mise en évidence ; elle traduit un comportement critique de l'énergie interfaciale coacervat/surnageant. Enfin, lorsque la fraction volumique en éthanol devient très importante, la transition liquide-liquide est remplacée par une transition liquide-solide générant un précipité comme dans le cas d'un système en forte interaction tel que le PDADMAC/PSSNa. Ceci souligne une fois encore le rôle clef de l'intensité de la complexation sur les mécanismes de formation et les caractéristiques structurales des PECs.

Mots clés : complexes de polyélectrolytes, coacervat complexe, interaction électrostatique, force de complexation, adsorption, tension interfaciale, transition liquide-liquide et liquide-solide, thermodynamique, structures locales, morphologies.

Title: Solid- and liquid-like polyelectrolyte complexes: interfacial tension, local structure and complexation strength

Abstract:

Polyelectrolyte complexes (PECs) are formed by oppositely charged polyelectrolytes (PEs), mainly through electrostatic interaction. They have many applications in technology and industry, such as cosmetics, biomedicine, biotechnology, water remediation and many others. In this study, the complexation between PEs was investigated using two model systems exhibiting a very different complexation strength: the weakly and strongly interacting poly (diallyldimethylammonium chloride)/poly (acrylic acid sodium salt) (PDADMAC/PANa) and poly (diallyldimethylammonium chloride)/poly (sodium 4-styrenesulfonate) (PDADMAC/PSSNa) pairs, respectively. At charge stoichiometry, the former shows a liquid-liquid phase transition leading to the formation of liquid coacervate microdroplets in equilibrium with the continuous phase, while the latter show a liquid-solid phase separation leading to a non-equilibrium solid precipitate. In a first part, we investigated the influence of the complexation strength on the surface area and interfacial tension by systematically studying the surface activity of the two different types of PEC suspensions as a function of the molar charge ratio Z (= [-]/[+]). This enabled us to show that simple surface tension measurements can be a very sensitive tool to characterize, discriminate and better understand the formation mechanism of the different structures encountered during the formation of PECs. In a second part, we have focused our work on the coacervate phase of the PDADMAC/PANa obtained for Z=1. In particular, we have studied the influence of the complexation strength on the interfacial tension, polymer volume fraction and local structure of such polymer-rich phase in equilibrium with the polymer-poor supernatant. For this purpose, we systematically investigated the effect of the PE concentration, temperature, ionic strength and ethanol content on the polymer network structure using complementary techniques such as TGA, DLS, SANS and interfacial tension measurements. We put in evidence that the lattice correlation length is strongly dependent on the complexation strength and also that the coacervate phase has a lower critical solution temperature (LCST) character, that is, a critical behavior of the coacervate/supernatant interfacial energy that cancels at high concentration where a unique phase appears, the so-called self-suppressed coacervate phase (SSCV). The latter can furthermore be diluted or heated to obtain a new coacervate phase with a different mesh size. Finally, when the ethanol fraction becomes very important, the liquid-liquid transition is replaced by a liquid-solid transition generating a solid precipitated as in the case of the strongly PDADMAC/PANa interacting system. Again, this highlights the key importance of interaction strength on the formation mechanisms and structural characteristics of PECs.

Keywords: polyelectrolyte complexes, complex coacervate, electrostatic interaction, complexation strength, adsorption, interfacial tension, liquid–liquid and liquid–solid transition, thermodynamic, local structures, morphologies.

Unité de recherche

Centre de Recherche Paul Pascal (CRPP), Equipe Colloïdes, Interfaces, Assemblages, UMR 5031, Unité mixte de recherche CNRS/Université de Bordeaux
115 Avenue du Docteur Schweitzer-33600 Pessac, France

Laboratoire de Chimie des Polymères Organiques (LCPO), Equipe Polymer self -assembly and life Sciences, UMR 5629, Unité mixte de recherche CNRS/Université de Bordeaux/Bordeaux INP, 16 avenue Pey Berland-33600 Pessac, France

Acknowledgements

This thesis was carried out at the Centre de Recherche Paul Pascal (CRPP) and the Laboratoire de Chimie des Polymères Organiques (LCPO) under the supervision of Jean-Paul Chapel and Christophe Schatz and funded by the China Scholarship Council (CSC).

I would like to thank Dr. Fabrice COUSIN and Dr. Jérôme Fresnais who devoted their precious time to the examination of the manuscript by their remarks and comments. I also thank Drs Amélie BANC, Cécile Zakri, Christophe Schatz and Jean-Paul Chapel for having participated in the defense as members of the jury.

I would like to express my sincerely appreciation to my supervisors Dr. Jean-Paul Chapel and Dr. Christophe Schatz. Their enthusiasm, patience, and positive attitude towards research and life were very encouraging to me, which is very important to adapt as quickly as possible to a new experimental project and environment. In addition, their extensive knowledge of polyelectrolyte complexes provided me with great support in my PhD work, which facilitated my entry into this new world and allowed me to carry out my thesis subject in the best possible way.

Then, I also would like to thank the members of our group:

Joanna Giermanska, who is a very nice research engineer in our group, helped me a lot with the equipment, especially the tensiometer which is one of the main tools in my work, and gave me many tips to get better experimental results. He gave me many tips to get better experimental results. He is also an easy person to talk to and likes to share news and topics about life. It is a good experience to work with her. I also want to thank Eric Laurichesse who is a very nice person to work with. He also warmly helped me to perform the tensiometry experiments and to find the experimental equipment I needed. Moreover, I am also grateful to Nouha Jemili, Flavia Mesquita Cabrini, Romain poupart, Martin Fauquignon, Tim Delas, Etienne Lepoivre... They are all warm, help me with my experiences and share their ideas about research and life, which makes me feel relaxed. I would also like to thank Patrick Snabre, who offered me a constructive discussion about my doctoral work and shared with me his opinions about research and his feelings about life and gave me some advice for my future

career. I would also like to thank Ahmed Bentaleb, who patiently helped me with the SAXS measurements. He loves to run and share some pictures and his experience with the marathon. I would also like to thank Alain Derre, for his help with the TGA measurements. He is very competent in this field and was able to repair the machine in the shortest possible time when it had some problems.

A big thank you to Lionel Porcar, local contact of the D22 spectrometer at ILL, who always allowed us to perform "extra" verification experiments outside the official runs!

The list will never end. I would like to thank many people: Francois Dole, Gilles Pécastaings……

I also express my gratitude to all the members of the departments of CRPP, LCPO and the University of Bordeaux. With their dedicated and warm help, I was able to manage all kinds of academic formalities and make the process of my PhD work smoother. The administrative staff helped me process the necessary documents; all the researchers and engineers created a great study environment, and I was able to get technical services from the CRPP IT team, including software and internet, etc. In addition, all the PhD students and postdoctoral fellows provided me with timely assistance.

In addition, I would like to thank my friends and colleagues who are in France and in China. They have encouraged me a lot to overcome all kinds of difficulties in research and in life. Without them, I would not know how to carry out the difficult doctoral work which is a totally new field for me.

Finally, I would like to thank all my family members who have provided vital support. In particular, my parents have contributed a lot for me since I was born and came into this world. They have truly made great sacrifices so that I could grow up healthy and receive a good education. They also taught me to be persistent and optimistic in life and encouraged me to expand my horizons for a better future. I sincerely wish them happiness in their whole life.

Thank you!

Hongwei Li

Pessac, January, 2022

Table of Contents

Introduction

Polyelectrolytes are macromolecules in which a substantial portion of the constitutional units contains ionic or ionizable groups, or both. These so-called electrolyte groups can dissociate in suitable solvents such as aqueous solutions, making the polymers charged. The PE properties are then between those of electrolytes and neutral polymers: PE solutions are indeed electrically conductive like salts and can be viscous like neutral polymers. They can be divided into strong and weak, positively and negatively charged polycations and polyanions, respectively. A "strong" PE dissociates completely in solution for most reasonable pH values, although a "weak" PE has a dissociation constant (pKa) between ~2 and ~10. Thus, their charge fraction can be modified by changing the solution pH, counter-ion concentration, or ionic strength. They can be natural (nucleic acids, proteins, polypeptides, polysaccharides) or synthetic (poly(acrylic acid), poly(sodium styrene sulfonate), poly(ethyleneimine), poly(allylamine hydrochloride) …). In short, they are one of the main building blocks of soft matter systems and play a fundamental role in determining the structure, stability and interactions of various molecular assemblies. They are nowadays found in many technological and scientific areas ranging from cosmetics, food, oil recovery, water treatment, coating, paper industries, pharmaceuticals and biomedicine to drug delivery and biomedicine.

Mixing dilute solutions of a polyanion and a polycation usually results in the formation of so-called polyelectrolyte complexes (PECs) formed by the spontaneous electrostatic complexation of these oppositely charged macromolecules, accompanied by the release of counterions (and water molecules). The study of these PECs began nearly a century ago with the pioneering work of Bungenberg de Jong and colleagues in the 1930’ on polysaccharide and protein systems. Most fundamental works have been published in the 70s and 80s by Michaels, Kabanov and Zezin, Dautzenberg, Tsuchida and Abe. They have received renewed attention in recent years due to several very different works that require a deeper understanding of the complexation process. In the late 1990s, Decher's invention of layer-by-layer deposition of oppositely charged PEs led to many potential applications in catalysis, membranes, and biomedicine. More recently, the increasing attention of biologists to the structures and

functions of the subcellular, membrane-less structures that are ubiquitous in cells has led to interest of an entirely different kind.

As these polymers may contain monomers and ions of very different nature they exhibit a large number of unique physicochemical or biological behaviors that are generally sensitive to ionic strength, pH, polymer concentration and temperature. In addition to the electrostatic interactions that mainly control the formation of PECs, secondary interactions of hydrophobic, hydrogen bonding or ion-dipole type can also participate in the complexation. The intrinsic characteristics of the PEs but also some formulation parameters such as the mixing pathways can also strongly influence the formation of PECs, such as PE charge density, solution dielectric constant and ionic strength, mixing charge ratio, pH, molecular weight, concentration or the mixing order to generate PECs with various properties and morphologies.

The interaction strength is central in the complexation of oppositely charged PEs as it will impact the final structure of the PECs. To further investigate this key issue, we have investigated in this PhD work the complexation between two PEs two model systems exhibiting a very different complexation strength: the weakly and strongly interacting poly (diallyldimethylammonium chloride)/poly (acrylic acid sodium salt) (PDADMAC/PANa) and poly (diallyldimethylammonium chloride)/poly (sodium 4- styrenesulfonate) (PDADMAC/PSSNa) pairs, respectively.

This will allow us to study the association of a strong polycation (PDADMAC) with a strong (PSSNa) or weak (PANa) polyanion. At charge stoichiometry, the former shows a liquid-liquid phase transition leading to the formation of microdroplets of liquid coacervate in equilibrium with the continuous phase, while the latter show a liquid-solid phase separation ultimately leading to a non-equilibrium solid precipitate.

In Chapter 1, the general and fundamental characteristics and concepts of PEs and PECS will be presented in order to better understand the nature of polyelectrolytes in solution, the associated physicochemical quantities and their interaction with oppositely charged polyelectrolytes, as well as some interesting applications and works from the literature to guide and inspire the experimental work performed in Chapters 2 and 3 on liquid and solid polyelectrolyte complexes.

In chapter 2, we investigated the influence of the complexation strength on the surface area and interfacial tension by systematically studying the surface activity of the two different PEC suspensions as a function of the molar charge ratio Z (= [-]/[+]). This enabled us to show that simple surface tension measurements can be a very sensitive tool to characterize, discriminate and better understand the formation mechanism of the different structures encountered during the formation of PECs.

In chapter 3, we have focused our work on the coacervate phase of the PDADMAC/PANa obtained at Z=1 (neutrality). In particular, we have studied the influence of the complexation strength on the interfacial tension, polymer volume fraction and local structure of such polymer-rich phase in equilibrium with the polymer-poor supernatant. For this purpose, we systematically investigated the effect of the PE concentration, temperature, ionic strength and ethanol content on the polymer network structure using complementary techniques such as TGA, DLS, SANS and interfacial tension measurements.

Chapter 1

Fundamentals in polyelectrolytes and polyelectrolyte complexes

Polyelectrolytes (PEs) and polyelectrolyte complexes (PECs) formed in aqueous solution by electrostatic interactions between oppositely charged entities have attracted considerable interest over the past several decades in many fields of science and technology, with several applications ranging from pharmaceuticals, drug delivery, sensors, cosmetics, surface coatings, the food industry, and water purification. This bibliographic part will introduce the general concepts necessary to better understand the nature of polylectrolytes in solution, the associated physicochemical quantities and their interaction with oppositely charged polylectrolytes in order to introduce the experimental work carried out during this PhD on *liquid* and *solid* polylectrolyte complexes.

1.1 Polyelectrolytes

Polyelectrolytes (PEs) are polymers containing a fraction f of charged monomers ($0 < f \leq 1$) composed of ionic or ionizable groups that can dissociate in a polar solvent like water[1], giving them unique physico-chemical and biological properties compared to their neutral alter egos. The charges carried by the polymers are accompanied by an oppositely charged counterion in order to respect electroneutrality. Depending on the charge carried by the backbone, PEs can be divided into two categories: positively charged polycations which in solution become positively charged and are surrounded by anionic counterions and polyanions surrounded by cationic counterions as illustrated in **Figure 1-1**. There are also polyampholytic species that carry cationic or anionic charged groups depending on the pH of the solution.

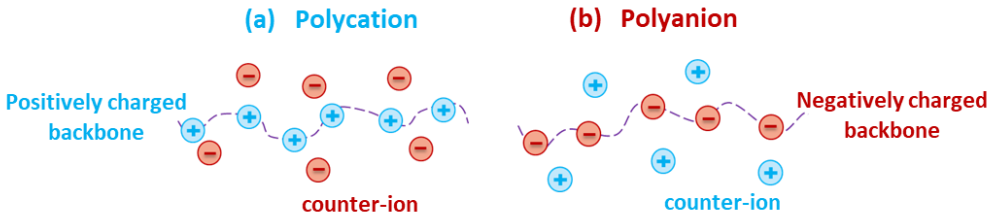

Figure 1-1. Schematic illustration of (a) a polycation and (b) a polyanion.

PE can be synthetic or natural. The main natural PEs are proteins, nucleic acids, polysaccharides, such as chitosan or alginate, extracted from natural brown algae and used in food or cosmetic formulations as gelling agents. Poly(acrylic acid) (PAA), Poly(sodium styrenesulfonate) (PSSNa) or poly(diallyldimethylammonium chloride) (PDADMAC) are well known examples of synthetic PEs (**Figure 1-2**). In the same way that acids or bases are weak or strong, PEs can also be classified into strong PEs in which all ionic groups are fully dissociated in solutions, regardless of pH, and weak PEs in which the effective charge distribution is dynamic, depending on the pH of the solution. In addition, the characteristics of PEs will also be influenced by many factors, for example, molecular weight, polymer concentration, temperature and ionic strength. In the following, some of these parameters and details will be demonstrated, including PE interactions and relevant theories.

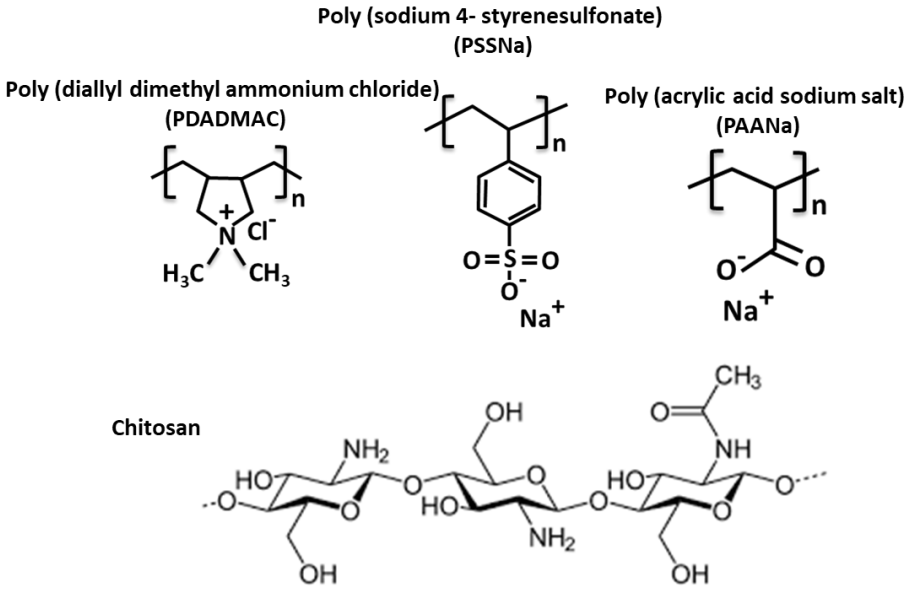

Figure 1-2. Examples of synthetic and natural PEs.[2]

1.1.1 Conformation and properties of polyelectrolytes

As with neutral polymers, a distinction is made between hydrophilic PEs, such as PAA and PDADMAC, that are in good solvent or solvent Θ in water, and hydrophobic polyelectrolytes that have low solubility in water and are therefore prone to hydrophobic interactions such as PSSNa, the reference hydrophobic PE where styrenic monomers are responsible for this behavior. Hydrophobicity of PEs can be determined by measurements of their specific heat or transfer energy[3, 4]. In aqueous media, a fraction of counter-ions is released, the polymer chains start to become more water soluble corresponding to distinct conformations where the chains are stretched like rigid rods. Indeed, in aqueous solutions, the charged segments of PEs have attractive interactions with polar water molecules and repulsive interactions with adjacent charged segments. In their uncharged state, they will have the appearance of more or less collapsed structures depending on the hydrophobicity of the uncharged PE chains whereas in a theta or good solvent, a random coil conformation is obtained. In a poor solvent, just like a hydrophobic uncharged polymer in water, they will be in a completely collapsed conformation. The hydrophobic interaction can be seen as the driving force behind these thermodynamic conformational changes from the stretched to coil state, as shown in **Figure 1-3**.[5]

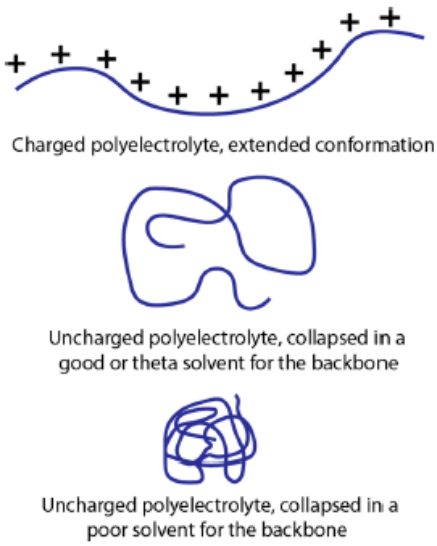

Figure 1-3. Schematic of the conformation of a charged polyelectrolyte vs. neutral polymer in good, theta, or bad solvent. [5]

Given the above, a number of counterions will be released if PEs are dissolved in polar aqueous solutions, leaving behind the charged monomer units. If a counterion escapes and is away from the backbone of the main chain, then the whole chain becomes charged. However, there may be another scenario. The counterion cannot easily pull away from the ionized monomer when the thermal motion is not strong enough. Instead, an "ion pair" will form between the counterion and the ionized monomer. In other words, the counterion will remain in close proximity to the charged monomer (at an average distance r) with a dipole formed by the two charges. If such multiple dipole-dipole ion pairs occur among all the counterions and the corresponding charged monomer units, then the chain is called an ionomer. The existence of multiple counterions is one of the unique characteristics of polyelectrolytes. The distribution of counterions is a complex situation influenced by electrostatic attraction and nature's requirement for entropy maximization.[6-8]

The interaction between the charged chain and the counterions has been an important topic for a long time. The distribution of counterions can be visualized by small-angle neutron scattering by using inorganic ions with a large neutron scattering cross section as a probe for counterions. The adsorption (or condensation) and desorption (unbound) of counterions on the polyelectrolyte chain is a dynamic exchange process in solution as found by neutron

scattering and neutron spin echo spectroscopy.[9, 10] The concentration of free counterions is much lower than the value predicted by the counterion condensation model, which means a much lower effective charge density of the polyelectrolyte chains as found by conductivity measurements.[11]

In addition to the above, neutron scattering and neutron spin echo spectroscopy are used to study the radial distribution of counterions, and electrical conductivity measurements are used to study the extent of counterion condensation. The distribution of counterions is also studied by applying several techniques such as pulsed field gradient NMR to study the self-diffusion of counterions[12], dielectric spectroscopy[13], capillary electrophoresis[14], osmotic pressure measurements[15] to measure the effective charge of polyelectrolytes, and electron paramagnetic resonance spectroscopy.[16]

Further evidence for the counterion adsorption process was found in a recent single-molecule study, in which the extreme dilution situation exposed the effect of entropy on the effective charge of the polyelectrolyte. Single-molecule fluorescence fluctuation spectroscopy, fluorescence correlation spectroscopy (FCS), and photon number histogram (PCH) were used to study the first-order conformational transition of single chains. A cationic fluorescent molecule (rhodamine 6G) was adopted as a probe to monitor the counterions of the anionic polyelectrolyte (sodium polystyrene sulfonate, PSSNa), and FCS was used to study the diffusion of the counterion probes in the PSSNa solution.[17]

There are two types of counterion probes: one is freely diffusing and the other is bound to the polymer chain. Both are confirmed by the presence of different diffusion coefficients. According to the results of **Figure 1-4** obtained, with the change of the concentration and molecular weight of the PSSNa molecule, the fraction of these two species can also be different. In other words, with the increase of PSSNa concentration, more counterions will be bound to the polymer chain as result of a lowered translational entropy at high polymer concentration. Furthermore, with increasing molecular weight of PSSNa, counterion binding is also enhanced, which is attributed to the effect of the chain end on counterion distribution. The dynamic exchange process of free counterions (desorption) and bound counterions (adsorption) is also indicated by substituting the different bound probes and increasing the salt content in the solution.

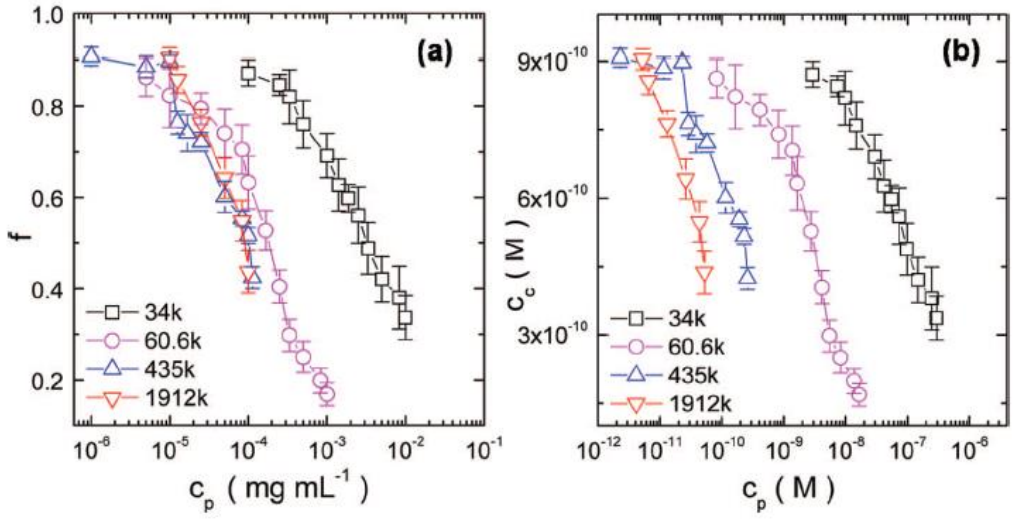

Figure 1-4. (a) The fraction of free counterions as a function of the mass concentration of PSSNa (b) The molar concentration of free counter ions as a function of the molar concentration of PSSNa for different PSSNa molecular weights. [17]

1.1.2 Theory of polyelectrolytes

1.1.2.1 Coulomb's law

Electrostatic interactions can be described by Coulomb's law due to the existence of attraction or repulsion between two charged points (q_1 and q_2) at a spatial distance r causing an electrostatic force F as indicated by equation (1.1) where all parameters are considered as scalar to simplify the calculation.

$$F = \frac{q_1 q_2}{4\pi\varepsilon_0\varepsilon_r r^2} \qquad (1.1)$$

with $\varepsilon_0$the vacuum permittivity and ε_r the relative static permittivity of the medium which is usually water in PEs solutions.

Here we assume that the charges of the dissociated monomer and the counterion are point charges of the same magnitude equal to the electronic charge e. Then the energy of the Coulomb interaction of the ions pair is $e^2/\varepsilon r$ with $\varepsilon = \varepsilon_0\varepsilon_r$ the dielectric constant of the medium. If this this energy is much less than the characteristic energy of thermal motion $k_B T$:

$$\frac{e^2}{\varepsilon r} < k_B T \quad or \quad \frac{e^2}{\varepsilon r\, k_B T} < 1 \quad (1.2)$$

where k_B is the Boltzmann's constant, and T the absolute temperature, then counter-ions break off the chain[18] and we get the polyelectrolyte regime.

On the contrary, if this energy is much larger than k_BT:

$$\frac{e^2}{\varepsilon r} > k_B T \quad or \quad \frac{e^2}{\varepsilon r\, k_B T} > 1 \quad (1.3)$$

then the counterions cannot detach from the chain, which means that thermal motion cannot break the ion pairs, and the chain is considered an ionomer, as shown in **Figure 1-5**.

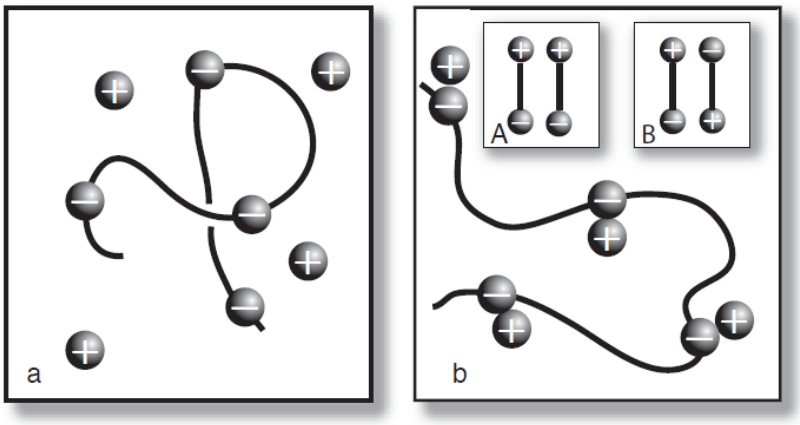

Figure 1-5. The polyelectrolyte regime (a) with all counterions free and detached from the polymer chain; the ionomer regime (b) with counterions "condensed" onto the main chain forming ion pairs with the charged monomers. Inset: The dipoles (ion pairs) are free to choose any orientation relative to each other. The one they prefer is (B), because it gives a lower energy than (A). It corresponds to an attraction. [18]

As previously described, proteins, DNA, PSSNa, PAA, PDAMAC are all polyelectrolytes when dissolved in water (polar solvent). One point to note is that the dielectric constant of water is quite high ($\varepsilon \approx 80$) which can result in the ratio $e^2/\varepsilon r k_B T$ being relatively small with then the inequality (1.2) holding. However, if other solvents with much smaller ε values (typically less than 40) are used, then the inequality (1.3) is verified and as a result the polymer

is an ionomer rather than a polyelectrolyte. Therefore, the dielectric constant is an extremely important factor to consider when choosing the appropriate solvent. This is the reason why the polyelectrolyte regime is typical of charged (bio)polymers dissolved in water while the ionomer regime is the one favoured in organic solvents.

1.1.2.2 Debye-Hückel model

The Debye length, obtained from Coulomb's law, is defined as the distance from a charge surrounded by other point charges at which the interaction potential is shielded. The Debye length (κ^{-1}) accounts for the local charge density and the local concentration of counterions [5, 19] :

$$\kappa^{-1} = \sqrt{\frac{\varepsilon_r \varepsilon_0 k_B T}{2 N_A e^2 I}} \qquad (1.4)$$

with ε_r the permittivity of the medium, ε_0 the vacuum permittivity, k_B the Boltzmann constant, T the temperature, N_A the Avogadro's number, e the elementary charge and I the ionic strength of the electrolyte solution.

For simple electrolytes (salts), this is acceptable; for polyelectrolytes this approach finds its limits. Indeed, the model treats the ions as a point charge, whereas the charges are distributed along a chain and are therefore no longer point charges in the case of polyelectrolytes.[20] The charged functional groups of polyelectrolytes dissociated in water are periodic along the backbone or on a dangling chain. Although the model is not perfect, the Debye length is commonly used to theoretically treat the interaction between charged chain segments.[21]

1.1.2.3 Screening of electrostatic interaction

When a finite concentration of salt is present in the solution, which is often the case in experiments, the solution becomes a conductive rather than a dielectric medium due to dissociation of the salt. According to the basic understanding, the Coulomb interaction between the charged monomers can be screened by the salt ions. Thus, distant parts of the

chain will no longer interact because the electrostatic potential created by a monomer, or group of monomers, decreases exponentially rather than algebraically with distance.

Furthermore, by combining the Debye-Hückel model, the Debye length κ^{-1} range can be much larger than the monomer size, which sets the typical interaction range in neutral polymers. Depending on the ionic strength, κ^{-1} can typically range from less than 1 nm to more than 100 nm. It should be noted, however, that the concept of effective interaction between monomers, obtained by integrating the degrees of freedom of small ions, is only useful for the calculation of static properties. Dynamic properties such as diffusion constants or viscosities need not be identical to those of a hypothetical polymer solution in which the monomer-monomer interaction is given by (1.6). Ionic degrees of freedom can play a nontrivial role in the dynamics, as they do in charged colloid suspensions [1]:

$$v_{DH}(r) = k_B T \frac{l_B}{r} \exp(-\kappa r) \qquad (1.6)$$

with l_B being the Bjerrum length which is defined as the distance between two charges at which the interaction strength can be comparable in magnitude to the thermal energy, $k_B T$. This is commonly used to describe the strength of the electrostatic interaction in polyelectrolytes.[22] The expression for Bjerrum length l_B is:

$$l_B = \frac{e^2}{4\pi\varepsilon_r\varepsilon_0 k_B T} \qquad (1.7)$$

1.1.2.4 Manning condensation

Electrostatic interactions of polyelectrolytes are highly sensitive to their oppositely charged counterions, which can be free in solution or tightly associated to the chain (condensed); hence counterions can decrease the overall apparent polymer charge and neutralize the charges effectively. Instead of treating polyelectrolytes as point charges, Manning developed a theory aiming to determine the extent of counterion condensation by using the Debye-Hückel approximation. Considering the polyelectrolyte chain as an infinite line charge with a given linear charge density β , this theory indicates[23, 24]:

$$\beta = \frac{Z_p e}{b} \qquad (1.8)$$

where Z_p is the polyion valency, e is the elementary charge and b is the distance between charges on the polymer. It has been shown that the statistical mechanical phase integral for such an infinite line charge diverges at high charge densities. This essentially means that the system is unstable at linear charge densities greater than a critical value β_{crit} . Manning introduced the so-called charge parameter (ξ):

$$\xi = \frac{e^2}{\varepsilon k_B T b} = \frac{l_B}{b} \qquad (1.9)$$

For a counter-ion i, the system is unstable for values of $\xi \geq |Z_i Z_p|^{-1} = \xi_{crit}$, where Z_i is the valence of the counterion, or $\xi \geq 1$ for monovalent ions. When the system is unstable for values of $\xi > \xi_{crit}$, then counterions will "condense", or associate closely to the polymer chain until ξ approaches ξ_{crit} (1 for systems of monovalent ions). Because ξ is the ratio of the Bjerrum length l_B to the average charge spacing, the critical charge spacing for a system with monovalent ions is equal to l_B and for multivalent counter-ions to l_B/Z_i.

It follows that for strongly charged polyelectrolytes, the electrostatic potential on the chain will be quite high and condensation of the counter ions will occur if the energy gain is greater than the entropy loss associated with the loss of mobility of the condensed counter ions leading to effective charges lower than nominal monomer charges. The effective charge fraction, f_{eff}, is then calculated as

$$f_{eff} = \frac{1}{\xi} \qquad (1.10)$$

The condensed counter-ion sheath around a polyelectrolyte chain is electrically polarizable which can induce attractive interactions between polyelectrolyte chains. Below the Manning condensation threshold $(\xi < 1)$, the counterions are not condensed and are essentially free. The osmotic pressure of the polyelectrolyte solution is one of the directly measurable quantities which is strongly depended on the condensation of the counterions. In many cases, the osmotic pressure of a polyelectrolyte solution is dominated by the counterions, while the contribution of the polyelectrolyte chains plays only a very small role.

Several other physical quantities such as the electrical conductivity of the solution or the electrophoretic mobility of the chains[25] strongly depend on the condensation of the counter-ions and are dominated by the free counter-ions. In general, their determination is in good agreement with Manning condensation theory.

For polymers, heat transfer is quite efficient in the molecular chain backbone direction due to strong covalent bonds, while it is much less efficient in the inter-chain direction due to weak non-bonding interactions.[26-32] High thermal conductivity polymers for example can be used in many applications, such as flexible electronic devices [30, 33] and Li-ion batteries [31, 32]. However, for polyelectrolytes, the heat transfer mechanism will be more complex due to the direct effect on heat transfer but also an indirect contribution due to the conformational changes of the chain influenced by the strong coulombic interactions between the ionized polymer chain and the counterions.[34-36] Regarding the role of counterions, their effect on the thermal conductivity of polyelectrolytes is still under debate. In polyelectrolytes, it is reported that the counterion-counterion, counterion-polymer and polymer-polymer interactions are strongly dependent on the partial charge and ionic size of the counter-ions. [34, 37-39]

Given the importance of polyelectrolytes used in many fields, including but not limited to electronic devices and batteries, the thermal conductivity of polyelectrolytes with different counterions is studied using molecular dynamics (MD) simulations, as shown in **Figure 1-6**.[40] The results show that the radius of the counterions has a strong negative dependence on the thermal conductivity. By analyzing the heat flow at the molecular level, it is found that the thermal conductivity generally shows an increasing trend with respect to the non-bonding interatomic forces and atomic velocities. Furthermore, a positive correlation, which can also be attributed to the same origin at the molecular level, is also established between the MD calculated thermal conductivity and the minimum thermal conductivity model result. With these results, new insights are provided into the physics of heat transfer in polymers, which can be used as a reference for developing thermal conductivity tailored polyelectrolytes.

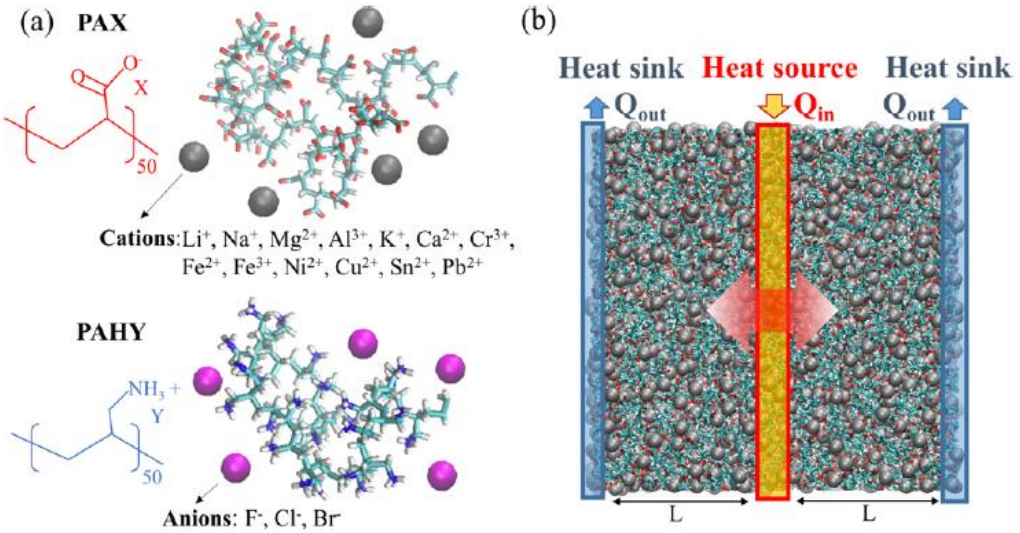

Figure 1-6. (a). Schematic illustrations of various polyelectrolytes with different cations and anions (b) Schematic of the non-equilibrium MD simulation (NEMD) model setup for thermal conductivity calculation.[40]

The charge state of the main chain is the most important factor in controlling the conformation of charged macromolecules and has been confirmed to be strongly related to the interaction between the chain and its counterions. Dissociation of charged or ionizable groups provides charges to the main chain, while binding of counterions neutralizes the original charges.[23, 41] Much new knowledge has been gained on this important topic which has been the subject of intensive efforts. Through the development and application of new techniques in recent years, it has been shown that multiple factors such as the concentration of charged macromolecules, molecular weight, molecular topology, and salt concentration, strongly impact the binding of counterions and thus the effective charge density of the main chain.[42, 43] The distribution of counterions around the main chain is under the dynamic exchange between adsorbed and desorbed (free) counterions governed by electrostatic interactions and thermal activation.[41] In addition, the details of adsorption and desorption of a counterion on the polyelectrolyte chain are an important issue to study in such a thermal equilibrium state.

In aqueous solution, the dynamic exchange of adsorption and desorption of counterions on a polyelectrolyte chain is studied at the single molecular level. As **Figure 1-7** showed, the study is performed using a fluorescence resonance energy transfer (FRET) process between a

fluorescence donor chemically attached to the end of a model polyanion (PSSNa) and a positively charged fluorescence acceptor (Atto 610), which serves as a counterion probe in solution.[44] Dual color fluorescence correlation spectroscopy (DC-FCS) is a popular technique used to estimate the adsorption and desorption rate of the counterion probe on the charged main chain and the multiple factors that affect it. If the desorption rate is greater than the adsorption rate, the overall equilibrium will tip in favor of desorption and leave the main chain effectively charged. The adsorption rate increases with the concentration of the fluorescent probe due to a reduced entropy penalty while the desorption rate remains unchanged.

Moreover, with the addition of salt (NaCl) in the solution, the analysis of the experimental data shows a competition of the adsorption between the sodium ions and the fluorescent probe. At very high salt concentration, a greater adsorption of sodium ions is observed which causes a conformational change with the contraction of the polyelectrolyte chain.

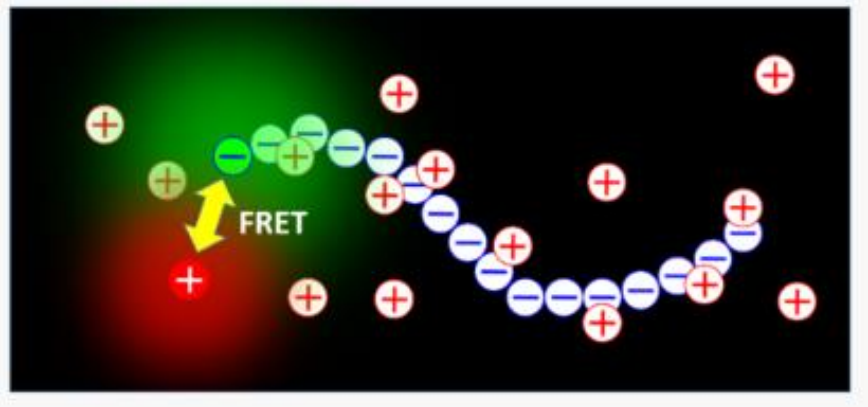

Figure 1-7. Schematic illustration of dynamic adsorption of counterions on a polyelectrolyte chain. [44]

1.1.3 Weak and strong polyelectrolytes

Under the effect of electrostatic forces, the interaction and structure of PEs can be controlled to a large extent in a solvent (usually water).[45-47] The interaction can lead to a strong repulsion between the intramolecular charges which strongly stretches the PEs in the high dilution regime generating rod-shaped chains.[45] If a PE is dissolved in the solution in the presence of salt, the charges of the PE chain will be further screened by the ions of the

salt, causing the interaction strength to decay with the Debye length κ^{-1}.[47] As discussed earlier, charge density plays an important role in the interaction between polyelectrolyte monomer groups.[45] Some groups present a charge that is strongly dependent on the pH of the solution, such as the carboxylic groups (COOH) of poly(acrylic acid) (PAA) for example. They are then considered "weak" polyelectrolytes.[47]

In contrast, PEs that carry monomeric groups that are virtually unaffected by pH, such as the sulfonate group of PSSNa or the quaternary ammonium group of PDADMAC, are considered "strong" polyelectrolytes.[46, 47] The average charge density or directly the free energy was used in earlier theories like those of Kuhn [45] or Overbeek [48]. Pierre-Gilles De Gennes is one of the first authors who introduced the idea of a coupling constant to describe the intra- and intermolecular of interaction PEs.[49]

For weak PEs, the PE molecule can remain rigid and rod-like in the case where the PE blob size is small compared to the chain length.[49, 50] Therefore, the entropy change upon dilution or complex formation of such a PE is small.[47] Meanwhile, the electrostatic repulsion is smaller than k_BT, and therefore, polymer segments can have a Gaussian coil-like conformation in the blobs if the PE is weakly charged. The entropy of segments in blobs is similar to that of uncharged polymers. To describe the solution behavior of a weak PE macromolecule, the free energy of a PE in solution is considered as both enthalpy and entropy in a Flory-type mean-field system (**Figure 1-8**), as shown in the following equation [2, 45]:

$$F \approx \frac{L^2}{b^2\,N} k_BT + k_BT \frac{l_B (fN)^2}{L} ln\left(\frac{L}{b\sqrt{N}}\right) \qquad (1.11)$$

with N the polymerization degree, f the charged fraction, L the length of the (coiled or elongated) PE, l_B the Bjerrum length and b the thickness of the (partially coiled) PE.

The first term on the right-hand side of (1.11), inversely related to the entropy, is the elastic contribution of the chain conformation to the free energy. If the entropy decreases (i.e. the chain elongates), L increases, then the first term of (1.11) will also increase. The second term illustrates the electrostatic contribution of the PE to the free energy. Therefore, the overall structure of the PE based on the fraction of charged monomers can be determined by Equation (1.11). This can be used to calculate and evaluate the degree of PE coiling as a

function of the charged fraction, as well as to compare the viscosity prediction from the PE structure with experimental measurements of the viscosity of the corresponding solutions.[45]

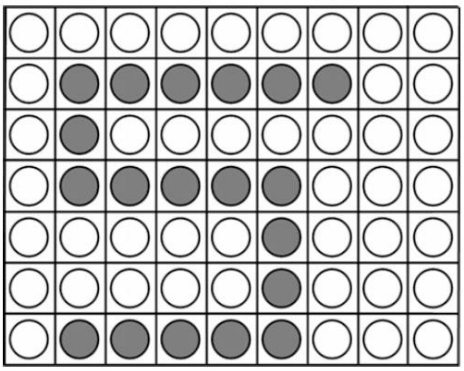

Figure 1-8. Graphical visualization of the Flory-Huggins mean field theory. The solvent is symbolized by the lattice positions with the white circles and the PE is illustrated by the gray circles. It is assumed that each field has the same size with no field or chain overlap, all field positions are occupied, all polymer-polymer interactions are the same (all chain parts are the same). [51]

The behavior of weak PEs can be controlled by the pH and ionic strength in most cases. For example, when the pH causes a very low charge density, the interaction between the PEs is controlled by hydrophobic forces and hydrogen bonds[52], as well as within the same coil.

Strong PEs however exhibit a fundamentally different dilution and complex formation behavior than weak PEs. The dilution is mainly due to the increase in entropy due to the release of counter ions and not, as in the case of weak PEs, to changes in enthalpy.[46, 53] And during these processes, there is little change in the structure of the PE itself, as well as in its enthalpy. [52, 54]

1.2 Polyelectrolyte complexes

A growing number of papers on polyelectrolyte complexes testifies to the increasing scientific and industrial interest in this field, both on the experimental and theoretical levels.[55-62] Basically, polyelectrolyte complexes can be divided into two types: the first type (PECs) is a complex of cationic and anionic polyelectrolytes, called polyelectrolyte-polyelectrolyte complex. The second type (PESCs) consists of complexes of polyelectrolytes

and surfactants of opposite charge. The complex formation of PECs and PESCs is closely related to self-assembly processes when the two oppositely charged species-polyelectrolyte and polyelectrolyte or polyelectrolyte and surfactant-are mixed in aqueous solution. Multilayer films of PECs on solid substrates were also prepared by physisorption from a solution with the help of the well known the layer-by-layer technique and synonymous of electrostatic self-assembly. [63]

However, a number of different procedures for forming PECs and PESCs have been developed. The main difference between PECs and PESCs is in their solid-state structures. In contrast to the ladder and scrambled egg structures of PECs [64], solid-state PESCs exhibit typically highly ordered mesophases. [65] There are two reasons for the high ordering of PESCs: one is related to the cooperative binding phenomena of surfactant molecules on polyelectrolyte chains [66, 67] and the other one is related to the amphiphilicity of surfactant molecules. The cooperative zipper complexation could be an additional mechanism between a polyelectrolyte and oppositely charged surfactant molecules mixed at stoichiometry. A microphase separation in PECs is promoted by the amphiphilicity of surfactants, which may result in periodic nanostructures with repeat units. In contrast, no such periodic nanostructures can be obtained with PECs normally. In this chapter, polyelectrolyte-polyelectrolyte complexes (PECs) will be mainly discussed as a preamble to the experimental work that will be described in the forthcoming chapters.

1.2.1 Polyelectrolyte complexes (PECs)

Under certain conditions, the formation of PECs depends primarily on the rapid kinetics of the process and will be influenced by multiple factors, including the natural characteristics of the polyelectrolyte, temperature, ionic strength, and mixing mode. Polyelectrolyte complexes form spontaneously with some counterions released during the mixing of polyanion and polycation solutions. Normally, the low molecular weight counterions are more or less localized near the free polyelectrolyte chains, which leads, in the case of high charge densities, to condensation of the counterions, as shown above. Complex formation can occur either between polyacids and polybases or between their metal and halogen salts. The released low molecular weight counterions can lead to an increase in entropy, which is the

driving force behind complex formation. In addition, hydrogen bonds or hydrophobic interactions may also play a secondary role.

The following equation illustrates the polyelectrolyte complex formation reaction [5].

$$(>-A^-c^+)_n + (>-C^+a^-)_m \Leftrightarrow (>-A^-C^+)_x + (>-A^-c^+)_{n-x} + (>-C^+a^-)_{m-x} + xa^- + xc^+ \quad (1.12)$$

where $A^-$and $C^+$are the charged groups on the polyelectrolyte chain and their counterions $a^-$and c^+, n and m are representative of the number of anionic and cationic groups in solution, n/m or $n/m = x$ is the molar mixing ratio, when $n < m$, then $\theta = x/n$, or when $n > m$, then $\theta = x/m$, θ is the degree of conversion.

The degree of conversion determines whether the ionic sites of the effective components are completely bound by oppositely charged polyelectrolytes or whether low molecular weight counterions remain partly in the complex. Another characteristic quantity is the overall composition of the PEC structures at any mixing ratio. Even if the ionic bonding stoichiometry is 1:1, the main component may be bound in excess, leading to an overcharging of the PEC particles. The formation of PECs leads to quite different structures, depending on the characteristics of components used and the external conditions of the reaction. As limiting cases for the resulting structures of polyelectrolyte complexes, two models are discussed in the literature. [68] The first one is called the ladder-like model. The complex formation takes place on a molecular level via conformational adaptation (zip mechanism); the second one is called the scrambled egg model where the complexed PE chains adopt a random conformation. A great number of chains are incorporated into a particle. In addition to determining the stoichiometry of PECs, detailed characterization of PEC structures can provide insight into the effects of various factors on complex formation and their different properties.

1.2.1.1 Water-soluble PECs

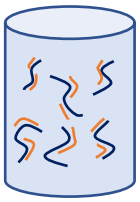

Figure 1-9. Schematic illustration of water-soluble PECs.

Comprehensive and systematic studies about soluble PECs (as **Figure 1-9** showed) began with the pioneering work of the Kabanov [69, 70] and Tsuchida[71, 72] groups. They showed that the formation of PECs can result in soluble complexes between polyions with weak ionic groups and significantly different molecular weights in non-stoichiometric systems with appropriate salt concentration. According to the ladder model, these PECs are structured into single-stranded hydrophilic and double-stranded hydrophobic segments. Predominantly, various polycations have been used to combine with polyanions containing carboxyl groups. Due to the presence of a small amount of salt, the processes can be rearranged and exchanged, meanwhile, the reaction is able to be shifted to thermodynamic equilibrium, leading to uniform short-chain components among all the long chains of the counterpart. With the addition of salt, this can initially lead to a shrinkage of the PECs due to the screening of their charges by the electrolyte. When a critical concentration of salt is exceeded, a disproportion of the guest short chains occurs, which can lead to the formation of fully complexed and precipitated species and free host polyelectrolyte chains in solution.[69]

If the salt concentration increases continuously, then the precipitate will be dissolved again with the presence of free polyelectrolyte chains for both components in solution. Changing the pH value can induce the same result.[70] While PECs exhibit high stability at low ionic strength, they can take part in polyion exchange and substitution reactions at higher ionic strengths. In particular, the addition of a higher molecular weight component or stronger ionic groups can lead to substitution reactions. Therefore, polyelectrolyte complexes can be considered as “living systems” that are quite sensitive to the environment change and make the appropriate respond. Thus, very specific conditions are required for the preparation of soluble PECs.[21]

1.2.1.2 Stoichiometry of the PECs (precipitate /coacervate)

Mixing oppositely charged polyelectrolytes in aqueous solutions can lead to associative phase separation of the polyelectrolyte chains, leading to dense polymer-rich phases known as polyelectrolyte complexes.[5, 73-78] There are several examples of complexation in natural and biological systems - the glue that holds together the habitat of sand worms, bacterial nucleotides and DNA-enzyme complexes.[79, 80] The compaction of long DNA strands around histones to form chromatin fibers in eukaryotic cells is perhaps the most important biological consequence of polyelectrolyte complexation.[81] Then, to encapsulate biomolecules and enhance biological activities, liquid complexes have also been used as membrane-free compartments.[82-84]

Polyelectrolyte complexes can be viscous water-rich liquids, called "coacervates", or solid complexes resembling hydrated polymer glass, considered as "precipitates" as shown in **Figure 1-10**. At the beginning of the twentieth century, the scientific interest for this kind of systems appeared following the seminal work of Bungenberg de Jong on coacervates and precipitates.[85] Studies on the complexation of natural polymers have been the focus for decades, including gelatin and gum arabic.[86, 87] Due to the recent development of synthesis and purification capabilities, a range of synthetic polyelectrolytes, polypeptides, proteins and charged nanoparticles[88-92] can be studied by researchers to better understand complexation. These developments may also have enhanced the creative work of countless self-assemblies, including spherical, cylindrical and vermicular micelles, multilayer films, membranes, capsules, vesicles, fibers and hydrogels.[93-103] Water-rich coacervate-based assemblies are of great interest in current biomedical applications such as drug and nucleotide encapsulation and delivery, bioadhesives and tissue growth scaffolds.[104-106]

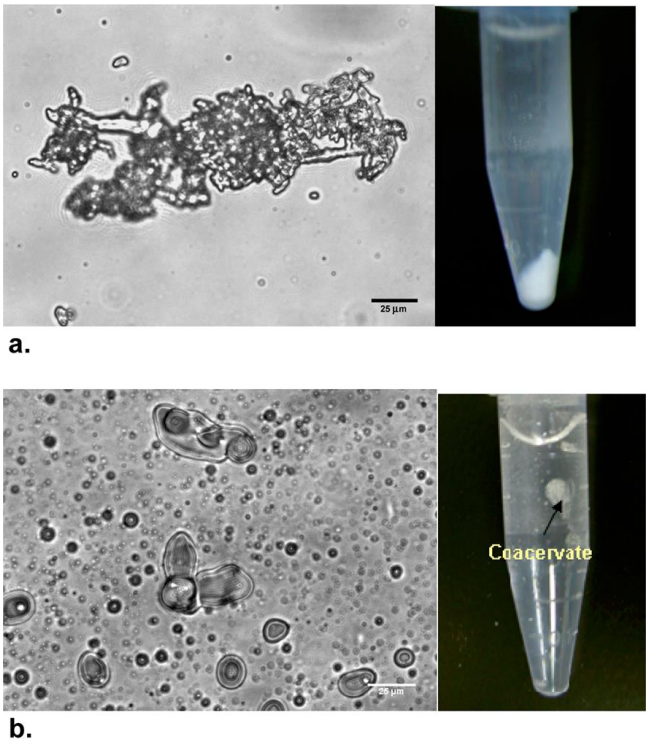

Figure 1-10. Observation of the PEC phase of mixtures prepared from PAH- poly(allylamine hydrochloride) and fully neutralized PAA (sodium salt of polyacrylic acid) after centrifugation (in the flask) and by optical microscopy without (a) and with salt addition at 2M (b). Systems are prepared at 1:1 stoichiometry of acid/base units with a total polyelectrolyte concentration of 0.05 wt%. [107]

Solid-like precipitates can also be formed in a solution of polyelectrolyte-surfactant complexes (PESC) with various structures.[108, 109] Many reports demonstrate the structure and formation of well-ordered precipitates or colloidal nanoparticles.[110]

1.2.1.3 Potential Applications of PECs in Solution

A range of chain lengths, PE composition, salt concentrations can be tuned to design complexes sensitive to external factors such as ionic strength, solution pH or temperature. To some extent, these complexes should have great prospects in the future as potential transport systems for drugs, enzymes or DNA, as these charged species can be easily combined in complex structures, as shown in **Figure 1-11**. Polypeptide/polyelectrolyte complexes can be used as pharmaceutical carriers, such as polylysine/polyanion complexes, with interests for basic research on biomolecular recognition at the conformational level and for applications.

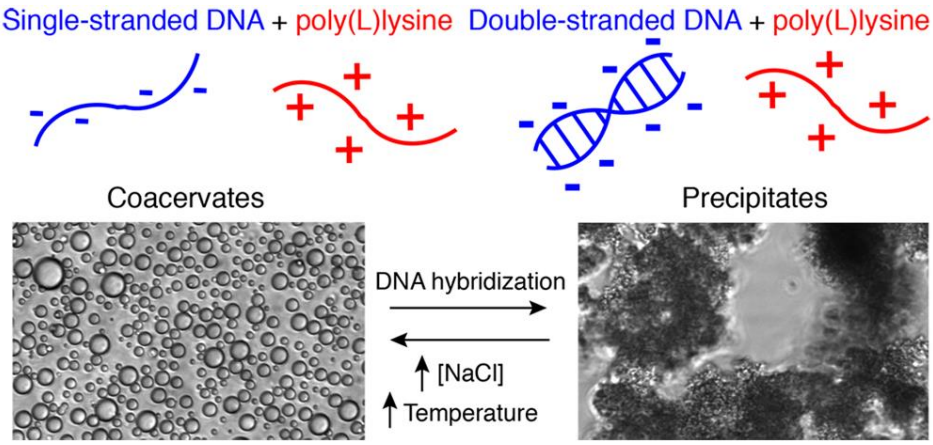

Figure 1-11. Poly(L-lysine) and DNA with different hybridization states form different phase separated complexes and transition with the effect of salt and temperature.[111]

Polyelectrolyte-enzyme complexes

The formation of complexes between proteins and polyelectrolytes has been extensively studied.[112, 113] A mechanism of protection-activation of enzymes was described by Kabanov about the pH-induced liquid/solid transition of their complexes with polyelectrolytes.[112] The direct association of an enzyme with a polyelectrolyte often leads to a strong loss of its activity. Therefore, it has been proposed to immobilize the enzymes in a complex matrix of synthetic polyelectrolytes[112] based on the fact that under optimal pH conditions, PEC formation can be achieved for incorporation of an enzyme into the complex. Thus, it becomes possible that there is no enzyme released from the PEC matrix by adjusting the pH to a value allowing the highest activity. The immobilization procedures were optimized according to the pH, nature and molecular weight of the components as well as the enzyme/polyelectrolyte mass ratio for trypsin and amyloglucosidase.[114] In addition, the complex was entrapped in polyvinyl alcohol gel particles, which allowed the enzyme to be easily manipulated in industrial fields and used multiple times without loss of activity.[114]

DNA-Polycation Complexes

It is well known that many diseases can be caused by a single genetic defect. By introducing DNA or DNA fragments into cells, gene therapy can offer the possibility of correcting such defects, whereas traditional medicine can only treat the symptoms. However,

in this case, one of the most difficult problems is to find appropriate carrier systems that guarantee a high rate of cell transfection with low cell mortality. Kabanov presented a good study in this research area.[115] In gene delivery systems, DNA or oligonucleotide complexes with polycations have proven to have great potential.[116] However, the low colloidal stability can lead to a serious problem, especially when the mixing ratio of anionic and cationic groups is close to the stoichiometry or when complexes are exposed to physiological salt conditions. The situation has obviously improved by using doubly hydrophilic polycations.[117] However, in many cases, high level of aggregation of the complexes are observed, which can result in several thousand DNA fragments introduced into one cell, especially for oligonucleotides. Based on the generation of soluble PECs, the aggregation level can be significantly decreased under certain conditions.[118]

1.2.2 Influence of ionic strength and temperature on PECs assembly and structure

1.2.2.1 Effect of salt/ ionic strength

Similar to the effect of salt on the formation of soluble PECs, salt is also expected to play a decisive role in the formation of highly aggregated PECs, as it can weaken the electrostatic interaction and enhance the rearrangement processes, and some details have already been studied.[119] Extensive studies of various PEC systems have revealed that there is a large difference, highly dependent on the polyelectrolyte components used, in the response of polyelectrolyte complexes to the addition of NaCl.[119, 120] In aqueous KBr, polyelectrolyte complexes (PEC) can be dissociated and dissolved. On the contrary, oppositely charged polyelectrolyte can re-associate when the salt is diluted by adding water.[121] Compared to NaCl, the chaotropic KBr has a higher doping constant. If the KBr concentration is less than 1.3 M, it would take about an hour to reach doping equilibrium for a 1 mm diameter PEC fiber in, whereas it would take days or weeks to achieve a stable coacervate composition starting with dry PEC.[121, 122] As an alternative pathway, sufficient KBr was also added to completely dissolve the PEC then water was added to the solution to dilute the salt to a final concentration to obtain the coacervate phase as shown in **Figure 1-12**. [121]

Figure 1-12 (a) shows the change in equilibrium material morphology from dry PEC without salt to coacervate and fully soluble state with increasing KBr concentration. At low salt concentration, PEC appears in a solid state, with a fairly opaque appearance and the consistency of a very soft rubber. By increasing the amount of KBr, the complex changes from an opaque solid state to a clear, mobile liquid state, resulting in a significant increase in the volume of the PEC. With the salt concentration continuously increased to about 1.80 M, a transparent and soluble single phase will be realized, which means that the PEC is absolutely dissolved at a high salt concentration.

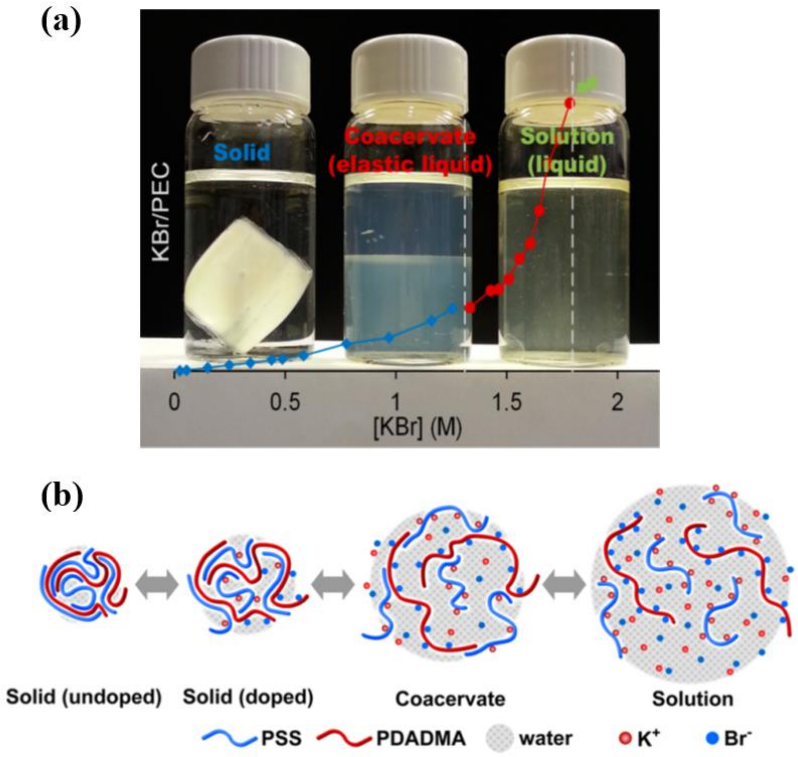

Figure 1-12. (a) After proper equilibration, these mixtures prepared from the strongly interacting poly(styrenesulfonate) (PSSNa)/poly(diallyldimethylammonium) (PDADMA) system at stoichiometry yielded compositions ranging from complexes (solids) to coacervates (elastic liquids) and dissolved solutions with increasing KBr. (b) Schematic illustration of the effect of salt addition on the microstructure of PEC solid (undoped), solid (doped), coacervate, and solution from left to right. All steps are reversible and all compositions are in equilibrium.[121]

The water content in the PEC increases due to the increasing salt concentration as a result of hydration. Meanwhile, the salt can also break the association between the polymer ion pairs. **Figure 1-12** (b) shows the general evolution of PEC as a function of the amount of

salt. Initially, the PEC shows a highly condensed solid appearance due to the closed association of the polymer in water without addition of salt. When a certain amount of KBr is doped into the PEC, the additional water is also introduced into the gap of the polymer molecules. And at the same time, the salt ion will make a pair with the charged monomer unit leading to the interaction breakage between two charged polyelectrolyte segments. If the salt concentration is higher, more charges of the polyelectrolyte will be screened, and the association between the polymers will be weakened, so the crosslinking density will be much lower. In the end, the PEC dissolves completely and the polyelectrolyte molecules are pulled apart, with all ion pairs being broken between the polyelectrolytes, leaving the chains free.

As mentioned above, the interaction between ion pairs is strong and can result in a solid-like precipitate at low salt concentrations. Increasing the added salt will reduce the number of ion pairs and weaken the ion pair strength, resulting in sticky and unstable connections between oppositely charged polyelectrolyte segments forming a liquid-like coacervate.[123, 124] The boundary between the solid-like precipitate phase and the liquid-like coacervate phase is broad and has been identified as a continuum by Wang and Schlenoff. [121]

The electrostatic interactions between polyelectrolyte chains and their relaxation mechanism within the complex phase are of fundamental interest. [125] Through ion pairing between anionic and cationic polyelectrolyte segments, these interactions have already been modeled through the formation of thermoreversible bonds.[121, 126] And for the relaxation mechanism of polymer chains across this continuum, it is expected to exhibit a stepwise evolution.

Depending on the salt ion concentrations and sizes, a mixture of linear anionic and cationic polyelectrolytes in aqueous medium leads to different phases. At low NaCl salt concentrations, sodium poly(styrene sulfonate) (NaPSS) and poly(diallyl dimethyl ammonium chloride) (PDADMAC) solutions at a stochiometric mixing ratio of 1:1 separate into a polymer-poor supernatant and polymer-rich precipitates that are stiff and turbid, as shown in **Figure 1-13** (a) and (b) corresponding to two representative salt concentrations lower than 2 M. When the amount of salt is increased, the polymer-rich phase gradually becomes softer and fluid, as shown in **Figure 1-13** (c) and (d) corresponding to NaCl concentrations of 2.4 M and

2.6 M, respectively. When the salt concentration is increased further, the polymer-rich phase becomes fluid and looks more liquid-like and transparent, as shown in **Figure 1-13** (e)–(g) corresponding to NaCl concentrations higher than 3 M.

If NaCl is replaced by a KBr salt, whose hydration shell size of the dissociated salt ions is larger in the potassium poly(styrene sulfonate) (KPSS)/poly(diallyl dimethyl ammonium bromide) (PDADMAB) system, there will be a noticeable effect on the complexation behavior.[127] In this situation, it will be shifted to lower salt concentrations and the rigid and turbid precipitate will appear even if the KBr concentration is about 0.5 M, as shown in **Figure 1-13** (h). However, a similar trend is observed, then with increasing KBr concentration, the soft and fluid phase can appear at C_{KBr} = 1.2 M as shown in **Figure 1-13** (i). As the salt concentration increases, the polymer-rich phase becomes progressively more liquid, as shown in **Figure 1-13** (j)-(l) corresponding to KBr concentrations of 1.4 M, 1.6 M and 1.8 M, respectively. When the KBr concentration is higher than 1.85 M as shown in **Figure 1-13** (m) there is only one phase in the solution where no complexation will take place between oppositely charged polyelectrolytes, because the charges on the polyelectrolyte chains are screened by salt ions.

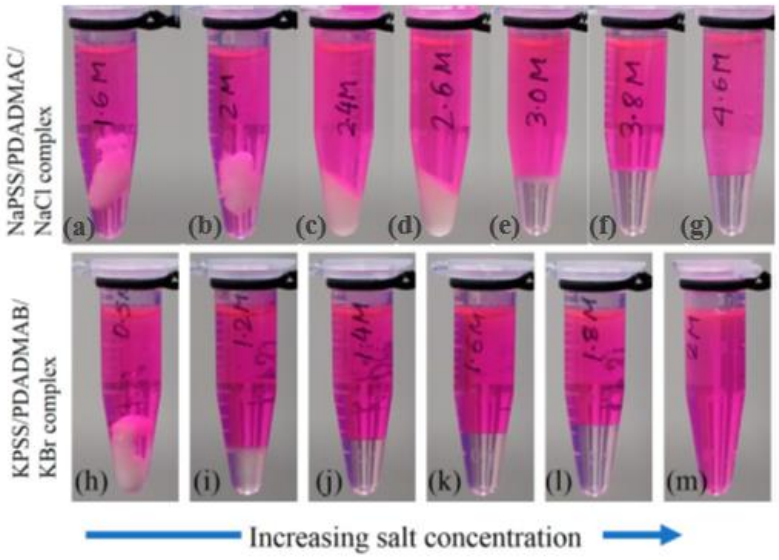

Figure 1-13. Photographs of complexes obtained after centrifugation for NaPSS/PDADMAC at increasing concentrations of NaCl (a–g) and KPSS/PDADMAB at increasing concentrations of KBr (h–l). Rhodamine-B dye was added to the supernatant to show the interface between supernatant at the top and complexes at the bottom in the microcuvettes.[128]

1.2.2.2 Temperature sensitive PECs

Poly(N-isopropylacrylamide) (PNIPAM) is one of the most typical thermosensitive polymers whose behavior in aqueous solution has been extensively studied. At low temperatures, PNIPAM is soluble in water; however, with increasing temperature, it starts to be insoluble and exhibits a lower critical solution temperature (LCST) behavior leading to the coil-to-globule transition. [129] When PNIPAM is part of a polymer network (gel or microgels), a strong volume change of the network can be observed within a narrow temperature range,. With the introduction of ionic groups, it is possible to vary the properties of microgels to a large extent. [130, 131]

Compared to the preparation of thermosensitive gels by covalent crosslinking in general, there is a promising new route to provide the preparation of tailored nanoscale gel particles that can be achieved by the formation of polyelectrolyte complexes between ionically modified thermosensitive polymers. As reported by Dautzenberg, recent studies on the formation of PECs between ionically modified PNIPAM have shown that nearly monodisperse, sphere-like complex particles on the scale of 100 nm can be prepared that exhibit reversible, temperature-controlled swelling-deflating behavior of nearly a factor of 10 at about 35 °C. [132]

The lower critical solution temperature (LCST) behavior can also be observed in the complexation between potassium-poly(styrenesulfonate) (KPSS) and poly(diallyl dimethylammonium bromide) (PDADMAB) as shown in **Figure 1-14**. By heating the mixtures, the phase separation can be shown experimentally. At low temperatures, between 5 and 10 °C, there will be a single stable phase. With increasing temperature, the transmittance first decreases gently, then begins to drop sharply until the temperature reaches the cloud point temperature. If the temperature is continuously increased above the cloud point temperature, the solution becomes completely cloudy with micrometer-sized spherical droplets inside that can be detected by optical microscopy. This phenomenon is reversible upon cooling of the mixtures. Furthermore, when the separated coexisting phase is heated again, a new equilibrium tries to be reached in the sodium poly(styrene sulfonate) (NaPSS) and poly(diallyldimethylammonium chloride) (PDADMAC) system with the presence of NaCl.

For phase separation, the driving force can be increased by increasing the Bjerrum length or reducing the excluded volume parameter.[133] Indeed, the Bjerrum length is considered to be closely related to phase separation of electrostatic origin according to theoretical studies.

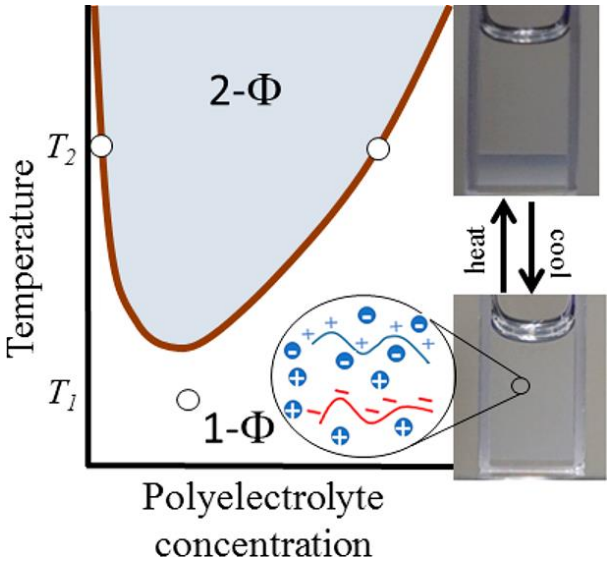

Figure 1-14. Lower Critical Solution Temperature Behavior in Polyelectrolyte Complex Coacervates obtained from KPSS/PDADMAB prepared at C_{Br}= 2.15M.[134]

Adhikari and Muthukumar also tried to give a possible theoretical explanation based on the mean field theory.[135] They reported that an increase in Bjerrum length with temperature can lead to electrostatic LCST; however, the temperature dependence of the Flory-Huggins interaction parameter and solvation effects must also be considered. From the analysis, the solvent dielectric constant and the temperature-dependent solvent-polymer interaction parameter can lead to the occurrence of complex coacervate phase behavior. And the LCST behavior can take place only in the case where the solvent dielectric constant decreases and the solvent-polymer interaction parameter increases with temperature. The theoretical approach they followed is as follows:

For the temperature dependence of the Bjerrum length $l_B(T)$, one can obtain:

$$l_B(T) = \frac{e^2}{4\pi\varepsilon_r(T)\varepsilon_0 k_B T} \qquad (1.13)$$

where e is the electronic charge, $\varepsilon_r(T)$ is the dielectric constant of the medium depend on temperature, ε_0 is the permittivity of vacuum, k_B is the Boltzmann constant and T is the absolute temperature.

If the medium is water, the temperature dependence of its dielectric constant $\varepsilon_r(T)$ can be empirically modeled by : add ref

$$\varepsilon_r(T) = 87.740 - 0.40008(T-273) + 9.398\times10^{-4}(T-273)^2$$
$$-1.410\times10^{-6}(T-273)^3 \qquad (1.14)$$

where ε(T) is a monotonically decreasing function of the absolute temperature (T).

Therefore, based on the relationship between these parameters, the dielectric constant $\varepsilon_r(T)$ in equation (1.14) will decrease with increasing temperature with a Bjerrum length $l_B(T)$ that will eventually increase with temperature.

This highlights the increase in the magnitude of the dipole-dipole interaction energy, which will favor the onset of LCST behavior at higher temperature leading to phase separation. On the contrary, if the magnitude of the dipole-dipole interaction energy increases with decreasing temperature, the upper critical solution temperature (UCST) behavior will tend to be induced.

The behavior of UCST-like phase and LCST-like transition was reported by Ye and Wu in PSSNa and PDADMAC PECs with the same salt concentration but different polymer concentration.[136] As shown in **Figure 1-15** (a)-(c), by adjusting the initial polymer concentrations, they experimentally observed UCST behavior with a gel-to-sol transition at about 9 °C for low polymer concentration and LCST behavior with a coil-to-globule transition at about 43 °C for high polymer concentration. The effects of hydration and cation-anion interactions were studied in depth by Raman spectroscopy. If the temperature is lower than UCST, the more hydrophobic polyelectrolyte chains can lead to a high proportion of contact ion pairs (CIPs) compared to solvent-separated ion pairs (SIPs). This was shown by monitoring the hydration state of the polymer chains at various temperatures as well as CIP and SIP peaks

by Raman spectroscopy. With increasing temperature, the dissociation of CIPs leads to a UCST-type solid-liquid phase transition that can be considered as a "CIPs-SIPs-free ions" transition corresponding to the dissociation of cation-anion interactions, as shown in **Figure 1-15** (d)-left.

While at higher concentrations of PECs, there are fewer hydrophobic polyelectrolyte chains due to greater solvation (hydration) caused by counterions, which indicates a lower ratio of CIPs to SIPs and leads to a LCST-like liquid-liquid phase transition that can be considered as "free ions-SIPs-CIPs" corresponding to the dehydration-induced association of the cation-anion interaction, as shown in **Figure 1-15** (d)-right. These results illustrate the influence of cation-anion interactions on the thermally sensitive phase transition at the molecular level in the formation of PECs and may provide a better understanding of the mechanism of PEC systems.

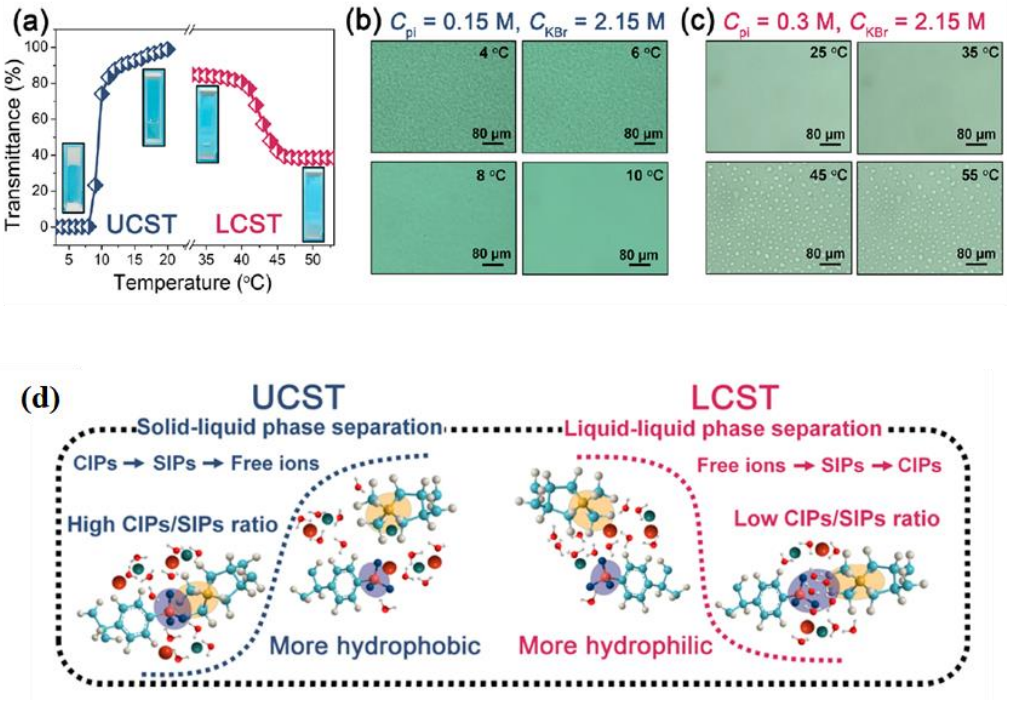

Figure 1-15. Turbidity changes of UCST and LCST behavior transitions in aqueous PSS/PDADMAC PEC solutions at 2.15 M KBr (a) and corresponding optical micrographs of both solutions (b, c). Schematic illustration of the phase transition mechanisms at different concentrations of PECs in 2.15 M KBr solutions during the heating process (d).[136]

In addition, the distinct contributions of electrostatic and hydrophobic interactions are also investigated on nanostructures composed of two oppositely charged diblock copolymers sharing a common heat-sensitive nonionic block pNIPAM.[137] The strength of electrostatic and hydrophobic interactions can be controlled by adjusting the ionic strength and changing the temperature. Micelles are formed with a coacervate core and a hydrated pNIPAM shell at low salt concentration and low temperature as shown in **Figure 1-16 A**. On the shell, there is always a chain of polyanions that can provide the negative charge. However, the structure of the shell will be changed with increasing temperature, resulting in increased interactions and weak local association of the polymer chains. In this case, the pNIPAM chains can be relatively concentrated by making a semi-diluted polymer solution, as shown in **Figure 1-16 B**. If the temperature is continuously increased above the LCST of pNIPAM, this leads to a strong association between the nanostructures, and a cluster structure can be formed with a hydrophobic core polyelectrolyte shell (pNIPAM) associated by electrostatic interaction, as shown in **Figure 1-16 C**.

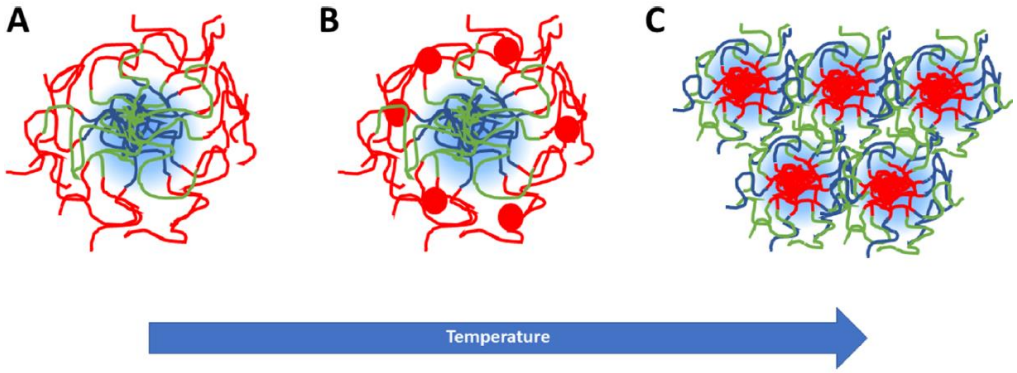

Figure 1-16. Schematic representation of the structure change due to temperature increase corresponding to the coacervate core and hydrated pNIPAM shell (A), the coacervate core and concentrated pNIPAM shell (B), and the cluster structure (C) symbolized by the polycation chain (blue segments), polyanion chain (green segments), and pNIPAM blocks (red segments). The red circles represent the local association of pNIPAM chains. [137]

1.2.2.3 PEs and PECS surface activity

In aqueous systems, polyelectrolyte complexes have already received increasing attention over the past several decades due to their many potential applications, including water treatment[138], paper making[139], cosmetics[140] and others. These properties can be associated with their adsorption ability at various interfaces, as we will show experimentally in Chapter 2.

B.A.Noskov and co-workers[141] reported about individual solutions of sodium poly(styrenesulfonate) (PSSNa) at different concentrations, the electrostatic interaction was examined after the addition of NaCl at different concentrations, which can lead to the acceleration of the first step of the adsorption process resulting in a decrease of the surface tension curves, but the surface tension equilibrium will take a long time (more than 5 hours), which is comparable to the results illustrated by Theodoly *et al.*[142] Furthermore, with the addition of oppositely charged surfactants or polyelectrolytes to varying concentrations of PSS solutions, the surface activity can be changed in an obvious way. Indeed, the surface tension of these complexes shows a significant decrease with increasing temperature and addition of salts at different concentrations of PSS, as shown in **Figure 1-17** on the PSS / benzyldimethylhexadecylammonium chloride (BAC) complex.

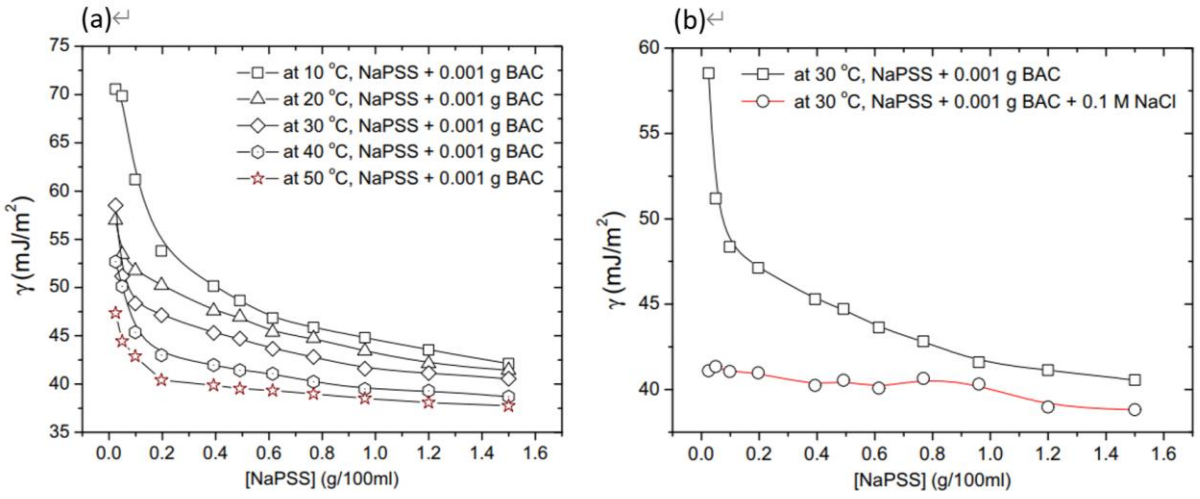

Figure 1-17. Surface tensions of NaPSS solutions at temperatures from 10 to 50 °C with a fixed added amount of BAC of 0.001 g (a). Surface tensions of aqueous solutions of NaPSS plus 0.001 g BAC at 30 °C without (open squares) and with (open circles) 0.1 NaCl added (b).[143]

1.2.3 Mean field theories: the Voorn–Overbeek model

Aqueous solutions of oppositely charged polyelectrolytes, when mixed under appropriate conditions (charge stoichiometry), can result in associative phase separation resulting in a dense polymer-rich coacervate phase in equilibrium with a surrounding polymer-poor phase comprising only the very dilute solution of one or both polymers. Bungenberg de Jong and H. R. Kruyt were the first to describe such a phenomenon almost a century ago on a system of gum arabic and gelatin, two natural polyampholytes.[85] Based on these results, Voorn and Overbeek (VO) were the first, in the late 1950s, to develop a mean field theory of this phase separation.[48, 53] This theory remains today the basic conceptual foundation of complex coacervation associated among other things with the origin of liquid-liquid phase coexistence phenomena in biology[144, 145].

The VO theory is anchored in the competition between the configurational entropy of charged polyions and electrostatic correlation attraction between them. The former is evaluated within the Flory-Huggins polymer mixing framework (FH), while the latter is based on the Debye-Hückel dilute electrolyte theory (DH). Various assumptions were made to keep this set of equations simple. The mixtures we are interested in consist of three components: a polymer salt P^+P^- composed of two equally long polyelectrolytes P^+ and P^- of length N and charge density σ= z/N (z the overall charge of the chains), a (simple) salt (for example NaCl) composed of two monovalent ions (Na^+ and Cl^-, with N = 1 and σ= 1) and water. The volume fractions of the polymer salt, salt, and water are φ_p, φ_s and (1 -φ_p -φ_s), respectively. $\varphi_i = a^3 N_i c_i$ with c_i the concentration of the PEs and the salt. The monomers, salt and water molecules are all assumed to have the same molecular volume, $v = a^3$ with a the size of the monomer. The rather simple total free energy per unit lattice site in k_{BT} units from both FH and DH contributions follows:

$$\frac{F_{total} a^3}{V k_{BT}} = f_{FH} + f_{DH} + \frac{1}{2}\sum_{i,j} \chi_{ij}\, \varphi_j \varphi_k$$

$$f_{FH} = \sum_i \sigma_i \varphi_i ln \varphi_i \text{ and } f_{DH} = -\alpha(\sum_i \sigma_i \varphi_i)^{3/2} = -\frac{(\kappa_D a)^3}{12\pi} \text{ and } \alpha = \frac{2}{3}\sqrt{\frac{\pi}{a^3}}\, l_B^{\frac{3}{2}} \qquad (1.15)$$

V is the total volume, κ_D^{-1} the Debye screening length, l_B the Bjerrum length. The χ_{ij}term describe the short-range interactions of non-electrostatic nature such as the van der Waals interactions, which is also frequently included in later formulations of the theory. f_{FH} and f_{DH} are the Flory-Hugging and Debye-Hückel free energies. A two-phase equilibrium is found when the two coexisting phases have a lower free energy than a homogeneous mixture of all components ($\Delta F = F_{p1} + F_{p2} - F_{mix} < 0$). The compositions of the coexisting phases can be derived from the equality of the electrochemical potentials of all components in the two phases: $(\mu_i \pm z_i\psi)_1 = (\mu_i \pm z_i\psi)_2$. For equal lengths and charge densities of both polymers, the electrostatic potential difference between both phases must be zero: $\Delta\psi = 0$. This approach can be further simplified by assuming that the salt concentrations in the two phases are nearly equal. In that case, the binodal compositions can be found from a common tangent construction in the graph of free energy versus polymer volume fraction. The spinodes can be obtained numerically from ($\frac{\partial^2 F}{\partial \varphi^2} = 0$). The binodal points are extracted from the condition of equal tangents using the first derivative of the free energy. Finally, the critical point can be derived from the ($\frac{\partial^3 F}{\partial \varphi^3} = 0$) condition.

Spruijt *and al* [146] were able recently to quantitatively describe all experimentally aspects of the associative phase separation in the PAA and PDMAEMA (poly(N,N-dimethylaminoethyl methacrylate)) system using α=0.9 and the experimentally known chain lengths and charge densities of both PEs as illustrated in **Figure 1-18**. Their results show that the VO model can be applied successfully to associative phase separation of strongly charged flexible polyelectrolytes, as long as the salt concentration is high to ensure that high surface potentials are strongly screened and the complexation is reversible.

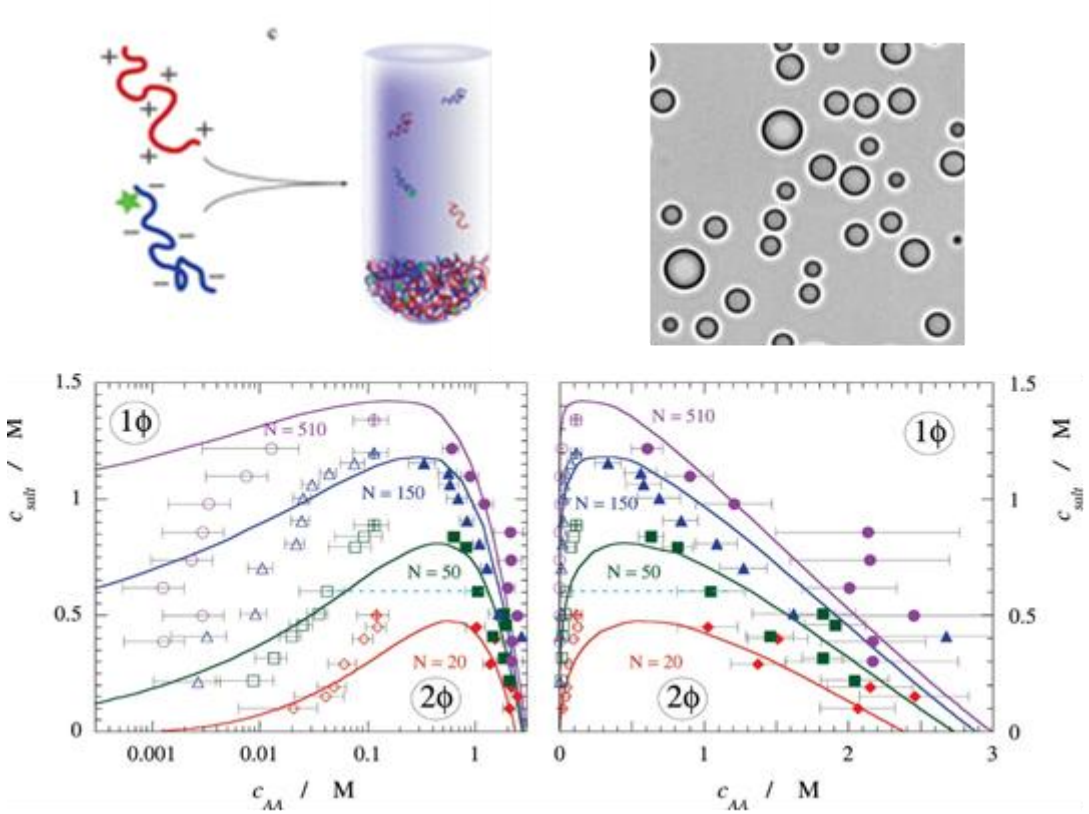

Figure 1-18. (Upper Left) Schematic illustration of the PAA/PDMAEMA two-phase system after the macroscopic phase separation. (Upper Right) Optical microscopy image of the mixture right after the associative liquid-liquid phase transition generating polymer-rich droplets surrounded by a polymer-poor continuum phase. (Bottom) Salt-polymer phase diagram for associative phase separation between PAA and PDMAEMA at pH 6.5 (σ= 0.95) on a logarithmic scale (left) and a linear scale (right) of polymer concentrations. Symbols indicate experimentally measured binodal compositions of the coexisting phases. Crossed symbols indicate lowest salt concentrations for which phase separation was no longer observed. Solid lines are theoretical predictions of the phase behavior based on the VO model. The dotted lines are examples of tie lines.[146]

1.3 Conclusions

As we have just seen, polyelectrolytes in all their forms (hydrophobic, hydrophilic, amphiphilic...) are macromolecules that combine the properties of neutral polymers and those of charged entities. These characteristics give them unique behaviors and properties such as their ability to form spontaneously, by mixing two polyelectrolytes of different charge, complexes in solution and at interfaces (mainly) by electrostatic interactions. These complexes are of great interest in many scientific, technological and industrial fields and their properties depend on the physicochemical nature of the charged chains, but also on the conditions of implementation and formation, or in other words, how they are brought into intimate contact. Even if many results have been reported for several decades, the understanding of some complexation mechanisms such as coacervation and the influence of the interaction intensity on the structure and properties of some PECs still needs to be deepened and rationalized.

References

[1] Barrat, J.-L. and F.o. Joanny, *Theory of Polyelectrolyte Solutions*, in *Advances in Chemical Physics*. 1996. p. 1-66.

[2] Dobrynin, A. and M. Rubinstein, *Theory of polyelectrolytes in solutions and at surfaces.* Progress in Polymer Science, 2005. **30**(11): p. 1049-1118.

[3] Sugai, S. and G. Ebert, *Conformations of hydrophobic polyelectrolytes.* Advances in Colloid and Interface Science, 1985. **24**: p. 247-282.

[4] Kogej, K., *Thermodynamic Analysis of the Conformational Transition in Aqueous Solutions of Isotactic and Atactic Poly(Methacrylic Acid) and the Hydrophobic Effect.* Polymers (Basel), 2016. **8**(5).

[5] Thünemann, A.F., et al., *Polyelectrolyte Complexes*, in *Polyelectrolytes with Defined Molecular Architecture II*. 2004. p. 113-171.

[6] Hoagland, D.A., E. Arvanitidou, and C. Welch, *Capillary Electrophoresis Measurements of the Free Solution Mobility for Several Model Polyelectrolyte Systems.* Macromolecules, 1999. **32**(19): p. 6180-6190.

[7] Stellwagen, E., Lu, and N.C. Stellwagen, *Unified Description of Electrophoresis and Diffusion for DNA and Other Polyions.* Biochemistry, 2003. **42**(40): p. 11745-11750.

[8] Fischer, S., A. Naji, and R.R. Netz, *Salt-induced counterion-mobility anomaly in polyelectrolyte electrophoresis.* Phys Rev Lett, 2008. **101**(17): p. 176103.

[9] Prabhu, V.M., et al., *Counterion associative behavior with flexible polyelectrolytes.* The Journal of Chemical Physics, 2004. **121**(9): p. 4424-4429.

[10] Prabhu, V.M., *Counterion structure and dynamics in polyelectrolyte solutions.* Current Opinion in Colloid & Interface Science, 2005. **10**(1): p. 2-8.

[11] Truzzolillo, D., et al., *Counterion condensation of differently flexible polyelectrolytes in aqueous solutions in the dilute and semidilute regime.* Physical Review E, 2009. **79**(1): p. 011804.

[12] Schipper, F.J.M., J.G. Hollander, and J.C. Leyte, *Counterion self-diffusion in polyelectrolyte solutions.* Journal of Physics: Condensed Matter, 1997. **9**(50): p. 11179-11193.

[13] Bordi, F., et al., *Determination of Polyelectrolyte Charge and Interaction with Water Using Dielectric Spectroscopy.* Macromolecules, 2002. **35**(18): p. 7031-7038.

[14] Popov, A. and D.A. Hoagland, *Electrophoretic evidence for a new type of counterion condensation.* Journal of Polymer Science Part B: Polymer Physics, 2004. **42**(19): p. 3616-3627.

[15] Essafi, W., et al., *Anomalous counterion condensation in salt-free hydrophobic polyelectrolyte solutions: Osmotic pressure measurements.* EPL (Europhysics Letters), 2005. **71**(6): p. 938.

[16] Hinderberger, D., H.W. Spiess, and G. Jeschke, *Radial counterion distributions in polyelectrolyte solutions determined by EPR spectroscopy.* EPL (Europhysics Letters), 2005. **70**(1): p. 102.

[17] Jia, P., et al., *Dynamic exchange of counterions of polystyrene sulfonate.* The Journal of chemical physics, 2012. **136**(8): p. 084904.

[18] Grosberg, A.Y. and A.R. Khokhlov, *Giant Molecules*. 2010: WORLD SCIENTIFIC. 348.

[19] Tadmor, R., et al., *Debye Length and Double-Layer Forces in Polyelectrolyte Solutions.* Macromolecules, 2002. **35**(6): p. 2380-2388.

[20] Harris, F.E. and S.A.J.T.J.o.P.C. Rice, *A chain model for polyelectrolytes. I.* The Journal of Physical Chemistry, 1954. **58**(9): p. 725-732.
[21] Nagarajan, R., *Thermodynamics of nonionic polymer—micelle association.* Colloids and Surfaces, 1985. **13**: p. 1-17.
[22] Norwood, D.P., E. Minatti, and W.F. Reed, *Surfactant/Polymer Assemblies. 1. Surfactant Binding Properties.* Macromolecules, 1998. **31**(9): p. 2957-2965.
[23] Manning, G.S., *Limiting Laws and Counterion Condensation in Polyelectrolyte Solutions I. Colligative Properties.* The Journal of Chemical Physics, 1969. **51**(3): p. 924-933.
[24] Manning, G.S., *Limiting Laws and Counterion Condensation in Polyelectrolyte Solutions II. Self-Diffusion of the Small Ions.* The Journal of Chemical Physics, 1969. **51**(3): p. 934-938.
[25] Wall, F.T. and P.F. Grieger, *Theory of Ion Exchange for Polyelectrolytes Undergoing Electrolytic Transference.* The Journal of Chemical Physics, 1952. **20**(8): p. 1200-1206.
[26] Luo, T. and G. Chen, *Nanoscale heat transfer – from computation to experiment.* Physical Chemistry Chemical Physics, 2013. **15**(10): p. 3389-3412.
[27] Kim, G.-H., et al., *High thermal conductivity in amorphous polymer blends by engineered interchain interactions.* Nature Materials, 2015. **14**(3): p. 295-300.
[28] Wei, X., T. Zhang, and T. Luo, *Chain conformation-dependent thermal conductivity of amorphous polymer blends: the impact of inter- and intra-chain interactions.* Physical Chemistry Chemical Physics, 2016. **18**(47): p. 32146-32154.
[29] Lu, T., et al., *Thermal transport in semicrystalline polyethylene by molecular dynamics simulation.* Journal of Applied Physics, 2018. **123**(1): p. 015107.
[30] Bisri, S.Z., et al., *Endeavor of iontronics: from fundamentals to applications of ion-controlled electronics.* Advanced Materials, 2017. **29**(25): p. 1607054.
[31] Liu, W., et al., *Enhancing ionic conductivity in composite polymer electrolytes with well-aligned ceramic nanowires.* Nature Energy, 2017. **2**(5): p. 17035.
[32] Huang, Q., et al., *Cycle stability of conversion-type iron fluoride lithium battery cathode at elevated temperatures in polymer electrolyte composites.* Nature Materials, 2019. **18**(12): p. 1343-1349.
[33] Huang, Y., et al., *A self-healable and highly stretchable supercapacitor based on a dual crosslinked polyelectrolyte.* Nature Communications, 2015. **6**(1): p. 10310.
[34] Berezney, J.P. and O.A. Saleh, *Electrostatic Effects on the Conformation and Elasticity of Hyaluronic Acid, a Moderately Flexible Polyelectrolyte.* Macromolecules, 2017. **50**(3): p. 1085-1089.
[35] Shanker, A., et al., *High thermal conductivity in electrostatically engineered amorphous polymers.* Science Advances, 2017. **3**(7): p. e1700342.
[36] Kawagoe, Y., et al., *Molecular dynamics study on thermal energy transfer in bulk polyacrylic acid.* AIP Advances, 2019. **9**(2): p. 025302.
[37] Wong, J.E., et al., *Specific Ion versus Electrostatic Effects on the Construction of Polyelectrolyte Multilayers.* Langmuir, 2009. **25**(24): p. 14061-14070.
[38] Yu, J., et al., *Structure of Polyelectrolyte Brushes in the Presence of Multivalent Counterions.* Macromolecules, 2016. **49**(15): p. 5609-5617.
[39] Brettmann, B., P. Pincus, and M. Tirrell, *Lateral Structure Formation in Polyelectrolyte Brushes Induced by Multivalent Ions.* Macromolecules, 2017. **50**(3): p. 1225-1235.
[40] Wei, X., R. Ma, and T. Luo, *Thermal Conductivity of Polyelectrolytes with Different Counterions.* The Journal of Physical Chemistry C, 2020. **124**(8): p. 4483-4488.

[41] Muthukumar, M., *Theory of counter-ion condensation on flexible polyelectrolytes: Adsorption mechanism.* The Journal of Chemical Physics, 2004. **120**(19): p. 9343-9350.
[42] Zheng, K., et al., *Counterion Cloud Expansion of a Polyelectrolyte by Dilution.* Macromolecules, 2018. **51**(12): p. 4444-4450.
[43] Zhao, J., *Studying the physics of charged macromolecules by single molecule fluorescence spectroscopy.* The Journal of Chemical Physics, 2020. **153**(17): p. 170903.
[44] Shi, Y., et al., *Counterion Binding Dynamics of a Polyelectrolyte.* Macromolecules, 2021. **54**(10): p. 4926-4933.
[45] Kuhn, W., O. Künzle, and A. Katchalsky, *Verhalten polyvalenter Fadenmolekelionen in Lösung.* Helvetica Chimica Acta, 1948. **31**(7): p. 1994-2037.
[46] Ōsawa, F., N. Imai, and I. Kagawa, *Theory of strong polyelectrolyte solutions. I. Coiled macro ions.* Journal of Polymer Science, 1954. **13**(68): p. 93-111.
[47] Schönhoff, M., *Layered polyelectrolyte complexes: physics of formation and molecular properties.* Journal of Physics: Condensed Matter, 2003. **15**(49): p. R1781-R1808.
[48] Overbeek, J.T. and M.J. Voorn, *Phase separation in polyelectrolyte solutions; theory of complex coacervation.* J Cell Physiol Suppl, 1957. **49**(Suppl 1): p. 7-22; discussion, 22-6.
[49] De Gennes, P.G., et al., *Remarks on polyelectrolyte conformation.* Journal de physique, 1976. **37**(12): p. 1461-1473.
[50] De Gennes, P.-G., *Scaling concepts in polymer physics*. 1979: Cornell university press.
[51] P.M, V., O. Bayraktar, and G. Picó, *Polyelectrolytes: Thermodynamics and Rheology*. 2014.
[52] Bekturov, E.A. and L.A. Bimendina. *Interpolymer complexes*. in *Speciality Polymers*. 1981. Berlin, Heidelberg: Springer Berlin Heidelberg.
[53] Michaeli, I., J.T.G. Overbeek, and M.J. Voorn, *Phase separation of polyelectrolyte solutions.* Journal of Polymer Science, 1957. **23**(103): p. 443-450.
[54] Schlenoff, J.B., A.H. Rmaile, and C.B. Bucur, *Hydration contributions to association in polyelectrolyte multilayers and complexes: Visualizing hydrophobicity.* Journal of the American Chemical Society, 2008. **130**(41): p. 13589-13597.
[55] Thünemann, A.F., *Polyelectrolyte–surfactant complexes (synthesis, structure and materials aspects).* Progress in Polymer Science, 2002. **27**(8): p. 1473-1572.
[56] Peng, B. and M. Muthukumar, *Modeling competitive substitution in a polyelectrolyte complex.* The Journal of chemical physics, 2015. **143**(24): p. 243133.
[57] Lueckheide, M., et al., *Structure–property relationships of oligonucleotide polyelectrolyte complex micelles.* Nano letters, 2018. **18**(11): p. 7111-7117.
[58] Rathee, V.S., et al., *Role of associative charging in the entropy–energy balance of polyelectrolyte complexes.* Journal of the American Chemical Society, 2018. **140**(45): p. 15319-15328.
[59] Schlenoff, J.B., et al., *Ion Content of Polyelectrolyte Complex Coacervates and the Donnan Equilibrium.* Macromolecules, 2019. **52**(23): p. 9149-9159.
[60] Shaheen, S.A., et al., *Water and ion transport through the glass transition in polyelectrolyte complexes.* Chemistry of Materials, 2020. **32**(14): p. 5994-6002.
[61] Neitzel, A.E., et al., *Polyelectrolyte complex coacervation across a broad range of charge densities.* Macromolecules, 2021. **54**(14): p. 6878-6890.
[62] Subbotin, A.V. and A.N. Semenov, *The structure of polyelectrolyte complex coacervates and multilayers.* Macromolecules, 2021. **54**(3): p. 1314-1328.

[63] Bertrand, P., et al., *Ultrathin polymer coatings by complexation of polyelectrolytes at interfaces: suitable materials, structure and properties.* Macromolecular rapid communications, 2000. **21**(7): p. 319-348.

[64] Kötz, J., S. Kosmella, and T. Beitz, *Self-assembled polyelectrolyte systems.* Progress in Polymer Science, 2001. **26**(8): p. 1199-1232.

[65] Antonietti, M., J. Conrad, and A. Thuenemann, *Polyelectrolyte-surfactant complexes: a new type of solid, mesomorphous material.* Macromolecules, 1994. **27**(21): p. 6007-6011.

[66] Hayakawa, K. and J.C.T. Kwak, *Surfactant-polyelectrolyte interactions. 1. Binding of dodecyltrimethylammonium ions by sodium dextransulfate and sodium poly (styrenesulfonate) in aqueous solution in the presence of sodium chloride.* The Journal of Physical Chemistry, 1982. **86**(19): p. 3866-3870.

[67] Hayakawa, K. and J.C.T. Kwak, *Study of surfactant-polyelectrolyte interactions. 2. Effect of multivalent counterions on the binding of dodecyltrimethylammonium ions by sodium dextran sulfate and sodium poly (styrene sulfonate) in aqueous solution.* The Journal of Physical Chemistry, 1983. **87**(3): p. 506-509.

[68] Philipp, B., W. Dawydoff, and K.J. Linow, *Polyelektrolytkomplexe—Bildungsweise, Struktur und Anwendungsmöglichkeiten.* Zeitschrift für chemie, 1982. **22**(1): p. 1-13.

[69] Zezin, A.B. and V.A. Kabanov, *A new class of complex water-soluble polyelectrolytes.* Russian Chemical Reviews, 1982. **51**(9): p. 833.

[70] Kabanov, V.A. and A.B. Zezin, *Soluble interpolymeric complexes as a new class of synthetic polyelectrolytes.* Pure and applied chemistry, 1984. **56**(3): p. 343-354.

[71] Tsuchida, E., Y. Osada, and H. Ohno, *Formation of interpolymer complexes.* Journal of Macromolecular Science, Part B: Physics, 1980. **17**(4): p. 683-714.

[72] Tsuchida, E. and K. Abe, *Interactions between macromolecules in solution and intermacromolecular complexes.* Interactions between macromolecules in solution and intermacromolecular complexes, 1982: p. 1-119.

[73] Michaels, A.S., *Polyelectrolyte complexes.* Industrial & Engineering Chemistry, 1965. **57**(10): p. 32-40.

[74] Philipp, B., et al., *Polyelectrolyte complexes—recent developments and open problems.* Progress in Polymer Science, 1989. **14**(1): p. 91-172.

[75] Liu, X., et al., *Early stage kinetics of polyelectrolyte complex coacervation monitored through stopped-flow light scattering.* Soft Matter, 2016. **12**(44): p. 9030-9038.

[76] Liu, X., J.-P. Chapel, and C. Schatz, *Structure, thermodynamic and kinetic signatures of a synthetic polyelectrolyte coacervating system.* Advances in colloid and interface science, 2017. **239**: p. 178-186.

[77] Liu, X., et al., *Early stage kinetics of polyelectrolyte complex coacervation monitored through stopped-flow light scattering.* Soft Matter, 2016. **12**(44): p. 9030-9038.

[78] Liu, X., J.P. Chapel, and C. Schatz, *Structure, thermodynamic and kinetic signatures of a synthetic polyelectrolyte coacervating system.* Adv Colloid Interface Sci, 2017. **239**: p. 178-186.

[79] Zhao, H., et al., *Cement proteins of the tube-building polychaete Phragmatopoma californica.* Journal of Biological Chemistry, 2005. **280**(52): p. 42938-42944.

[80] De Vries, R., *DNA condensation in bacteria: Interplay between macromolecular crowding and nucleoid proteins.* Biochimie, 2010. **92**(12): p. 1715-1721.

[81] Widom, J., *Structure, dynamics, and function of chromatin in vitro.* Annual review of biophysics and biomolecular structure, 1998. **27**(1): p. 285-327.

[82] Zaitsev, S.Y., et al., *General approach for lipases immobilization in polyelectrolyte complexes.* Colloids and Surfaces A: Physicochemical and Engineering Aspects, 2003. **221**(1-3): p. 209-220.
[83] Sokolova, E., et al., *Enhanced transcription rates in membrane-free protocells formed by coacervation of cell lysate.* Proceedings of the National Academy of Sciences, 2013. **110**(29): p. 11692-11697.
[84] Lindhoud, S. and M.M.A.E. Claessens, *Accumulation of small protein molecules in a macroscopic complex coacervate.* Soft Matter, 2016. **12**(2): p. 408-413.
[85] Bungenberg de Jong, H.G. and H.R. Kruyt. *Coacervation (partial miscibility in colloid systems)*. 1929.
[86] Veis, A. and C. Aranyi, *Phase separation in polyelectrolyte systems. I. Complex coacervates of gelatin.* The Journal of Physical Chemistry, 1960. **64**(9): p. 1203-1210.
[87] Weinbreck, F., et al., *Complex coacervation of whey proteins and gum arabic.* Biomacromolecules, 2003. **4**(2): p. 293-303.
[88] Chollakup, R., et al., *Phase behavior and coacervation of aqueous poly (acrylic acid)–poly (allylamine) solutions.* Macromolecules, 2010. **43**(5): p. 2518-2528.
[89] Kayitmazer, A.B., et al., *Protein–polyelectrolyte interactions.* Soft Matter, 2013. **9**(9): p. 2553-2583.
[90] Priftis, D., et al., *Complex coacervation of poly (ethylene-imine)/polypeptide aqueous solutions: Thermodynamic and rheological characterization.* Journal of colloid and interface science, 2013. **398**: p. 39-50.
[91] Kim, H.J., et al., *Precise engineering of siRNA delivery vehicles to tumors using polyion complexes and gold nanoparticles.* ACS nano, 2014. **8**(9): p. 8979-8991.
[92] Park, J.I., et al., *Terminal supraparticle assemblies from similarly charged protein molecules and nanoparticles.* Nature communications, 2014. **5**(1): p. 1-9.
[93] Decher, G., *Fuzzy nanoassemblies: toward layered polymeric multicomposites.* science, 1997. **277**(5330): p. 1232-1237.
[94] Harada, A. and K. Kataoka, *Chain length recognition: core-shell supramolecular assembly from oppositely charged block copolymers.* Science, 1999. **283**(5398): p. 65-67.
[95] Johnston, A.P.R., et al., *Layer-by-layer engineered capsules and their applications.* Current opinion in colloid & interface science, 2006. **11**(4): p. 203-209.
[96] Koide, A., et al., *Semipermeable polymer vesicle (PICsome) self-assembled in aqueous medium from a pair of oppositely charged block copolymers: physiologically stable micro-/nanocontainers of water-soluble macromolecules.* Journal of the American Chemical Society, 2006. **128**(18): p. 5988-5989.
[97] Capito, R.M., et al., *Self-assembly of large and small molecules into hierarchically ordered sacs and membranes.* Science, 2008. **319**(5871): p. 1812-1816.
[98] Yan, Y., et al., *Spherocylindrical coacervate core micelles formed by a supramolecular coordination polymer and a diblock copolymer.* Soft Matter, 2008. **4**(11): p. 2207-2212.
[99] Lemmers, M., et al., *Multiresponsive reversible gels based on charge-driven assembly.* Angewandte Chemie, 2010. **122**(4): p. 720-723.
[100] Ma, G., et al., *Hyaluronic acid/chitosan polyelectrolyte complexes nanofibers prepared by electrospinning.* Materials Letters, 2012. **74**: p. 78-80.
[101] van der Kooij, H.M., et al., *On the stability and morphology of complex coacervate core micelles: From spherical to wormlike micelles.* Langmuir, 2012. **28**(40): p. 14180-14191.

[102] Krogstad, D.V., et al., *Effects of polymer and salt concentration on the structure and properties of triblock copolymer coacervate hydrogels.* Macromolecules, 2013. **46**(4): p. 1512-1518.
[103] Boas, M., et al., *Electrospinning polyelectrolyte complexes: pH-responsive fibers.* Soft Matter, 2015. **11**(9): p. 1739-1747.
[104] Stewart, R.J., C.S. Wang, and H. Shao, *Complex coacervates as a foundation for synthetic underwater adhesives.* Advances in colloid and interface science, 2011. **167**(1-2): p. 85-93.
[105] Kataoka, K., A. Harada, and Y. Nagasaki, *Block copolymer micelles for drug delivery: design, characterization and biological significance.* Advanced drug delivery reviews, 2012. **64**: p. 37-48.
[106] Cui, H., et al., *High performance and reversible ionic polypeptide hydrogel based on charge-driven assembly for biomedical applications.* Acta biomaterialia, 2015. **11**: p. 183-190.
[107] Chollakup, R., et al., *Polyelectrolyte molecular weight and salt effects on the phase behavior and coacervation of aqueous solutions of poly (acrylic acid) sodium salt and poly (allylamine) hydrochloride.* Macromolecules, 2013. **46**(6): p. 2376-2390.
[108] Antonietti, M., C. Burger, and J. Effing, *Mesomorphous polyelectrolyte-surfactant complexes.* Advanced Materials, 1995. **7**(8): p. 751-753.
[109] Antonietti, M. and M. Maskos, *Fine-tuning of phase structures and thermoplasticity of polyelectrolyte− surfactant complexes: Copolymers of ionic monomers with N-alkylacrylamides.* Macromolecules, 1996. **29**(12): p. 4199-4205.
[110] Nizri, G. and S. Magdassi, *Solubilization of hydrophobic molecules in nanoparticles formed by polymer–surfactant interactions.* Journal of colloid and interface science, 2005. **291**(1): p. 169-174.
[111] Vieregg, J.R., et al., *Oligonucleotide–peptide complexes: phase control by hybridization.* Journal of the American Chemical Society, 2018. **140**(5): p. 1632-1638.
[112] Bock, J., et al., *Macromolecular complexes in chemistry and biology.* Springer-Verlag GmbH & Co., Berlin, 1994: p. 33.
[113] Radeva, T., *Physical chemistry of polyelectrolytes*. Vol. 99. 2001: CRC Press.
[114] Czichocki, G., et al., *New and effective entrapment of polyelectrolyte-enzyme-complexes in LentiKats.* Biotechnology letters, 2001. **23**(16): p. 1303-1307.
[115] Kabanov, A.V., P.L. Felgner, and L.W. Seymour, *Self-assembling complexes for gene delivery.* From laboratory to clinical trial, 1998: p. 197-218.
[116] Wolfert, M.A., et al., *Polyelectrolyte vectors for gene delivery: influence of cationic polymer on biophysical properties of complexes formed with DNA.* Bioconjugate chemistry, 1999. **10**(6): p. 993-1004.
[117] Vinogradov, S.V., T.K. Bronich, and A.V. Kabanov, *Self-Assembly of Polyamine− Poly (ethylene glycol) Copolymers with Phosphorothioate Oligonucleotides.* Bioconjugate chemistry, 1998. **9**(6): p. 805-812.
[118] Bronich, T., A.V. Kabanov, and L.A. Marky, *A thermodynamic characterization of the interaction of a cationic copolymer with DNA.* The Journal of Physical Chemistry B, 2001. **105**(25): p. 6042-6050.
[119] Dautzenberg, H., *Polyelectrolyte complex formation in highly aggregating systems. 1. Effect of salt: polyelectrolyte complex formation in the presence of NaCl.* Macromolecules, 1997. **30**(25): p. 7810-7815.

[120] Dautzenberg, H. and N. Karibyants, *Polyelectrolyte complex formation in highly aggregating systems. Effect of salt: response to subsequent addition of NaCl.* Macromolecular Chemistry and Physics, 1999. **200**(1): p. 118-125.

[121] Wang, Q. and J.B. Schlenoff, *The polyelectrolyte complex/coacervate continuum.* Macromolecules, 2014. **47**(9): p. 3108-3116.

[122] Ghostine, R.A., R.F. Shamoun, and J.B. Schlenoff, *Doping and diffusion in an extruded saloplastic polyelectrolyte complex.* Macromolecules, 2013. **46**(10): p. 4089-4094.

[123] Spruijt, E., et al., *Structure and dynamics of polyelectrolyte complex coacervates studied by scattering of neutrons, X-rays, and light.* Macromolecules, 2013. **46**(11): p. 4596-4605.

[124] Salehi, A. and R.G. Larson, *A molecular thermodynamic model of complexation in mixtures of oppositely charged polyelectrolytes with explicit account of charge association/dissociation.* Macromolecules, 2016. **49**(24): p. 9706-9719.

[125] Sing, C.E., *Development of the modern theory of polymeric complex coacervation.* Advances in colloid and interface science, 2017. **239**: p. 2-16.

[126] Kudlay, A., A.V. Ermoshkin, and M. Olvera de La Cruz, *Complexation of oppositely charged polyelectrolytes: effect of ion pair formation.* Macromolecules, 2004. **37**(24): p. 9231-9241.

[127] Jha, P.K., et al., *pH and salt effects on the associative phase separation of oppositely charged polyelectrolytes.* Polymers, 2014. **6**(5): p. 1414-1436.

[128] Ali, S. and V.M. Prabhu, *Relaxation Behavior by Time-Salt and Time-Temperature Superpositions of Polyelectrolyte Complexes from Coacervate to Precipitate.* Gels, 2018. **4**(1): p. 11.

[129] Shibayama, M. and T. Tanaka, *Volume phase transition and related phenomena of polymer gels.* Responsive gels: volume transitions I, 1993: p. 1-62.

[130] Beltran, S., et al., *Swelling equilibria for weakly ionizable, temperature-sensitive hydrogels.* Macromolecules, 1991. **24**(2): p. 549-551.

[131] Lee, W.F. and C.H. Hsu, *Thermoreversible hydrogel. V. Synthesis and swelling behavior of the N-isopropylacrylamide-co-trimethyl methacryloyloxyethyl ammonium iodide copolymeric hydrogels.* Journal of applied polymer science, 1998. **69**(9): p. 1793-1803.

[132] Dautzenberg, H., Y. Gao, and M. Hahn, *Formation, structure, and temperature behavior of polyelectrolyte complexes between ionically modified thermosensitive polymers.* Langmuir, 2000. **16**(23): p. 9070-9081.

[133] Zhang, P., et al., *Polyelectrolyte complex coacervation: Effects of concentration asymmetry.* The Journal of chemical physics, 2018. **149**(16): p. 163303.

[134] Ali, S., M. Bleuel, and V.M. Prabhu, *Lower critical solution temperature in polyelectrolyte complex coacervates.* ACS macro letters, 2019. **8**(3): p. 289-293.

[135] Adhikari, S., V.M. Prabhu, and M. Muthukumar, *Lower critical solution temperature behavior in polyelectrolyte complex coacervates.* Macromolecules, 2019. **52**(18): p. 6998-7004.

[136] Ye, Z., S. Sun, and P. Wu, *Distinct Cation–Anion Interactions in the UCST and LCST Behavior of Polyelectrolyte Complex Aqueous Solutions.* ACS Macro Letters, 2020. **9**(7): p. 974-979.

[137] Fehér, B., et al., *Effect of temperature and ionic strength on micellar aggregates of oppositely charged thermoresponsive block copolymer polyelectrolytes.* Langmuir, 2019. **35**(42): p. 13614-13623.

[138] Wilts, E.M., J. Herzberger, and T.E. Long, *Addressing water scarcity: cationic polyelectrolytes in water treatment and purification.* Polymer International, 2018. **67**(7): p. 799-814.
[139] Schnell, C.N., et al., *Polyelectrolyte complexes for assisting the application of lignocellulosic micro/nanofibers in papermaking.* Cellulose, 2018. **25**(10): p. 6083-6092.
[140] Llamas, S., et al., *Adsorption of polyelectrolytes and polyelectrolytes-surfactant mixtures at surfaces: a physico-chemical approach to a cosmetic challenge.* Advances in Colloid and Interface Science, 2015. **222**: p. 461-487.
[141] Noskov, B.A., et al., *Dynamic surface properties of sodium poly (styrenesulfonate) solutions.* Macromolecules, 2004. **37**(7): p. 2519-2526.
[142] Theodoly, O., R. Ober, and C.E. Williams, *Adsorption of hydrophobic polyelectrolytes at the air/water interface: Conformational effect and history dependence.* The European Physical Journal E, 2001. **5**(1): p. 51-58.
[143] Owiwe, M.T., A.H. Ayyad, and F.M. Takrori, *Surface tension of the oppositely charged sodium poly (styrene sulfonate)/benzyldimethylhexadecylammonium chloride and sodium poly (styrene sulfonate)/polyallylamine hydrochloride mixtures.* Colloid and Polymer Science, 2020. **298**(9): p. 1197-1204.
[144] Brangwynne, C.P., P. Tompa, and R.V. Pappu, *Polymer physics of intracellular phase transitions.* Nature Physics, 2015. **11**(11): p. 899-904.
[145] Perry, S.L., *Phase separation: Bridging polymer physics and biology.* Current Opinion in Colloid & Interface Science, 2019. **39**: p. 86-97.
[146] Spruijt, E., et al., *Binodal Compositions of Polyelectrolyte Complexes.* Macromolecules, 2010. **43**(15): p. 6476-6484.

Chapter 2

Interfacial tension in polyelectrolyte complexes

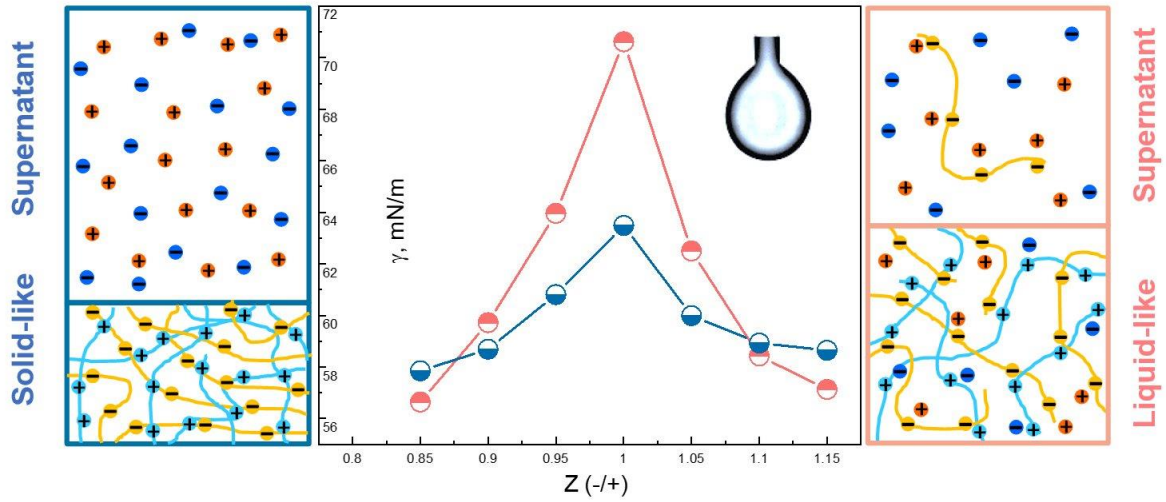

Abstract: We systematically investigate in this work, the surface activity of polyelectrolyte complex (PECs) suspensions as a function of the molar charge ratio Z (= [-]/[+]) from two model systems: the weakly and strongly interacting poly (diallyldimethylammonium chloride) / poly (acrylic acid sodium salt) (PDADMAC/PANa) and poly (diallyldimethylammonium chloride) /poly (sodium 4- styrenesulfonate) (PDADMAC/PSSNa) pairs respectively. For both systems, the PEC surface tension decreases as the system approaches charge stoichiometry (Z=1) whenever the complexation occurs in the presence of excess PDADMAC (Z < 1) or excess polyanion (Z > 1) consistent with an increased level of charge neutralization of PEs forming increasingly hydrophobic and neutral surface-active species. The behavior at stoichiometry (Z=1) is also particularly informative about the physical nature of the complexes. The PDADMAC/PANa system undergoes a liquid-liquid phase transition through the formation of coacervate microdroplets in equilibrium with macroions remaining in solution. In the PDADMAC/PSSNa system, the surface tension of the supernatant was close to that of pure water, suggesting that the PSSNa-based complexes have completely sedimented, consistent with a complete liquid-solid phase separation of an out-of-equilibrium system. Besides, the high sensitivity of surface tension measurements, which can detect the presence of trace

amounts of aggregates and other precursors in the supernatant allows for very accurate determination of the exact charge stoichiometry of the complexes. Finally, the very low water/water interfacial tension that develops between the dilute phase and the denser coacervate phase in the PDADAMAC/PANa system was measured using the generalized Young-Laplace method to complete the full characterization of both systems. The overall study showed that simple surface tension measurements can be a very sensitive tool to characterize, discriminate and better understand the formation mechanism of the different structures encountered during the formation of PECs.

Keywords: polyelectrolyte complexes; complex coacervates; liquid-liquid and liquid-solid transition; surface tension; pendant drop; interfacial tension.

2.1 Introduction

The complexation of oppositely charged polyelectrolytes (PEs) in aqueous solutions is a widespread associative process found in natural and man-made systems which takes place through mainly cooperative electrostatic interactions. Complementary interactions like short-range hydrogen-bonding or long-range hydrophobic effect can also participate in the complexation process. Such PE complexes or PECs have endless applications in different technological fields ranging from water treatment [1], paper making [2] and food industry [3] to pharmaceuticals [4], cosmetics [5], tissue engineering [6] and biomedicine [7]. The formation of PECs involves two distinct steps: the generation of primary PECs by ion pairing, followed by their aggregation/reorganization into larger structures [8]. At stoichiometry, when the amount of anionic and cationic charges are equal, two very different situations can occur depending on the intensity of the interaction. When the charged chains are strongly interacting (binding constant k_b>10^6 M^{-1}) the system undergoes a liquid-solid transition generating aggregates that eventually sediment with time as in the case of the PDADMAC/PSSNa system [9, 10]. When the interaction is weaker, the system undergoes a liquid-liquid phase transition generating highly hydrated and dense coacervate droplets in equilibrium with the surrounding continuous phase depleted in macromolecules as in the PDADMAC/PANa system (k_b ~10^3-10^4 M^{-1}) [11-13]. *Off* the stoichiometry, colloidal polyelectrolyte complexes are formed with a solvation, charge, hydrophobicity that vary with the molar charge ratio Z ([-]/[+]) [11-13].

The adsorption at the air/water interface of individual synthetic and natural polyelectrolytes, the main components of PECs, has been fairly well documented in the literature for several decades, particularly with the sodium poly(styrene sulfonate) (PSSNa) [14-24]. The adsorption of PEs differs in many respects from that of neutral polymers. Highly charged PEs are not hydrophobic enough to be surface active and therefore do not spontaneously adsorb at water-air interfaces at low concentrations [15, 16, 22]. In the presence of added electrolytes (salt) or at a sufficiently high concentration, they nevertheless adsorb with a much slower kinetics (a few hours) than in the case of neutral polymers where equilibrium is reached in a few minutes. A well-known effect due to the presence of an electrostatic barrier: the first adsorbing PE chains generate a negative adsorption potential

that slows down the subsequent adsorption of additional charged chains. In this context, the addition of salt increases the ionic strength of the solution, screening the electrostatic interaction and resulting in a larger and faster decrease in surface tension. At a sufficiently high salt concentration, the surface layer of PEs approaches that of neutral polymers.

If we add a second component of opposite charge in the solution, the surface activity properties of PEs can be completely different. A lot of work has been done in the last three decades to study the properties of PE/surfactant complexes (PESCs) at interfaces. Compared to neutral polymer/surfactant mixtures where only weak hydrophobic interactions can develop, PESCs have shown the coexistence of strong electrostatic and hydrophobic interactions [25-27]. This results in a complex but very rich adsorption pattern that has led to many important industrial applications ranging from enhanced oil recovery [28] and wastewater [29] to pharmaceuticals [30] and cosmetics [5]. Surface tension measurements of surfactants in the presence and absence of polymer were found to be particularly relevant to highlight the formation of specific interactions, if any, between the components [31].

Furthermore, if a PE replaces the surfactant, surprisingly few studies in the literature have focused on the interfacial properties of such PE complexes. Bago *et al.* recently highlighted the possibility of using PECs consisting of PDADMAC/PSSNa (solid-like colloidal PECs) and PDADMAC/PANa (near-neutral coacervate droplets) to stabilize oil/water emulsions while individual PEs are not emulsifiers because macroscopic phase separation occurs immediately after mixing [32, 33]. The surface activity of PSSNa/PAH and PDADMAC/PSSNa/lipase PECs were also highlighted by Owiwe *et al.* and Generalova et *al.* respectively [20, 34]. But in these very interesting works, it is difficult to know precisely which structures are responsible for these effects. Indeed, PECs can exist in different physical forms (soluble or insoluble colloidal complexes, coacervated droplets) which must have an impact on their surface activity properties, the objective of the study is precisely to establish this correlation. This will allow us to better use PECs to develop and modify the interfacial properties of various biphasic systems.

In this work, we systematically correlated the surface activity of PECs obtained at different molar charge ratios (Z) with the PEC structure determined by light scattering, zeta potential and microscopy. Two model systems were examined, the weakly interacting

PDADMAC/PANa system forming liquid-like PECs and the strongly interacting PDADMAC/PSSNa pair forming solid-like PECs. Our approach also showed that simple surface tension measurements at the air/water and water/water interface can be a very sensitive tool to characterize, discriminate and better understand the formation mechanism of the different structures encountered during the formation of PECs.

2.2 Experimental materials and methods

Polyelectrolytes (PEs). Poly (diallyldimethylammonium chloride) (PDADMAC, Mw ~ 100 000-200 000 $g.mol^{-1}$) was purchased from Aldrich as 20 wt. % solution in water (Lot # 03530MS). Poly(acrylic acid sodium salt) (PAANa, Mw ~ 2000 $g.mol^{-1}$) and Poly (sodium 4-styrenesulfonate) (PSSNa, M_w ~ 70 000 $g.mol^{-1}$ PDI=1.5~2) were purchased from Aldrich as powders (Lot # BCBF7673V) and (Lot # LR0001445584) respectively. Before any use, the three polyelectrolytes were purified by extensive dialyzes against pure water and then freeze-dried. These polymers were analyzed by size exclusion chromatography with a multi-angle light scattering detection to precisely determine the average molecular weights and dispersities (PDADMAC: Mw=44 200 $g.mol^{-1}$ with PDI=1.59 ; PANa: 2560 $g.mol^{-1}$ with PDI=1.45; PSSNa: M_w ~ 70 000 $g.mol^{-1}$ with PDI=1.5~2).[12] PANa, there is a certain amount of non-charged end groups. The content of acid groups was determined by conductometric titration experiments with 1M NaOH, giving a weight percentage of 84.2% for acid monomers. Individual stock solutions were made from the freeze-dried powders from filtered DI water using 0.2 µm Millipore membranes. The pH of each solution was set to 10 with the help of a 1M sodium hydroxide (NaOH). At such pH, the weak PANa polyanion is fully charged.[35]

Then, the stock solutions were diluted to the desired concentrations expressed in mM of repetitive units (0.62 mM, 6.2 mM, 18.6 mM, 62 mM, 434 mM, 930 mM) and the pH adjusted again to 10 (the volume of NaOH was taken into account for the final concentration). All solutions were filtered through 0.20 µm pore size cellulose acetate membranes (Millipore) before use.

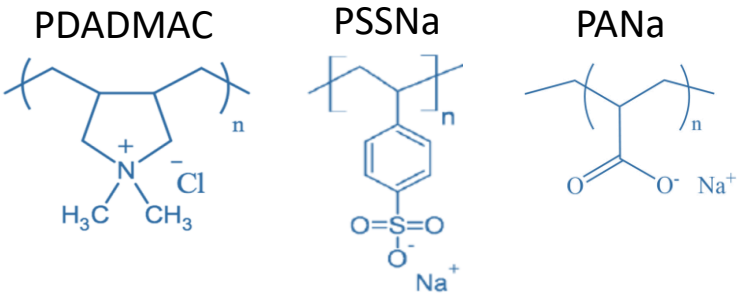

Figure 2-1. Chemical structure of PDADMAC, PSSNa and PANa.

Preparation of polyelectrolyte complexes (PECs). The PECs were formed at different molar charge ratios (Z) defined as $Z = \frac{[PANa]}{[PDADMAC]}$ or $Z = \frac{[PSSNa]}{[PDADMAC]}$ by considering the molar concentrations of repetitive units of respective PEs. PE solutions at 18.6 mM were used, so that the total PE concentration was also 18.6 mM regardless of the target Z value. This relatively low polymer concentration was chosen to minimize aggregation phenomena. The PECs were prepared by injecting a certain volume of PDADMAC solution into a vial containing either a PANa or a PSSNa solution. In some cases, the reverse order of addition was perfomed as well for comparison. The suspensions were thoroughly stirred for 2 minutes and rapidly used for DLS and surface tension measurements to avoid any significant sedimentation phenomena. The supernatants of PEC suspensions obtained at Z=1 were also collected and analyzed after 2 weeks.

Dynamical light scattering (DLS) and ζ-potential. Dynamic light scattering (DLS) experiments were performed by using an ALV laser goniometer, with a 22 mW linearly polarized laser (632.8 nm HeNe) and an ALV-5000/EPP multiple tau digital correlator with a 125 ns initial sampling time. The DLS autocorrelation functions were obtained at a scattering angle of 90° and a temperature of 20°C. The intensity-weighted relaxation time (τ) distributions were extracted from the autocorrelation data using the multi-exponential CONTIN method. The apparent diffusion coefficients (Dapp) were obtained by considering Dapp = (1/τq2) where τ is the mean relaxation time and q the scattering vector. The hydrodynamic radii (RH) were determined using the Stokes-Einstein relation, $R_H = \frac{k_B T}{6\pi\eta D}$ where kB is the Boltzmann constant, T the temperature, η the viscosity of the solvent and D the diffusion coefficient. ζ potential measurements were performed with a Zetasizer Nano-ZS (Malvern Instruments, UK) at an angle of 173° using a 4.0 mW He-Ne laser operating at a

wavelength of 632.8 nm. An automatic titrator MPT-2 (Malvern Instruments) was coupled to the Zetasizer allowing successive injections of one PE (titrant) into the second (titrated). The electrophoretic mobility of each solution was measured and converted to ζpotential (mV) by the Smoluchowski approximation model using the DTS program (Malvern).

Small-angle X-ray scattering (SAXS). SAXS profiles were acquired on a XEUSS set-up (Xenocs, Grenoble, France) with a microfocus copper anode source, a scatterless collimation system and a PILATUS 2-D detector, giving access to scattering wave vector q values from 0.009 to 0.5 $Å^{-1}$. The PECs and individual PEs were put in thin glass capillaries. The resulting 2D images were found to be isotropic, and the data were azimuthally averaged to give the intensity scattering curve I(q), corrected for the experimental background, as a function of $q = (4\pi/\lambda)\sin\theta$, where λ = 0.154 nm is the wavelength of the Cu Kα radiation and θ is half the scattering angle.

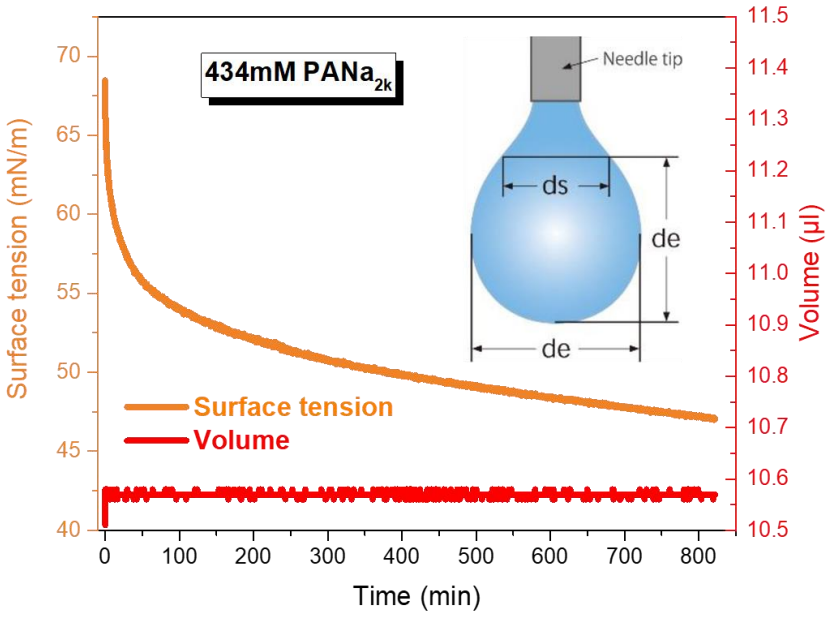

Figure 2-2. Dynamic surface adsorption at air-water interface

Dynamic air-water surface tension measurements. The dynamic surface tension of PEC solutions was measured using a pendant-drop set-up (Tracker, from Teclis Scientific, France). A drop of water of about 10 µL was generated with a syringe equipped with a Teflon needle, as shown in **Figure 2-2**. The pendant drop was generated in a closed cell saturated with water vapor with a feedback loop that maintained its volume throughout the experiment. This allowed measurements to be made over very long periods of time.The variation of the surface

tension at the solution/air interface was then monitored for more than 500 min at 22°C with a drop volume kept constant during the whole measurement. The time-dependent interfacial tension was deduced from the axisymmetric drop shape by fitting it with the Laplace equation. The pendant drop method is well suited for dynamic surface tension monitoring because i) it facilitates the creation of a pristine air/water interface, ii) it uses small volumes of solution, and iii) it avoids the problems of probe cleaning in force-based methods (Du Noüy ring or Wilhelmy plate) that can affect the final results [36].

Water-water interfacial tension measurements. Measurements of the water-water interfacial tension. These particular and delicate measurements will be described in more detail later

2.3 Results and Discussions

2.3.1 Surface tension of individual polyelectrolyte solutions

We first investigated the interfacial behaviour of the three individual polyelectrolyte solutions considered in this work prior to study the behaviour of PECs. **Figure 2-3** shows the dynamic surface tension of the different PE solutions at different concentrations. At low concentrations ($c \leq 6.2$ mM), almost no adsorption occurs due to the hydrophilic and charged nature of the polymer chains, as reported for various polyelectrolytes [14-24]. For higher concentrations ($c > 18.6$ mM), the surface tension significantly decreased due to the concomitant increase of the ionic strength in the medium when the PE concentration increased. Indeed, the concentration of free counterions scales with the PE concentration as $[C]_{free} \sim C_{PE} \times f_{eff}$, where f_{eff} is the effective charge density of the polyelectrolyte ($f_{eff} \sim 0.36$ for PANa and PSSNa and ~0.66 for PDADMAC) in relation with the Manning-Oosawa condensation [37, 38]. Therefore, by increasing the PE concentration, the electrostatic repulsions between the charged units become increasingly screened thus favoring the polymer adsorption at the air-water interface. In this concentration regime, it can be observed that adsorption mostly occurs at short times (< 1h) which is related to the diffusion of polymer chains, while at longer times, adsorption is much less important due to the formation of an electrostatic barrier generated by the previously adsorbed PE chains at the air-water interface.[16] This is a general trend well in line with the literature [14-23]. It emphasizes that the affinity of PEs with the

surface is mainly determined by the screening conditions rather than their chemical composition. Besides, it is important to note that the dynamic surface tension of the three PEs did not reach equilibrium values even after 500 minutes, as reported elsewhere for other PEs [16]. The small but still persistent adsorption at long times could be ascribed to the formation of metastable microdomains or aggregates at the interface, similar to those typically found in PE solutions [16].

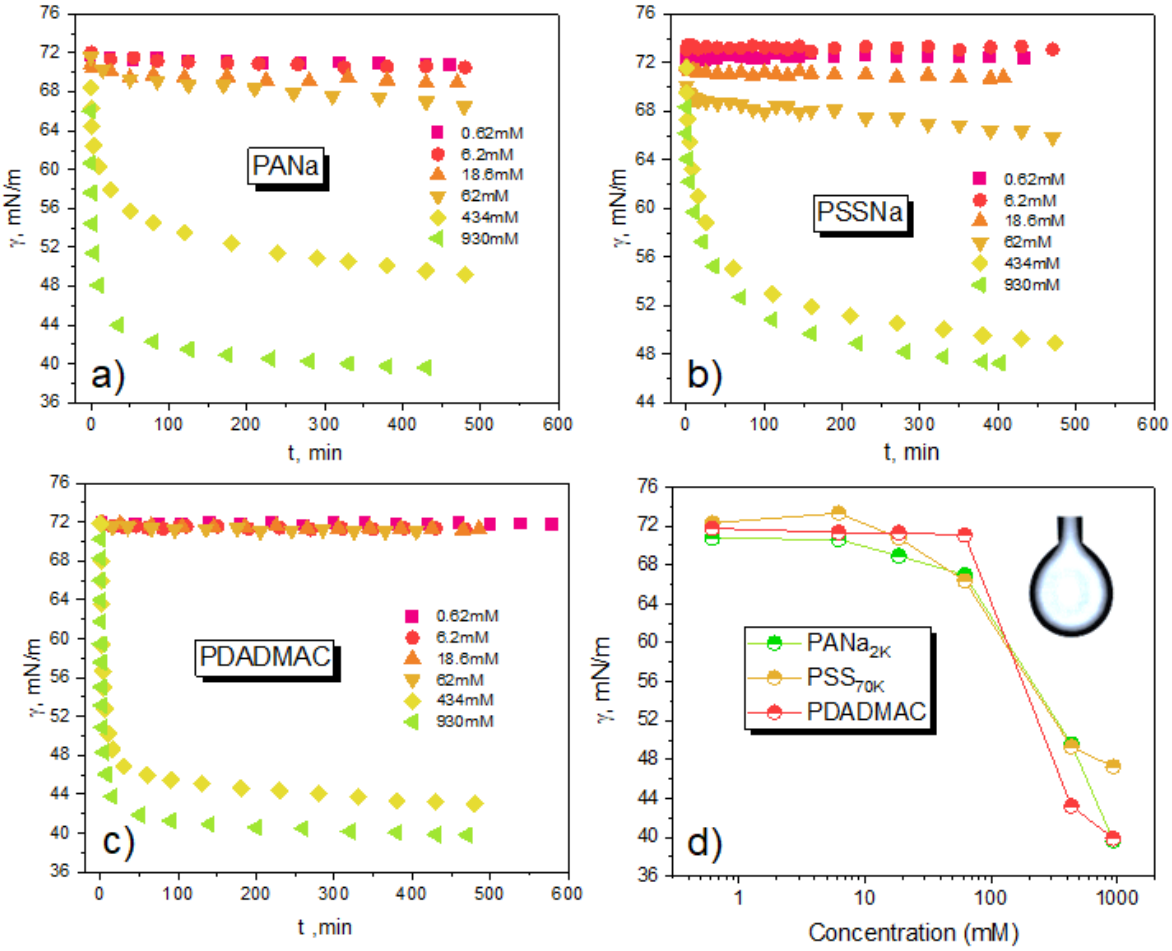

Figure 2-3. Dynamic surface tension (γ) of PANa (a), PSSNa (b) and PDADMAC (c) solutions at different concentrations (in repetitive units) determined by pendant-drop measurements. (d) Variation of the surface tension as a function of the concentration of the polyelectrolyte solution (PANa, PDADMAC, PSSNa) (b). Data were collected during 500 minutes.

From **Figure 2-3 d**, we can estimate the molar surface excess from the concentration dependence using the equilibrium Gibbs equation [15]

$$\Gamma_{PE} = -\frac{1}{RT(1+Nf_{eff})}\frac{d\gamma}{d(\ln c_{PE})} \qquad (2.1)$$

where f_{eff}, c_{PE} and N are the effective charge density, concentration and polymerization degree of the PE, respectively. The approximate surface excess was found to be 3.2 x 10^{-8} mol/m^2 (1.43 mg/m^2), 6.1 x 10^{-7} mol/m^2 (1.3 mg/m^2) and 2.9 x 10^{-8} mol/m^2 (2 mg/m^2) for PDADMAC, PANa and PSSNa respectively. A result suggesting that smaller chains of $PANa_{2k}$ can accommodate more easily than larger ones at the air/water interface.

We have just seen that free counterions decrease the repulsions between PEs chains which allows them to better adsorb at the water/air interface. The addition of salt to a given PEs solution should therefore produce the same effect as already documented in the literature [14-23] and in particular in the work of Noskov and co-workers [16] where the surface tension decreases strongly when NaCl is added to a dilute PSSNa solution (5 mM). **Figure 2-4** shows the surface tension of the three PE solutions at a concentration of 434 mM as a function of different amounts of added NaCl. As expected, the surface tension of PANa decreases well but only with a much higher NaCl concentration than the Na^+ counterions already present in the solution. The surface tension of PSSNa on the other hand does not change upon addition of salt which means that the surface activity of PSSNa at 434 mM is largely dominated by the hydrophobicity of the PE chain rather than the charges. The fact that the PSSNa quickly reaches its lowest surface activity is also in in agreement with its marked hydrophobic nature. The behavior of PDADMAC, however, is clearly unexpected with a surface tension that increases with the addition of NaCl. **Figure 2-4 d** shows a well-known result that the surface of NaCl solutions increases with the concentration.[39] This result can be rationalized by the presence of an ion depleted zone at the air/water interface which induces an increase in the surface tension according to the Gibbs equation (eq 2.1).

Highly hydrated ions such as Na^+ remain far from the interface where solvation is less efficient by definition. The ion hydration free energy influences then the surface tension at high concentration [40]. While the Na^+ structure-making ions tend to move away from the interface where they can better organize the water dipoles, the Cl^- structure-breaking ions are positively adsorbed at the air/water interface because bulk water can better organize its hydrogen bonds without them. Although we do not fully understand the unusual behavior of the PDADMAC chains upon addition of NaCl, we can nevertheless speculate that the presence

of a large excess of Cl^- ions from both the counterions and the salt may partially displace the large PDDAMAC chains adsorbed at the interface, thereby decreasing the surface tension. This effect is not observed in the case of PSSNa and PANa likely because the counterions are Na^+ and not Cl^-. Clearly, a more detailed study is needed to better understand this phenomenon which is not reported in the literature to our knowledge.

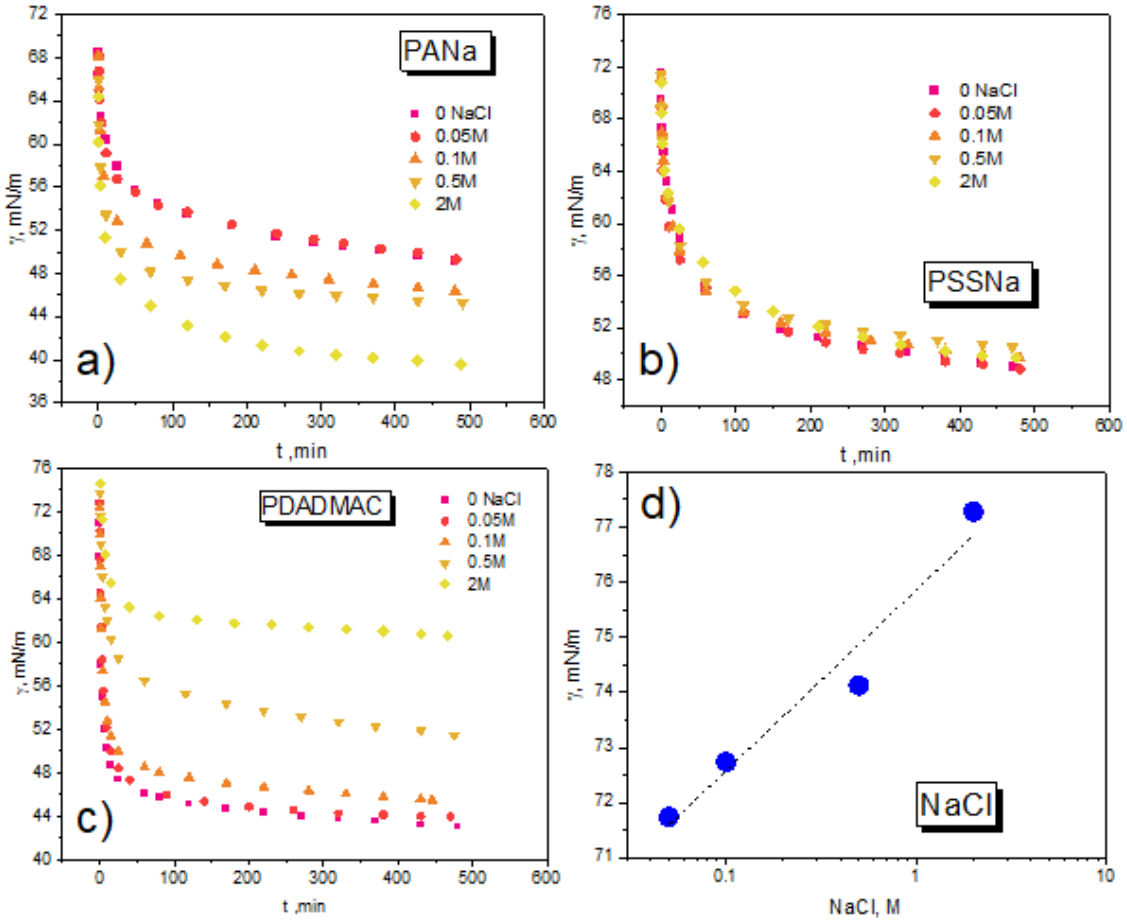

Figure 2-4. a,b,c) Influence of NaCl addition on the surface tension (γ) of PAANa, PSSNa and PDADMAC solutions prepared at 434mM. d) Surface tension of NaCl solutions prepared at various concentrations. The dotted line is a linear fit to the data. The surface tension values of NaCl solutions were constant throughout the measurements (500 min).

2.3.2 Dynamic light scattering analysis and zeta potential of PECs

PEC dispersions were generated by adding either PDADMAC into PANa and PSSNa solutions (*mixing route 1*) or PANa and PSSNa into PDADMAC solutions (*mixing route 2)* at

different molar charge ratios (Z=[-]/[+]) using PE solutions at 18.6 mM. They were then characterized by dynamic light scattering (DLS). **Figure 2-5** shows the relaxation time spectra of the two systems obtained from correlation functions by applying an inverse Laplace transform. For individual PDADMAC, PSSNa and PANa solutions, a fast mode was observed originating from the coupling of the PE motion with the dynamics of small and much faster counterions [41].

Following the route 1, so-called soluble complexes were formed at low Z [11, 12, 42] for the weakly complexing PDADMAC/PANa system due to the small size of PANa chains,. These structures were made of single PDADMAC chains complexed with few PANa ones. They carry a net positive charge as shown by zeta potential measurements (**Figure 2-6**) that is high enough to prevent self-association phenomena, as shown by the value of the hydrodynamic radius (R_H) around 5 nm, well in line with the coil size of a PDADMAC chain in presence of salt. It should be noted that soluble complexes represent a very specific kind of complex structure that can only be obtained under strict conditions of high chain length asymmetry between the two PEs [12, 42]. At higher Z (~0.6), where most charges of PDADMAC are neutralized through ion pairing with oppositely charged PANa chains, the relaxation times abruptly increased above 1 ms corresponding to R_H ~ 112 nm. In that case, PDADMAC chains are no longer hydrophilic and can self-assemble into small particles through hydrophobic interactions. Particles are stabilized by the excess of PDADMAC at Z < 1 and by the excess of PANa at Z > 1. In the strongly complexing PDADMAC/PSSNa system, colloidal complexes were generated from low Z values with R_H values of ~ 80 nm due to a much strongly interacting system with respect to the larger molar mass and higher hydrophobicity of PSSNa.

Furthermore, at charge stoichiometry (Z=1), a fundamental structural difference appears between the two systems. As expected, the highly complexing PDADMAC/PSSNa system undergoes a liquid-solid phase transition leading to solid aggregates while the weakly complexing PDADMAC/PANa system undergoes a liquid-liquid transition leading to coacervate droplets; a feature clearly visible in the optical microscopy images in **Figure 2-5 a** and **b**, which also generates a maximum turbidity at Z=1 just after mixing. It is also interesting to note that the suspension of PSSNa-based complexes *off* stoichiometry is more turbid compared to PANa-based complexes. It shows that larger and probably denser particles of complexes were

obtained with PSSNa as polyanion even though this was not readily detectable on the DLS size distributions due to the size dispersity of the structures and the presence of slow modes [43].

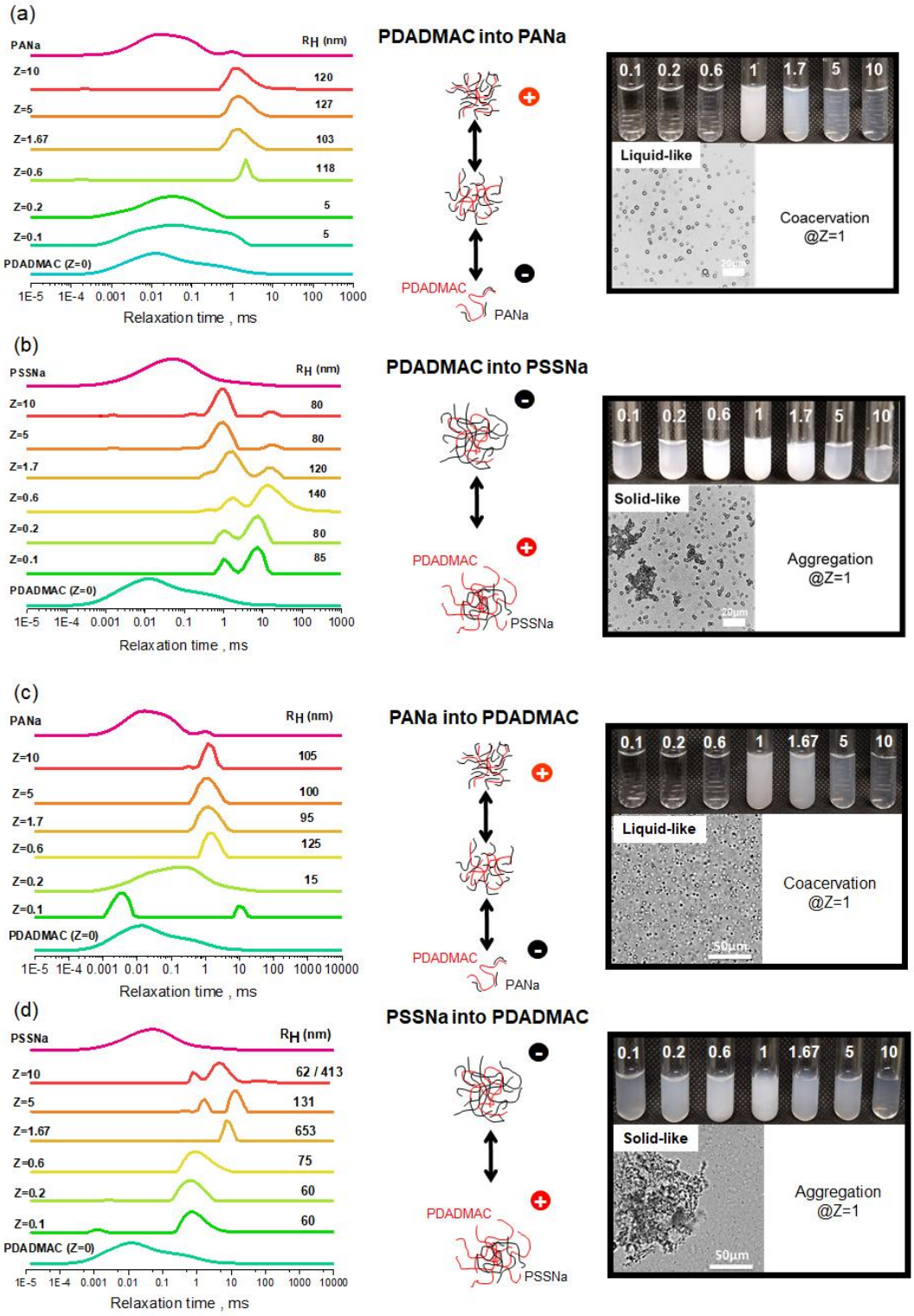

Figure 2-5. Spectra of the relaxation times (and hydrodynamic radii) and photographs of the PEC dispersions taken at different Z values together with microscopic images taken at charge stoichiometry (Z=1). Mixing route 1 (a) PDADMAC/PANa and (b) PDADMAC/PSSNa. Mixing route 2 (c)

PANa/PDADMAC and (d) PSSNa/PDADMAC. PECs were generated at different molar charge ratios (Z) from PE solutions prepared at 18.6 mM, pH 10 without added salt.

The variation of the zeta potential (ζ) (**Figure 2-6**) shows a typical charge inversion from positive ζ values when the polycation is in excess (Z < 1) to negative ones when the polyanion is in excess (Z > 1) in line with the recent work of Bago *et al*. [32]. What is more interesting is the pattern of the variation and the absolute values of ζ. The charge inversion is sharper in the case of complexes containing PSSNa. Overall, this shows that complexes made of PSSNa have a strict charge separation between the core and shell, whereas for PANa-based complexes, the charges are more evenly distributed throughout the complex structure. This supports a complexation mechanism where the hydrophobicity of PSSNa favors the formation of dense and solid-like complexes with little possibility for structural rearrangments. On the contrary, complexes made from PANa are softer, better hydrated and more prone to structural changes, thus favoring the transition from soluble complexes at Z < 0.6 to dispersed complexes at 0.6 < Z < 1 and coacervate droplets at Z close to 1. In a study on the influence of the hydrophobicity of PEs in PEC formation, Mende *et al*. concluded that PEs containing hydrophobic styrenic units favor the formation of compact structures compared to less hydrophobic PEs that instead lead to swollen particles.[44] Higher hydrophobicity leads also in general to lower colloidal stability. Finally, no significant variation of the pH was observed during the complexation which excludes all possibilities of acid-base reactions.

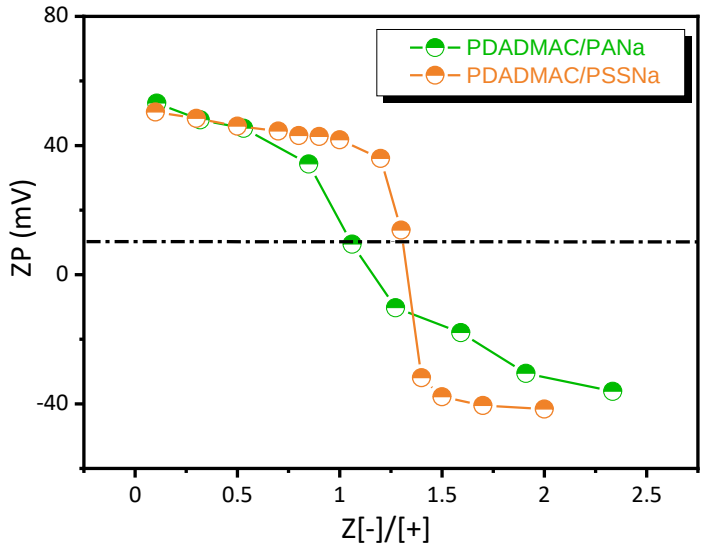

Figure 2-6. Zeta potential (ζ) of PECs prepared at various charge ratios (Z): PDADMAC/PANa (a) and PDADMAC/PSSNa (b). PECs were prepared from PE solutions at 18.6 mM, pH 10 without added salt.

Complexation is in general sensitive to the formulation route or the way the various components are brought into intimate contact. Indeed, the morphology of complexes is controlled by a competition between reaction and mixing times.[45, 46]. In some case the composition of complexes can be also dependent on the mixing order [9]. We then studied PECs generated by mixing route 2 where PDADMAC solutions were added to PSSNa or PANa solutions (**Figure 2-5 c** and **d**). It shows similar results as route 1 for the strongly interacting PDADMAC/PSSNa system, probably due to the relatively low concentrations of PE solutions allowing rapid homogenization of the mixture before the interaction begins to occur. At Z=1, very large objects are formed by a liquid-solid phase transition and eventually precipitate after 24 hours as in mixing path 1. For the weakly interacting PDADMAC/PANa system, we still detect solubles complexes at very low Z but with slighly larger R_H (~15nm) probably due to some bridging. At Z=0.6 we form colloidal PECs with R_H around 125 nm as in route 1. At Z=1 a liquid-liquid transition occurs to form a coacervate phase in equilibrium with a continuous phase depleted in macromolecules which finally separate macroscopically after 24h.

Since both routes yielded similiar results, PECs were then generated by mixing route 1 in the remainder of this study where the two polyanions (PSSNa and PANa) are added to the polycation solution (PDADMAC).

2.3.3 Surface tension of PEC dispersions

DLS analyses showed the presence of various colloidal structures in the PEC dispersions prepared from PE solutions at 18.6 mM. There was no large difference in size between the complexes obtained from PDADMAC/PANa and PDADMAC/PSSNa at various Z ratios even though their physical nature differs, liquid-like for the former and solid-like for the latter. In the following, we will show that these PECs have a specific interfacial signature, even if individual PEs barely adsorbed to the air/water interface at a concentration of 18.6 mM (**Figure 2-3**).

Figure 2-7 shows the time-dependent adsorption at the water/air interface of the different PECs generated as a function of the molar charge ratio (Z) at pH 10. For the two complex systems studied, the dynamic surface tension (γ) profiles are very different from those obtained with PEs alone (**Figure 2-3**). First, the γ values obtained with PECs are much lower than those found with PEs alone at similar concentration (the overall polymer concentration in PEC suspension was 18.6 mM for all Z values) (**Figure 2-7 a,b**). This highlights a more efficient charge screening of PDADMAC by complexation with a polyanion rather than by an increase of the ionic strength. **Figure 2-7 c** shows that γ values obtained after 500 min decreased as the system gets closer to stoichiometry (Z = 1) for both PDADMAC/PANa and PDADMAC/PSSNa complexes whenever the complexation takes place in presence of an excess of PDADMAC (Z < 1) or an excess of polyanion (Z > 1). This agrees well with an increased level of charge neutralization of PEs forming increasingly hydrophobic surface-active species. The fact that the variation of γ is symmetrical around Z = 1 also emphasizes that the interfacial activity of both systems depends greatly on the level of complexation and little on the positive or negative nature of the charges in excess at PEC surface. The behavior at stoichiometry (Z = 1) was particularly informative of the physical nature of the complexes. For PDADMAC/PANa at Z = 1 where the system undergoes a liquid–liquid phase transition forming coacervate microdroplets, the surface tension of the PEC suspension at Z=1 just after complexation is similar to that measured in the supernatant after sedimentation and coalescence of the droplets (**Figure 2-7 a**, symbol 1-sup). This shows that the surface-active species must be similar in both phases. Therefore, it rules out the possibility for large coacervate droplets to participate in the adsorption process. In fact, the adsorbing species are likely free macroions

or small complex particles in equilibrium with the coacervate droplets, in agreement, respectively, with the segregation mechanism proposed by Veis and the intercomplex disproportionation described by Shklovskii et al. [47, 48]. The two scenarios were reviewed by Kizilay et al. [49]. The fact that the surface tension drops quite rapidly with time at Z = 1 in the PEC suspension and supernatant (**Figure 2-7 a**) is also in line with the diffusion and adsorption at the liquid–air interface of small complexes or free macroions. For Z values different from 1, the adsorption kinetics of complexes is slower because of their larger size and higher charge density (**Figure 2-6** and **Figure 2-7 a**).

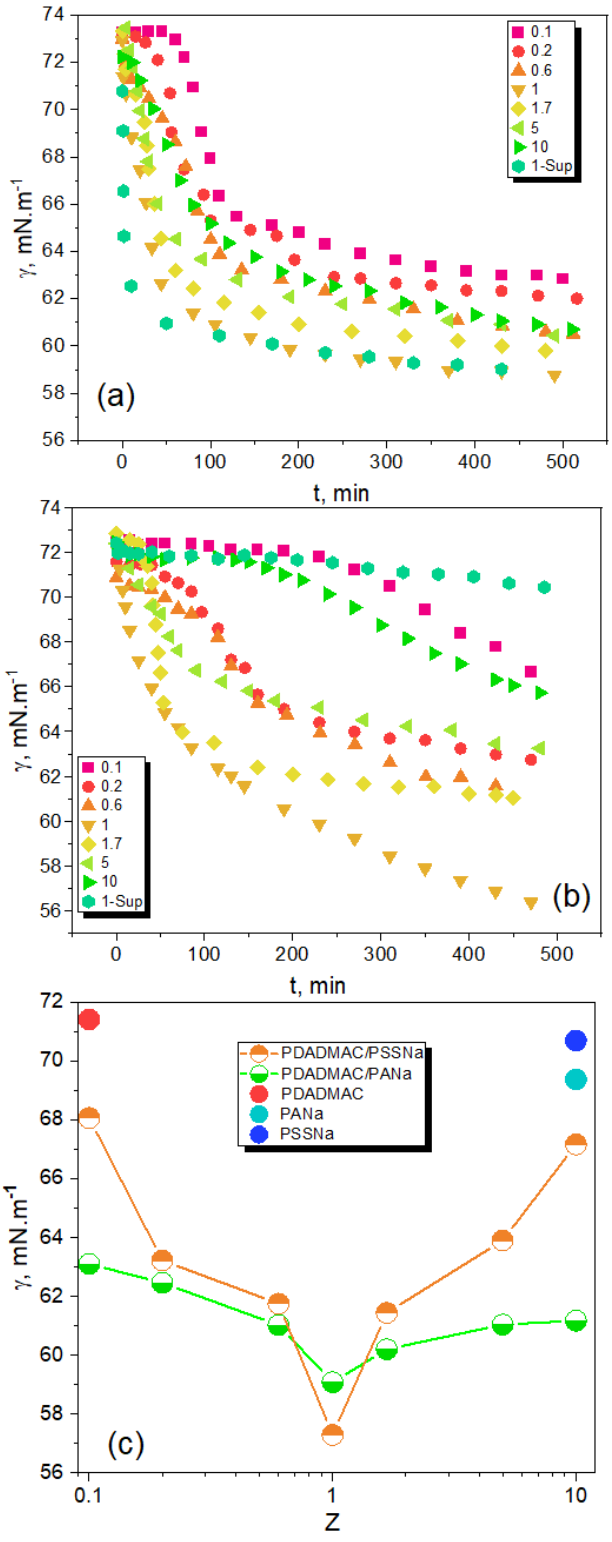

Figure 2-7. Dynamic surface tension (γ) of PDADMAC/PANa (a) and PDADMAC/PSSNa (b) PEC suspensions at different molar charge ratios (Z). Variation of γ obtained after 500 minutes as function of Z for the two PEC systems (c). PECs were prepared from PE solutions at 18.6 mM and pH 10 and rapidly analyzed after preparation. 1-sup in the (a) and (b) legend refer to the surface tension (γ) of the supernatant after the macroscopic phase separation occurring at Z=1 for both systems.

The interfacial behavior of PDADMAC/PSSNa was clearly different. First, the adsorption of complexes at the interface was much slower than for PDADMAC/PANa, especially for charge ratios far from stoichiometry (Z = 0.1, Z = 0.2 and Z = 10), as judged from the variations of γ (**Figure 2-7 b**). The surface tension values after 500 min were also higher for PSSNa-based complexes (**Figure 2-7 c**). These trends reflect the behaviour of rather large, dense, and highly charged particles (**Figure 2-6**) with less affinity with the water-air interface. In agreement with previous studies [44], it confirms the solid-like nature of PSSNa-based complexes in contrast to PANa-based complexes which are softer, more hydrated and thus with interfacial properties closer to those of polymer chains. It has been recently shown that solid particles have in general low interfacial affinity while particles decorated with polymer chains can adsorb at the water–oil interface depending on the hydrophobicity of the polymer. For example, latex particles decorated with polyamine chains can adsorb at the interface at pH 10 because amine groups are neutralized under such conditions [50]. PDADMAC/PSSNa complexes have such a core-shell structure with a dense and solid hydrophobic core resulting from the segregation of complexed segments and a stabilizing shell of excess PE. Then, the affinity of the shell with the water–air interface must depend greatly on the degree of complexation.

For Z close to 1 (Z = 0.6, Z = 1.7), a significant fraction of complex particles sedimented due to their large size and poor colloidal stability (**Figure 2-5 b**). Under these conditions, the few remaining particles capable of adsorbing at the interface were probably small and poorly charged, which would then explain the rapid and relatively large decrease in surface tension (**Figure 2-7 b**). For Z = 1, a fraction of the neutral complexes adsorbed rapidly and massively at the interface as seen by the variation of γ. Even though the equilibrium value of γ was not reached after 500 min, one can figure out the final state of the system. Indeed, the γ value in the supernatant after complete equilibration of complexes (2 weeks) was close to that of water (72 mN/m) (**Figure 2-7 b**), which means that PSSNa-based complexes have fully sedimented. It also implies that complexes were not in an equilibrium state in contrast to complexes obtained from PANa where free macroions or soluble complexes remain in solution. This is in agreement with a complete liquid-solid phase separation for the PDADMAC/PSSNa system.

We have shown so far that the measurement of the surface tension can be a very useful tool to better understand the formation mechanisms of PECs and to detect in a very sensitive way the presence of a very small amount of aggregates and other precursors in the supernatant phase. In **Figure 2-7 c**, the value of Z = 1 was obtained by simple manual mixing of two equimolar solutions of PEs of opposite charge. Is this method accurate enough to determine the exact charge stoichiometry? To answer this question, we slightly varied the stoichiometry of the mixture around Z = 1 and measured the surface tension of the supernatant to verify that it was indeed minimum.

Several insights can be drawn from data plotted in **Figure 2-8**. First, there is a value of Z equal to 1 that maximizes the surface tension of both supernatants and decreases symmetrically on both sides. This value can be considered as the experimental ''true'' charge stoichiometry. It is remarkable that the surface tension varies so strongly over such a small range of Z, thus emphasizing that this method is very efficient to determine precisely the stoichiometry in PECs systems. In particular, the method is more discriminating than turbidity measurements, which would yield optically transparent supernatants around Z = 1. It is also remarkable that the complexation stoichiometry was 1 despite the structural differences of the PEs. In fact, the PEs adopt an open extended conformation in salt-free solution, which favors the juxtaposition of long portions of oppositely charged PEs. Then, according to Michaels et al., the high local concentration of microions and the slow diffusion of the released microions from the sites of reaction allow sufficient charge screening so that rearrangements of rotational conformations can take place and favor the complete ionic pairing between PEs [51].

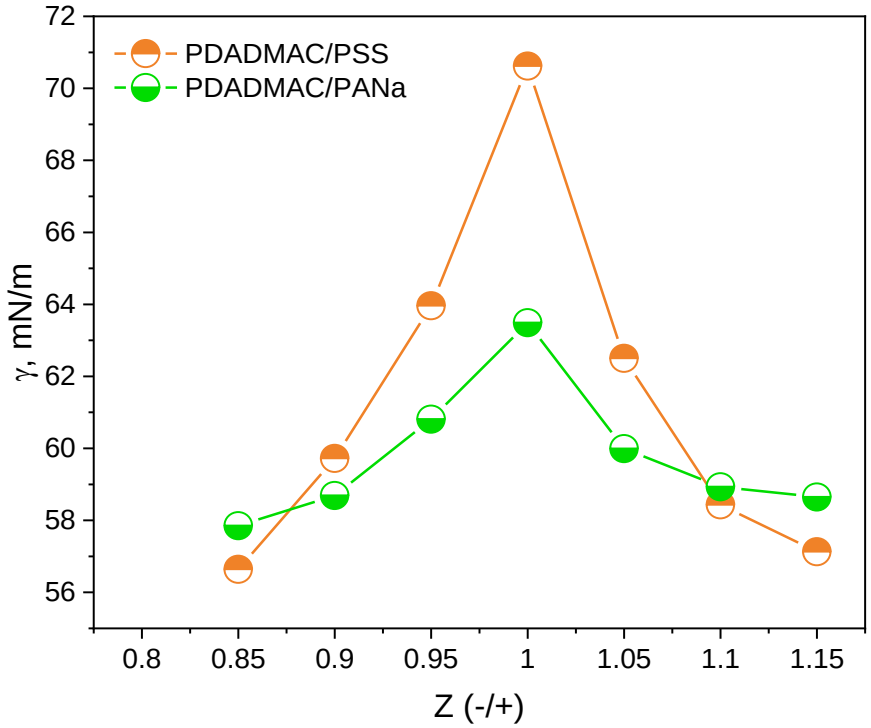

Figure 2-8. Surface tension (γ) measurements of the supernatant of PEC dispersions at different charge ratios (Z) around the charge stoichiometry (Z=1) for PDADAMAC/PANa (orange) and PDADMAC/PSSNa (green). PECs were prepared from 18.6 mM PE solutions, the supernatants were collected after a complete macroscopic phase separation (2 weeks), and the surface tension was measured after 500 min when the signal became constant.

Furthermore, the surface tension measured at Z = 1 for the aggregating PDADMAC/PSSNa system was similar to that of pure water, suggesting that all PE chains were indeed engaged in the formation of dense and solid aggregates during the liquid-solid phase transition, with the release of all counterions into the supernatant. This hypothesis was verified by measuring the conductivity of the supernatant at Z = 1 and of NaCl solutions prepared at various concentrations, as proposed a long time ago by Michaels et al. on a similar PEC system [51]. The conductivity in the supernatant corresponded to a NaCl concentration of 8.75 ± 0.51 mM, which is in good agreement with the complete release of counterions from PSS(Na+) and PDADMAC(Cl-) solutions prepared at 18.6 mM and mixed in equal volume, the theoretical NaCl concentration being then 9.3 mM.

For the PDADMAC/PANa system, the surface tension of the supernatant (at Z = 1.0) clearly indicates that the supernatant contains surface-active species in equilibrium with the coacervate droplets, as discussed previously. In order to know more precisely the structure of

these species, the supernatant was analyzed by SAXS (**Figure 2-9 a**). From the SAXS point of view, it appears that the supernatant contains little or no objects in solution while the interfacial tension measurements indicate the presence of surface-active species. It cannot be the PEs alone, as it would require at least a concentration of 100 mM (see **Figure 2-3**) to lower the surface tension to 64 mN/m, which would then be visible in SAXS. We then prepared PDADMAC/PANa PECs out of stoichiometry at a low concentration of 1 mM where neither SAXS nor DLS gave a consistent signal. Dynamic surface tension measurements performed on these diluted solutions (**Figure 2-9 b**) showed a slight decrease in surface tension for the three Z studied. These data suggest then that the supernatant probably contains very small numbers of PECs in equilibrium with the coacervate phase, an appealing hypothesis that needs to be confirmed by a dedicated and comprehensive study on the subject.

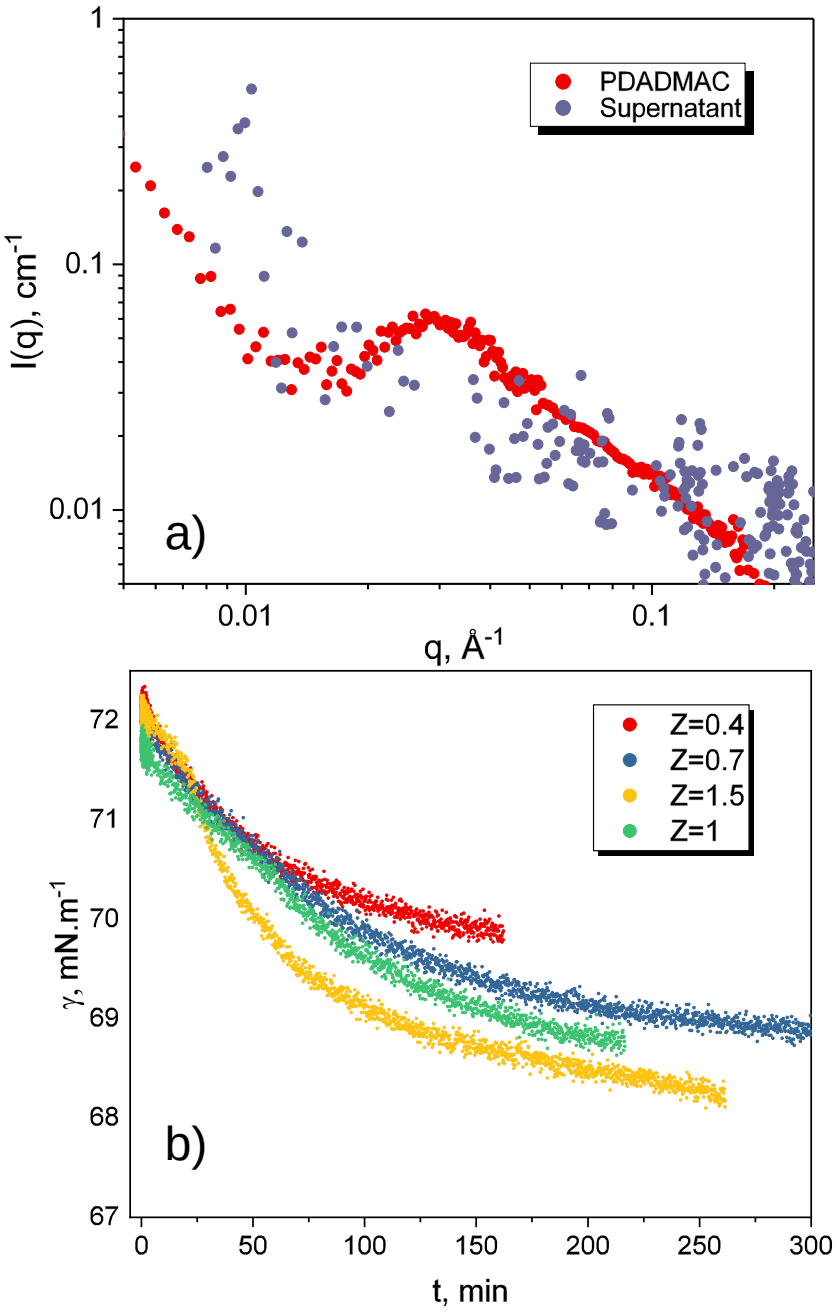

Figure 2-9. (a) Diffusion intensity I(q) of the supernatant phase at Z=1 measured by SAXS. The signature of an 18.6mM PDADMAC solution is also shown for comparison. We also note the presence of a polyelectrolyte peak (q~0.28 Å^{-1}) expected for this type of charged macromolecule. (b) Dynamic surface tension (γ) of PDADMAC/PANa complexes prepared at Z=0.4, 0.7, 1.0 and 1.5 from 1 mM PE stock solutions.

2.3.4 Interfacial tension between the dilute and the concentrated coacervate phase

At this point, all PEC dispersions were analyzed by surface tension measurements with the exception of the liquid–liquid interface formed during the complex coacervation of the PDADMAC/PANa system at Z = 1. The interfacial tension γ_{cc} between the dilute and the concentrated phases coexisting in the complex coacervate can be 10000 times lower than that of pure water, on the order of 1–100 µN/m, [52-56] and thus extremelly difficult to measure directly after complexation.

The dispersion of PECs obtained at a charge ratio Z = 1 was placed in a 2 mm-thick quartz cell with parallel walls. Within 14 days (or with the help of centrifugation) however, a complete macroscopic liquid–liquid phase separation is usually occurring giving rise to a net interface between the polymer-rich coacervate phase and the polymer-depleted supernatant phase as seen as seen in **Figure 2-10** a. In this particular geometry, the interfacial tension γ_{cc} can be accurately measured if the capillary length l_c defined as :

$$l_c = \sqrt{\frac{\gamma_{cc}}{\Delta\rho * g}} \qquad (2.2)$$

That sets the liquid-liquid interfacial profile is known togeter with the mass density difference $\Delta\rho = \rho_2 - \rho_1$ between the two phases [57].

The interfacial tension γ_{cc} between the dense complex coacervate (CC) and the macromolecule-depleted phase was then computed by measuring $\Delta\rho$ and l_c . $\Delta\rho$ was measured using a Density Meter (DMA 4100M, Anton Paar) with a resolution of 0.0001 g.m^{-3}. l_c was obtained by analyzing the static interfacial profile near the vertical wall of the cell with a shape given by the generalized Young–Laplace equation connecting capillary pressure with curvature and surface tension for the case of a flat wall as [57, 58]:

$$\Delta\rho\ g\ z(x,y) - \gamma\left[\frac{1}{R_1(x,y)} + \frac{1}{R_2(x,y)}\right] = constant \qquad (2.3)$$

With R_1 and R_2 the principal raddii of curvature of the geometry considered. This accounts for the balance existing at each point of the interface between the Laplace pressure and the interfacial tension. In the cell-wall geometry (where $1/R_1=0$) one can show that the equation reducew to [58] :

$$\frac{x}{l_c} = \left[arccosh\left(\frac{2l_c}{y}\right) - arccosh\left(\frac{2l_c}{h}\right) + \left(4 - \frac{h^2}{l_c^2}\right)^{\frac{1}{2}} - \left(4 - \frac{z^2}{l_c^2}\right)^{\frac{1}{2}} \right] \quad (2.4)$$

$$h = \sqrt{2l_c^2\,(1 - sin\theta)} \quad (2.5)$$

where x is the distance to the vertical wall, z the height of the profile above the flat level far away from the wall, and h is the meniscus contact height at x = 0 . h is the contact height. The (X,Z) profile was observed and recorded using an optical microscope (X4 objective) rotated by 90° equipped with a digital camera (**Figure 2-10** b) , computed using the ImageJ software and finally fitted to equation 2.4 (**Figure 2-10** c). The left and right profiles on both sides of the cell were measured and averaged.

γ_{cc} was found to be indeed very low (311 µN/m) in agreement with values found in the recent literature on water/water interfacial tension in both associative complex coacervates [52-56] and segregative aqueous two phase systems (ATPS) (dextran/PEG [59], dextran/gelatin [60]). A very small amount of energy is then sufficient to create an additional surface between the two coexisting PDADMAC/PANa phases; no ion pair break-up is then necessary but only their redistribution in the case of a neutral complex [61]. This low energy barrier will facilitate the transfer of actives into the denser dispersed phase. This key property is at the origin of the celebrated encapsulation/sequestration properties of these water-in-water emulsion system [62]. It is therefore essential for various applications to be able to stabilize these interfaces against coaserning in order to avoid any short-term macroscopic phase separation. [63]. This particular topic will be the subject of a future PhD in our group…

In the next chapter, the liquid-liquid interfacial tension will be measured in a systematic way in order to better understand the different factors influencing the internal structure of the coacervate phase.

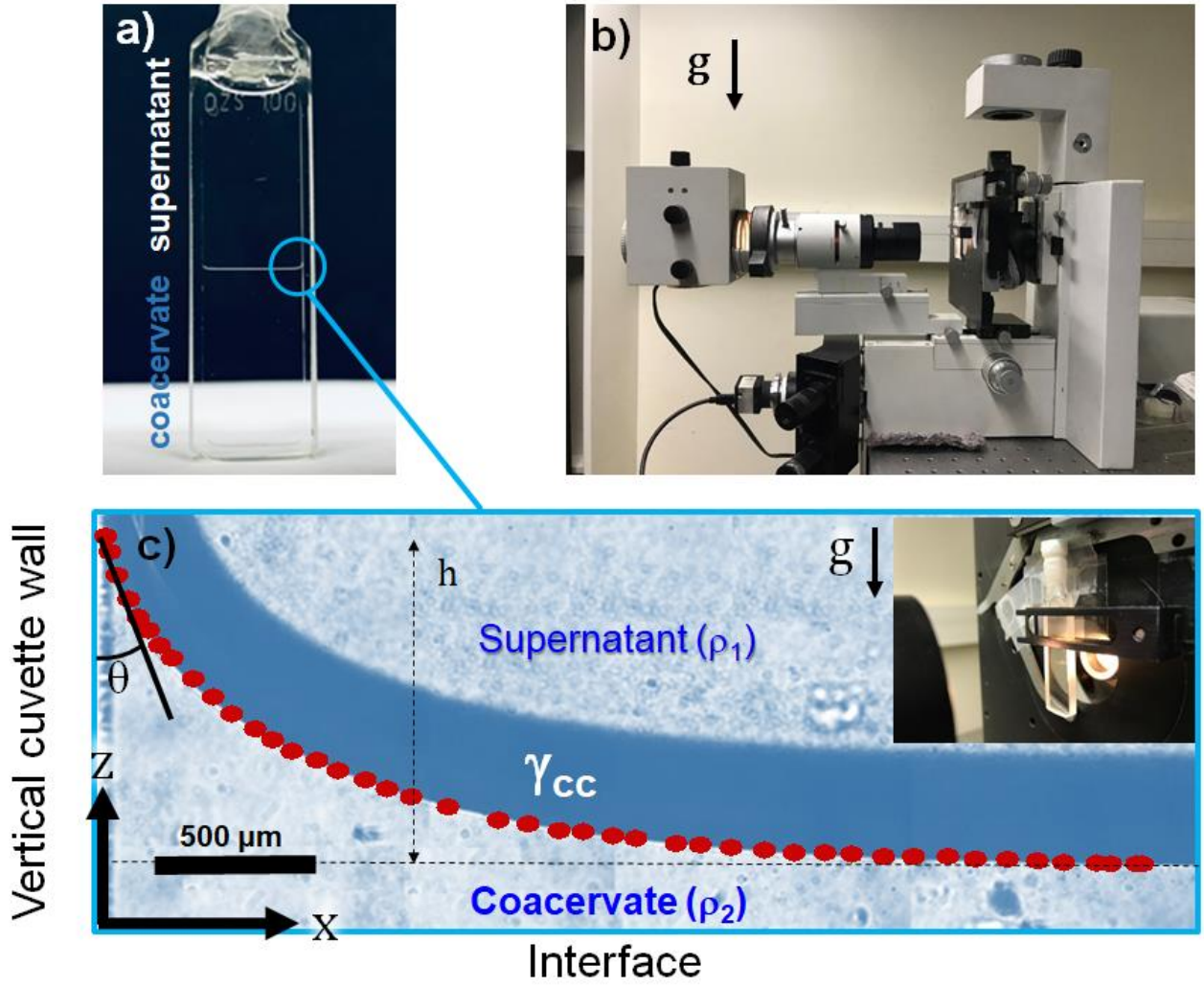

Figure 2-10. (a) Macroscopic phase separation obtained after 14 days after complexation of the PDADMAC/PANa system prepared from 18.6 mM PE solutions at charge stoichiometry (Z = 1). A clear separation between the dense coacervate phase and the macromolecule-depleted supernatant is visible. (b) Optical microscope setup (x4 objective) rotated 90° to image the liquid-liquid interfacial profile near the cell wall. (c) The static interfacial profile was fitted (red dots) to the generalize Laplace–Young equation (see Equation (2.3)) to extract the capillary length scale l_c to compute the interfacial tension $\gamma_{cc.}$

2.4 Conclusions

In this work, we highlighted that simple surface tension measurements at the air/water and water/water interface can be a very sensitive and discriminating tool to study the structure and formation mechanisms of polyelectrolyte complexes. This approach allows to finely characterize the different structures formed during the “electrostatic” complexation of polyelectrolytes of opposite charge as a function of the molar charge ratio Z = [-]/[+] and the interaction strength. For the strongly and weakly interacting PE systems studied in this work, the surface tension of the complexes decreases as the system approaches charge stoichiometry (Z = 1) whenever the complexation occurs in the presence of excess PDADMAC (Z < 1) or excess polyanion (Z > 1). A scenario consistent with an increased level of charge neutralization of PEs forming increasingly hydrophobic and neutral surface-active species, in agreement as well with zeta potential data.

In addition, the behavior at stoichiometry (Z = 1) was particularly informative about the physical nature of the complexes. In the PDADMAC/PANa system that undergoes a liquid–liquid phase transition at Z = 1 (formation of coacervate microdroplets), the surface tension of the suspension just after complexation is equal to that measured in the supernatant after macroscopic phase separation, suggesting that the surfaces-active species must be similar in both phases; a feature consistent with a system at equilibrium. In the PDADMAC/PSSNa system at Z = 1, the surface tension of the supernatant after two weeks was close to that of water, suggesting that the PSSNa-based complexes have completely sedimented, in contrast to the PANa-based ones where soluble complexes remain in solution; a feature consistent with the complete liquid–solid phase separation of a non-equilibrium system.

In addition, the high sensitivity of surface tension measurements, which can detect the presence of trace amounts of aggregates and other precursors in the supernatant while turbidity measurements yield optically transparent supernatants, allows for very accurate determination of the exact or “true” charge stoichiometry of the complexes.

To finalize the characterization of the weakly interacting PDADAMAC/PANa system, the water/water interfacial tension between the dilute phase (supernatant) and the concentrated phase of the coacervate was measured using the generalized Young–Laplace equation. A value

of ~311 μN/m was found in agreement with other macromolecular systems developing an ultra-low water/water interfacial tension (complex coacervates, biocondensates, and ATPS). This property allows these water-in-water (W/W) emulsions to efficiently encapsulate actives of interest in the dispersed phase but also makes them very difficult to stabilize [63, 64].

References

[1] Wilts, E.M., J. Herzberger, and T.E. Long, *Addressing water scarcity: cationic polyelectrolytes in water treatment and purification.* Polymer International, 2018. **67**(7): p. 799-814.

[2] Schnell, C.N., et al., *Polyelectrolyte complexes for assisting the application of lignocellulosic micro/nanofibers in papermaking.* Cellulose, 2018. **25**(10): p. 6083-6092.

[3] Schmitt, C. and S.L. Turgeon, *Protein/polysaccharide complexes and coacervates in food systems.* Advances in Colloid and Interface Science, 2011. **167**(1): p. 63-70.

[4] Meka, V.S., et al., *A comprehensive review on polyelectrolyte complexes.* Drug Discovery Today, 2017. **22**(11): p. 1697-1706.

[5] Llamas, S., et al., *Adsorption of polyelectrolytes and polyelectrolytes-surfactant mixtures at surfaces: a physico-chemical approach to a cosmetic challenge.* Adv Colloid Interface Sci, 2015. **222**: p. 461-87.

[6] Shakshi, R., S. Pramod Kumar, and M. Rishabha, *Pharmaceutical and Tissue Engineering Applications of Polyelectrolyte Complexes.* Current Smart Materials, 2018. **3**(1): p. 21-31.

[7] Buriuli, M. and D. Verma, *Polyelectrolyte Complexes (PECs) for Biomedical Applications*, in *Advances in Biomaterials for Biomedical Applications*, A. Tripathi and J.S. Melo, Editors. 2017, Springer Singapore: Singapore. p. 45-93.

[8] Lebovka, N.I., *Aggregation of Charged Colloidal Particles*, in *Polyelectrolyte Complexes in the Dispersed and Solid State I: Principles and Theory*, M. Müller, Editor. 2014, Springer Berlin Heidelberg: Berlin, Heidelberg. p. 57-96.

[9] Fu, J. and J.B. Schlenoff, *Driving Forces for Oppositely Charged Polyion Association in Aqueous Solutions: Enthalpic, Entropic, but Not Electrostatic.* Journal of the American Chemical Society, 2016. **138**(3): p. 980-990.

[10] Wang, Q. and J.B. Schlenoff, *The Polyelectrolyte Complex/Coacervate Continuum.* Macromolecules, 2014. **47**(9): p. 3108-3116.

[11] Liu, X., J.P. Chapel, and C. Schatz, *Structure, thermodynamic and kinetic signatures of a synthetic polyelectrolyte coacervating system.* Adv Colloid Interface Sci, 2017. **239**: p. 178-186.

[12] Liu, X., et al., *Early stage kinetics of polyelectrolyte complex coacervation monitored through stopped-flow light scattering.* Soft Matter, 2016. **12**(44): p. 9030-9038.

[13] Vitorazi, L., et al., *Evidence of a two-step process and pathway dependency in the thermodynamics of poly(diallyldimethylammonium chloride)/poly(sodium acrylate) complexation.* Soft Matter, 2014. **10**(47): p. 9496-9505.

[14] Ishimuro, Y. and K. Ueberreiter, *The surface tension of poly(acrylic acid) in aqueous solution.* Colloid and Polymer Science, 1980. **258**(8): p. 928-931.

[15] O. Theodoly, R.O., and C.E. Williams, *Adsorption of hydrophobic polyelectrolytes at the air/water interface: Conformational effect and history dependence.* The European Physical Journal E, 2001. **5**: p. 51-58.

[16] Miller, B.A.N.S.N.N.G.L.R., *Dynamic Surface Properties of Sodium Poly(styrenesulfonate) Solutions.* Macromolecules, 2004. **37**: p. 2519-2526.

[17] Noskov, B.A., et al., *Dynamic surface elasticity of polyelectrolyte solutions.* Colloids and Surfaces A: Physicochemical and Engineering Aspects, 2007. **298**(1-2): p. 115-122.

[18] Smith, H.Y.M.K.A.M.R.I.S.S.J.M.G.S., *Adsorption of Poly(styrenesulfonate) to the Air Surface of Water by Neutron Reflectivity.* Macromolecules, 2000. **33**: p. 6126-6133.

[19] Smith, H.Y.M.S.K.A.M.M.J.S.R.I.S.S.J.M.G.S., *Adsorption of Sodium Poly(styrenesulfonate) to the Air Surface of Water by Neutron and X-ray Reflectivity and Surface Tension Measurements: Polymer Concentration Dependence.* Macromolecules, 2002. **35**: p. 9737-9747.

[20] Owiwe, M.T., A.H. Ayyad, and F.M. Takrori, *Surface tension of the oppositely charged sodium poly(styrene sulfonate) /benzyldimethylhexadecylammonium chloride and sodium poly(styrene sulfonate)/polyallylamine hydrochloride mixtures.* Colloid and Polymer Science, 2020. **298**(9): p. 1197-1204.

[21] Dickhaus, B.N. and R. Priefer, *Determination of polyelectrolyte pKa values using surface-to-air tension measurements.* Colloids and Surfaces A: Physicochemical and Engineering Aspects, 2016. **488**: p. 15-19.

[22] Okubo, T. and K. Kobayashi, *Surface Tension of Biological Polyelectrolyte Solutions.* Journal of Colloid and Interface Science, 1998. **205**(2): p. 433-442.

[23] Ríos, H.E., et al., *Surface properties of cationic polyelectrolytes hydrophobically modified.* Colloids and Surfaces A: Physicochemical and Engineering Aspects, 2011. **384**(1): p. 262-267.

[24] Millet, F., et al., *Adsorption of Hydrophobically Modified Poly(acrylic acid) Sodium Salt at the Air/Water Interface by Combined Surface Tension and X-ray Reflectivity Measurements.* Langmuir, 1999. **15**(6): p. 2112-2119.

[25] Taylor, D.J., R.K. Thomas, and J. Penfold, *Polymer/surfactant interactions at the air/water interface.* Adv Colloid Interface Sci, 2007. **132**(2): p. 69-110.

[26] Khan, N. and B. Brettmann, *Intermolecular Interactions in Polyelectrolyte and Surfactant Complexes in Solution.* Polymers (Basel), 2018. **11**(1).

[27] La Mesa, C., *Polymer–surfactant and protein–surfactant interactions.* Journal of Colloid and Interface Science, 2005. **286**(1): p. 148-157.

[28] Budhathoki, M., et al., *Improved oil recovery by reducing surfactant adsorption with polyelectrolyte in high saline brine.* Colloids and Surfaces A: Physicochemical and Engineering Aspects, 2016. **498**: p. 66-73.

[29] Shulevich, Y.V., et al., *Purification of fat-containing wastewater using polyelectrolyte–surfactant complexes.* Separation and Purification Technology, 2013. **113**: p. 18-23.

[30] Mirtič, J., et al., *Polyelectrolyte–surfactant–complex nanoparticles as a delivery platform for poorly soluble drugs: A case study of ibuprofen loaded cetylpyridinium-alginate system.* International Journal of Pharmaceutics, 2020. **580**: p. 119199.

[31] Grządka, E., J. Matusiak, and M. Stankevič, *Interactions between fluorocarbon surfactants and polysaccharides.* Journal of Molecular Liquids, 2019. **283**: p. 81-90.

[32] Bago Rodriguez, A.M., B.P. Binks, and T. Sekine, *Emulsion stabilisation by complexes of oppositely charged synthetic polyelectrolytes.* Soft Matter, 2018. **14**(2): p. 239-254.

[33] Bago Rodriguez, A.M., B.P. Binks, and T. Sekine, *Novel stabilisation of emulsions by soft particles: polyelectrolyte complexes.* Faraday Discussions, 2016. **191**(0): p. 255-285.

[34] Generalova, A.N., et al., *Advantages of interfacial tensiometry for studying the interactions of biologically active compounds.* Colloids and Surfaces A: Physicochemical and Engineering Aspects, 2007. **298**(1): p. 88-93.

[35] Nekrasova, T.N., et al., *Potentiometric titration of polyacrylic acid, polymethacrylic acid and poly-l-glutamic acid.* Polymer Science U.S.S.R., 1965. **7**(5): p. 1008-1018.

[36] Chen, P., et al., *Axisymmetric Drop Shape Analysis (ADSA) and its Applications*, in *Studies in Interface Science*, D. MÖbius and R. Miller, Editors. 1998, Elsevier. p. 61-138.
[37] Manning, G.S., *Limiting Laws and Counterion Condensation in Polyelectrolyte Solutions I. Colligative Properties.* The Journal of Chemical Physics, 1969. **51**(3): p. 924-933.
[38] Oosawa, F., *Polyelectrolytes*. 1971 New York: M. Dekker.
[39] Abramzon, A.A. and R.D. Gaukhberg, *Surface tension of salt solutions.* Zhurnal Prikladnoj Khimii, 1993. **66**(9): p. 2145-2156.
[40] Leroy, P., et al., *Predicting the surface tension of aqueous 1:1 electrolyte solutions at high salinity.* Geochimica et Cosmochimica Acta, 2010. **74**(19): p. 5427-5442.
[41] Sedlak, M., *What can be seen by static and dynamic light scattering in polyelectrolyte solutions and mixtures?* Langmuir, 1999. **15**(12): p. 4045-4051.
[42] Kabanov, V.A. and A.B. Zezin, *A new class of complex water-soluble polyelectrolytes.* Die Makromolekulare Chemie, 1984. **6**(S19841): p. 259-276.
[43] Muthukumar, M., *Ordinary–extraordinary transition in dynamics of solutions of charged macromolecules.* Proceedings of the National Academy of Sciences, 2016. **113**(45): p. 12627-12632.
[44] Mende, M., et al., *Influence of the Hydrophobicity of Polyelectrolytes on Polyelectrolyte Complex Formation and Complex Particle Structure and Shape.* Polymers, 2011. **3**(3): p. 1363-1376.
[45] Qi, L., et al., *Influence of the Formulation Process in Electrostatic Assembly of Nanoparticles and Macromolecules in Aqueous Solution: The Mixing Pathway.* The Journal of Physical Chemistry C, 2010. **114**(30): p. 12870-12877.
[46] Qi, L., et al., *Influence of the Formulation Process in Electrostatic Assembly of Nanoparticles and Macromolecules in Aqueous Solution: The Interaction Pathway.* The Journal of Physical Chemistry C, 2010. **114**(39): p. 16373-16381.
[47] Zhang, R. and B.I. Shklovskii, *Phase diagram of solution of oppositely charged polyelectrolytes.* Physica A: Statistical Mechanics and its Applications, 2005. **352**(1): p. 216-238.
[48] Veis, A. and C. Aranyi, *Phase separation in polyelectrolyte systems. I. Complex coacervates of gelatin.* The Journal of Physical Chemistry, 1960. **64**(9): p. 1203-1210.
[49] Kizilay, E., A.B. Kayitmazer, and P.L. Dubin, *Complexation and coacervation of polyelectrolytes with oppositely charged colloids.* Advances in Colloid and Interface Science, 2011. **167**(1): p. 24-37.
[50] Manga, M.S., et al., *Measurements of Submicron Particle Adsorption and Particle Film Elasticity at Oil–Water Interfaces.* Langmuir, 2016. **32**(17): p. 4125-4133.
[51] Michaels, A.S., L. Mir, and N.S. Schneider, *A Conductometric Study of Polycation—Polyanion Reactions in Dilute Aqueous Solution.* The Journal of Physical Chemistry, 1965. **69**(5): p. 1447-1455.
[52] Spruijt, E., et al., *Interfacial tension between a complex coacervate phase and its coexisting aqueous phase.* Soft Matter, 2010. **6**(1): p. 172-178.
[53] Ali, S. and V.M. Prabhu, *Characterization of the Ultralow Interfacial Tension in Liquid-Liquid Phase Separated Polyelectrolyte Complex Coacervates by the Deformed Drop Retraction Method.* Macromolecules, 2019. **52**(19): p. 7495-7502.
[54] Prabhu, V.M., *Interfacial tension in polyelectrolyte systems exhibiting associative liquid–liquid phase separation.* Current Opinion in Colloid & Interface Science, 2021. **53**: p. 101422.

[55] Priftis, D., R. Farina, and M. Tirrell, *Interfacial Energy of Polypeptide Complex Coacervates Measured via Capillary Adhesion.* Langmuir, 2012. **28**(23): p. 8721-8729.
[56] Qin, J., et al., *Interfacial Tension of Polyelectrolyte Complex Coacervate Phases.* ACS Macro Letters, 2014. **3**(6): p. 565-568.
[57] Aarts, D.G.A.L., J.H.v.d. Wiel, and H.N.W. Lekkerkerker, *Interfacial dynamics and the static profile near a single wall in a model colloid polymer mixture.* Journal of Physics: Condensed Matter, 2002. **15**(1): p. S245-S250.
[58] *The Physical Properties of Fluids*, in *An Introduction to Fluid Dynamics*, G.K. Batchelor, Editor. 2000, Cambridge University Press: Cambridge. p. 1-70.
[59] Vis, M., et al., *Interfacial Tension of Phase-Separated Polydisperse Mixed Polymer Solutions.* The Journal of Physical Chemistry B, 2018. **122**(13): p. 3354-3362.
[60] Atefi, E., J.A. Mann, and H. Tavana, *Ultralow Interfacial Tensions of Aqueous Two-Phase Systems Measured Using Drop Shape.* Langmuir, 2014. **30**(32): p. 9691-9699.
[61] Gucht, J.v.d., et al., *Polyelectrolyte complexes: Bulk phases and colloidal systems.* Journal of Colloid and Interface Science, 2011. **361**(2): p. 407-422.
[62] Zhao, M. and N.S. Zacharia, *Protein encapsulation via polyelectrolyte complex coacervation: Protection against protein denaturation.* The Journal of Chemical Physics, 2018. **149**(16): p. 163326.
[63] Douliez, J.-P., et al., *Preparation of Swellable Hydrogel-Containing Colloidosomes from Aqueous Two-Phase Pickering Emulsion Droplets.* Angewandte Chemie International Edition, 2018. **57**(26): p. 7780-7784.
[64] Esquena, J., *Water-in-water (W/W) emulsions.* Current Opinion in Colloid & Interface Science, 2016. **25**: p. 109-119.

Chapter 3

Tunable interaction strength in PDADMAC / PANa complex coacervate system

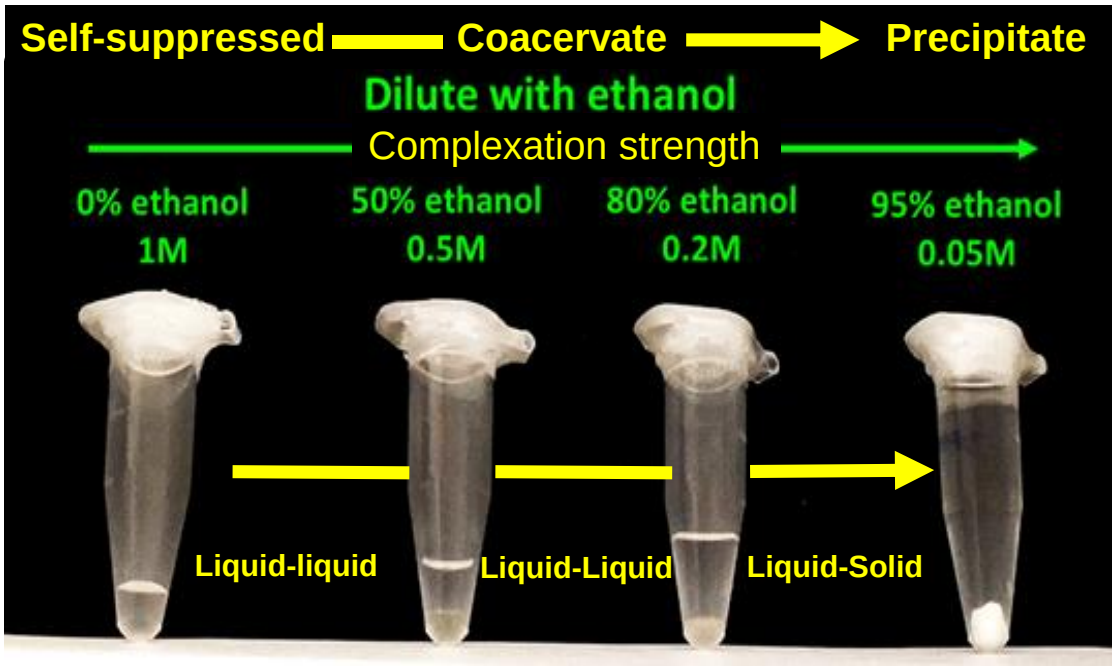

Abstract: In this chapter, we have focused our work on the coacervate phase of the PDADMAC/PANa obtained for Z=1. In particular, we have studied the influence of the complexation strength on the interfacial tension, polymer volume fraction and local structure of such polymer-rich phase in equilibrium with the polymer-poor supernatant. For this purpose, we systematically investigated the effect of the PE concentration, temperature, ionic strength and ethanol content on the polymer network structure using complementary techniques such as TGA, DLS, SANS and interfacial tension measurements. We put in evidence that the lattice correlation length is strongly dependent on the complexation strength and also that the coacervate phase has a lower critical solution temperature (LCST) character, that is, a critical behavior of the coacervate/supernatant interfacial energy that cancels at high concentration where a unique phase appears, the so-called self-suppressed coacervate phase (SSCV). The latter can furthermore be diluted or heated to obtain a new coacervate phase

with a different mesh size. Finally, when the ethanol fraction becomes very important, the liquid-liquid transition is replaced by a liquid-solid transition generating a solid precipitated as in the case of the strongly PDADMAC/PANa interacting system. Again, this highlights the key importance of interaction strength on the formation mechanisms and structural characteristics of PECs.

Keywords: polyelectrolyte complexes; complex coacervates; electrostatic interaction; complexation strength; interfacial tension; thermodynamic; local structures; morphologies.

3.1 Introduction

The previous chapter focused on PECs generated at low polymer concentration (18 mM) without salt addition for different Z molar charge ratios for the strongly and weakly interacting PDADMAC/PSSNa and PDADMAC/PANa systems, respectively. This chapter will be devoted to the study of the very peculiar and attractive complex coacervate phase generated around the charge stoichiometry in the PDADMAC/PANa system.

As briefly discussed in Chapter 1, these complex coacervate phases produced by an associative liquid-fluid phase transition (LLPS) generate chemically enriched microdroplets that have emerged in recent years as promising compartments for the construction of rudimentary forms of artificial cells.[1, 2] Due to their differential chemical composition and physical properties compared to the continuous phase, these crowded droplets spontaneously and selectively accumulate various solutes, [1, 2] including molecular dyes,[3] proteins or polynucleotides[4]. This effect due to the peculiar physicochemical environment found in the coacervate phase provides a simple means of localizing and concentrating functional species although the exact mechanism is not yet known in part because the local structure of this phase and the parameters that influence it are not systematically studied in the literature.

In this chapter, we will study the influence of the interaction force between oppositely charged PEs on the coacervate phase. To do so, we will adjust different physicochemical conditions such as the concentration and ionic strength of the PE stock solutions, the temperature or the addition of a cosolvent such as ethanol in the mixture. The impact of some of these parameters on different key characteristics of the coacervate phase such as liquid-liquid interfacial tension, polymer content, bulk density, rheology and local polymer network structure will be studied.

3.2 Experimental materials and method

Polyelectrolytes (PEs). Poly (diallyldimethylammonium chloride) (PDADMAC, Mw ~ 100 000-200 000 g.mol-1) was purchased from Aldrich as 20 wt. % solution in water (Lot # 03530MS) and Poly (acrylic acid sodium salt) (PAANa, Mw ~ 2000 g.mol-1) were purchased

from Aldrich as powders (Lot # BCBF7673V), respectively. Before any use, the two polyelectrolytes were purified by extensive dialyzes against pure water and then freeze-dried. Both polymers were analyzed by size exclusion chromatography with a multi-angle light scattering detection to precisely determine the average molecular weights and dispersities (PDADMAC : Mw=44 200 g.mol-1 with PDI=1.59 - PANa : 2560 with PDI=1.45).[5] PANa, there is a certain amount of non-charged end groups. The content of acid groups was determined by conductometric titration experiments with 1M NaOH, giving a weight percentage of 84.2% for acid monomers. Individual stock solutions were made from the freeze-dried powders from filtered DI water using 0.2 µm Millipore membranes. The pH of each solution was set to 10 with the help of a 1M sodium hydroxide (NaOH). At such pH, the weak PANa polyanion is fully charged.[6]

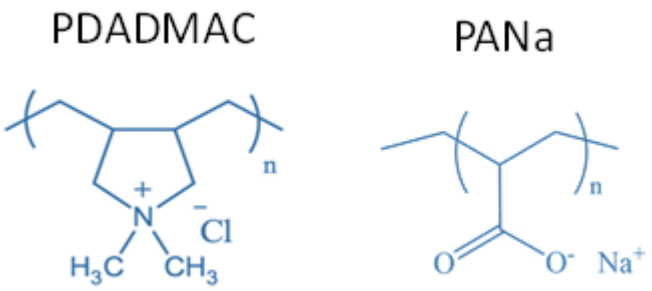

Figure 3-1. Chemical structure of PDADMAC and PANa.

Formulation of the coacervate phase. The coacervate phase was formed at stoichiometry with a molar charge ratio Z=1 defined as Z (-/+) = n(PANa) / n(PDADMAC) =1 where n(PDADMAC) and n(PANa) are the molar monomer concentrations of the individual PE solutions. In practice, the coacervate dispersion is obtained by mixing solutions of PDADMAC and PANa at the same (monomer) concentration. A monomeric molecular weight M_{w0} of 161 and 94 $g.mol^{-1}$ was used for PDADMAC and PANa, respectively, meanwhile all PEs solutions were filtered through Millipore membranes of 0.2 µm pore size.

The coacervation was studied under different conditions of PE concentration, ionic strength (NaCl), temperature and by adding ethanol. In the following, the concentration refers to the total PE concentration after mixing equivalent volumes of equimolar PDADMAC and

PANa solution. As such, the total concentration also corresponds to initial concentrations of individual PEs. The coacervate formation was studied at PE concentrations ranging from 18.6mM to mM. For the study of the ionic strength, the coacervate phase was generated from 0.3M PE solutions containing different concentrations of NaCl: 0.05M, 0.1M and 0.2M. The coacervate phase generated from 0.7 M stock solutions in PEs was also studied at different temperatures: 22°C (RT), 35°C, 40°C and 50°C.The coacervate phase generated from 0.5M stock solutions was also prepared with different volume fractions of ethanol: 0%, 20%, 30% and 50%.

In all cases, a certain volume of PDADMAC solution was injected rapidly with a syringe into a vial containing same volume of PANa solution, followed by vigorous shaking for 2 minutes and centrifugation for 10 minutes at 3600 rpm. The mixtures were then left to stand for at least a week (preferentially 3 weeks) at room temperature to get as close as possible to equilibrium of the system. We used a hot plate equipped with a temperature probe to heat the solutions in a water bath, shown in **Figure 3-2**. For SANS analyses at various temperatures, an oven was used to equilibrate the quartz cuvettes filled with the coacervate phase in equilibrium with the supernatant.

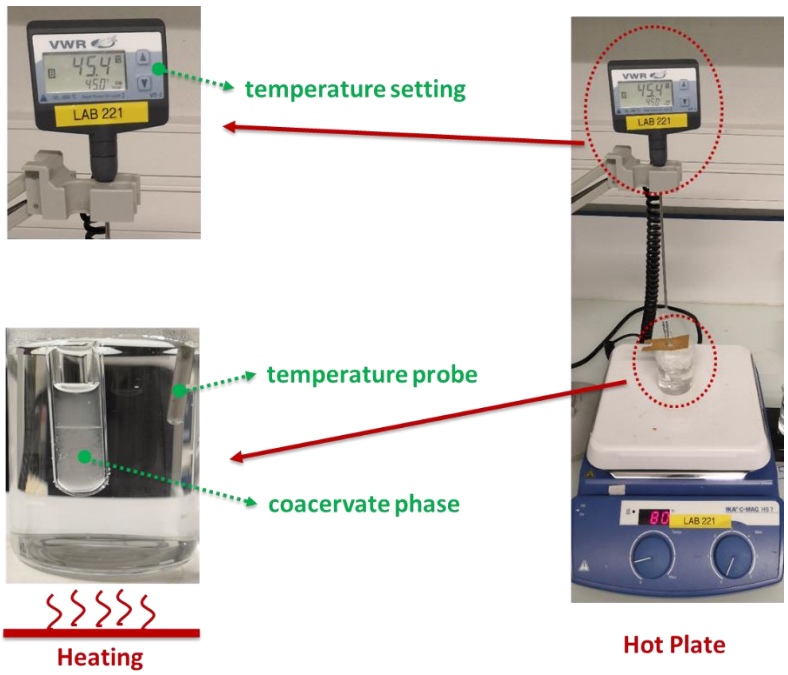

Figure 3-2. Heating system with a temperature probe in water bath.

Small-angle neutron scattering (SANS). SANS experiments were performed on D22 installed at the high-flux reactor of the Institut Laue-Langevin (ILL, Grenoble, France). The SANS intensity was measured at two sample-to-detector distances, 5.6 and 17.6m, using a 6-Å˚ neutron beam to cover a q range from 3×10^{-3} to 0.6 $Å^{-1}$. The measured two-dimensional scattering pattern was converted to a one-dimensional scattering profile by following the standard procedure: circular averaging, correction of transmission, and substations of buffer scattering and background. Thereafter, the SANS profiles with sample-to-detector distances of 5.6 and 17.6 m were merged into one profile using GRASP software (https://www.ill.eu/fr/users-en/scientific-groups/large-scale-structures/grasp/). All polymer solutions were made in D_2O. Deuterated ethanol (EtOD) was also used to make binary water/ethanol mixtures. The solution pD was ajusted using NaOD. Exposure time of 1h was necessary to obtain good statistics.

For other experimental techniques, details were provided in chapter 2.

These coacervates formed at charge stoichiometry under different conditions of PE concentration, ionic strength, temperature and ethanol fraction were then studied by using complementary techniques such as TGA, optical microscopy, X-ray and neutron scattering (SAXS and SANS), dynamic light scattering and liquid-liquid interfacial tension measurements.

3.3 Results and Discussions

3.3.1 The effect of concentration

In most studies related to complex coacervation, the PE concentration is held constant and the ionic strength and/or molecular weight of the chains are often used as adjustable parameters to study the phase diagram. The impact of the overall PE concentration is rarely studied in a systematic way, especially for high values.

In this work, we studied the effect of PE stock solution concentration on coacervation yield, composition and structure. Four different concentrations were used: 18.6, 100, 400, 700 and 800 mM (total concentration in PE). As mentioned in the materials and methods section,

after preparation, each coacervate phase was allowed to stand for at least one week to allow the system to equilibrate.

3.3.1.1 Interfacial tension

In a first set of experiments, the density of the supernatant and coacervate phases as well as the density difference $\Delta\rho$ were measured by using a Density Meter (DMA 4100M, Anton Paar) with a resolution of 0.0001 g.m^{-3}. It can be clearly seen in **Table 3-1** that the density of the supernatant increases with the concentration of the stock solution while that of the coacervate decreases.

Table 3-1. Density (kg/m^3) of the coacervate and supernatant phases, difference in bulk density between the two phases and capillary length l_c for different PE concentrations.

Concentration (mM)	18.6	100	400	700	800
Coacervate phase	1081.1	1073.4	1056.0	1034.2	1025
Supernatant phase	998.7	1001.1	1007.9	1019.8	
$\Delta\rho$ (kg/m^3)	82.4	72.3	48.1	14.4	0
l_c (µm)	620	600	350	285	0

The data are then plotted in **Figure 3-3.** The density in the coacervate and the supernatant vary linearly and symmetrically with the PE concentration. As the concentration increases, the coacervate phase generated becomes lighter with, consequently, a denser supernatant until a particular concentration where a monophasic phase is obtained (~ 800 mM). This concentration refers to the ***self-suppressed coacervation***. We will come back to this very important point later on.

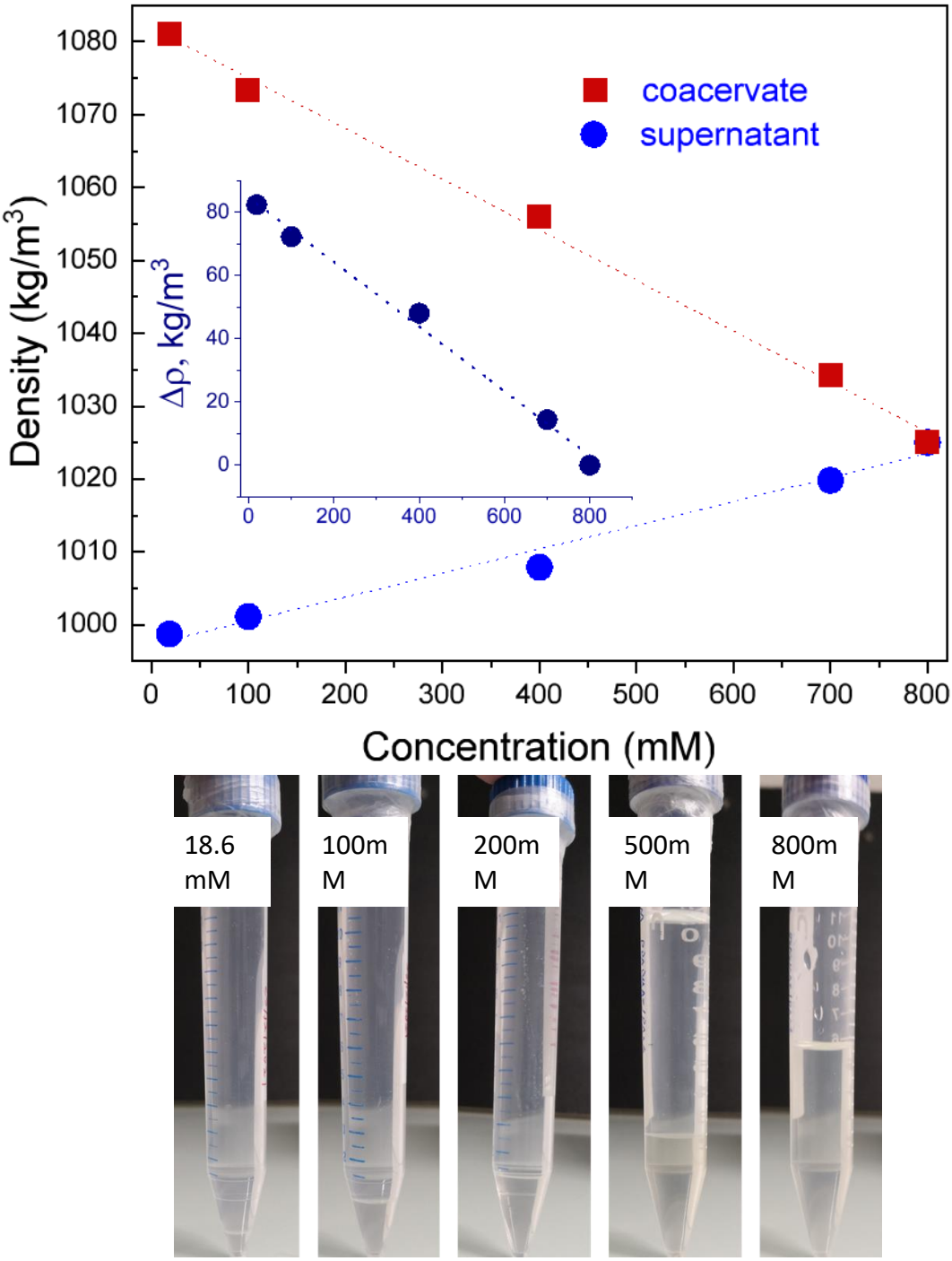

Figure 3-3. Variation of the density of both the supernatant and coacervate phase as a function of the PE concentration for the PDADMAC/PANa system at pH 10 without added salt. Insert: variation of $\Delta\rho$. The dotted lines are a linear fit to the data.

In a second set of experiment, the surface tension of the supernatant (γ_s) and the interfacial tension γ_{cc} between the dense complex coacervate (CC) and the macromolecule-depleted phase were measured as described in chapter 2. γ_s was measured using the pendant drop method (**Figure 3-4**).

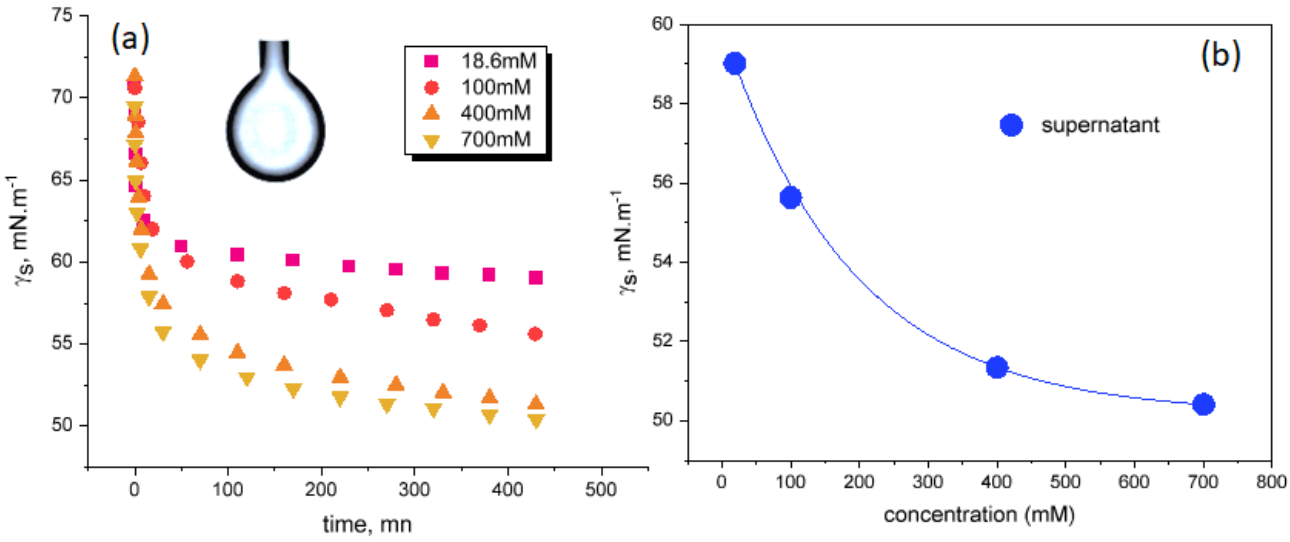

Figure 3-4. (a) Dynamic and (b) static surface tension γ_s of the supernatant (liquid/air interface) for different stock solution concentrations measured using the pendant drop method. The static surface tension was measured after 450 mn. The solid line is a guide for the eyes.

As expected from the density results, the surface tension after 450 min decreases well with the PE concentration in agreement with denser supernatants where more polymer complexes will adsorb at the air-water interface as discussed in chapter 2. At ~800 mM where we have a single phase, the surface tension of the concentrated solution containing both PEs is the lowest. An effect that is qualitatively similar with the case of individual PEs seen in chapter 2 where the surface tension decreases with PE concentration. An effect that has been attributed to the screening effect of free counter ions (see chapter 2).

In order to obtain γ_{cc}, the capillary length scale l_c was obtained by analyzing the static interfacial profile near the vertical wall of the cell with a shape given by the generalized Young-Laplace equation connecting capillary pressure with curvature and surface tension for the case of a flat wall (see Eq. 2.4).

Figure 3-5. shows the four profiles. It can be clearly seen that the profiles and then $l_c(=\sqrt{\frac{\gamma_{cc}}{\Delta\rho * g}})$ (see **Table 3-1**) are quite different suggesting that the interfacial tension γ_{cc} does indeed vary with the concentration of the stock solution.

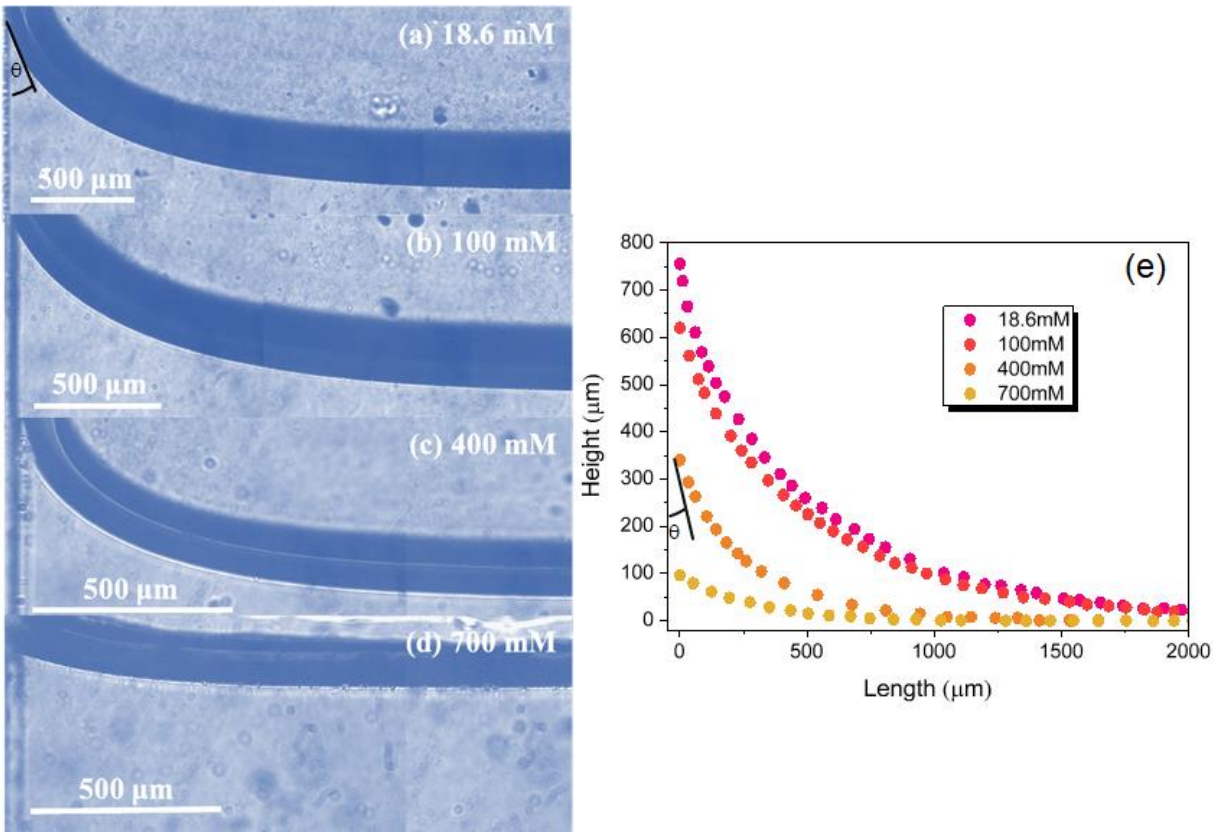

Figure 3-5. Optical microscopy images (x4 objective) of the liquid-liquid interfacial profile near the cell wall between the supernatant and the coacervate phase for PDADMAC/PANa system obtained at charge stoichiometry at pH 10 for different PE concentrations (a) 18.6mM, (b) 100mM, (c) 400mM and (d) 700mM near the cell wall. (e) Extracted profile using Image J.

We can clearly see that the interfacial tension decreases with the concentration until a critical value of about 800mM where coacervation is suppressed, as we have seen earlier, with the presence of a single phase containing both types of PEs. This critical concentration for which $\gamma_{cc} = 0$ by definition will be called hereafter self-suppressed coacervate concentration or CSSCV.

Figure 3-6 shows the variation of the interfacial tension γ_{cc} as a function of the PE concentration. We can clearly see that the interfacial tension decreases with the concentration until a critical value of about 800mM where coacervation is suppressed, as we have seen earlier, with the presence of a single phase containing both types of PEs. This critical concentration for which $\gamma_{cc} = 0$ by definition will be called hereafter self-supressed coacervation concentration or C_{SSCV}.

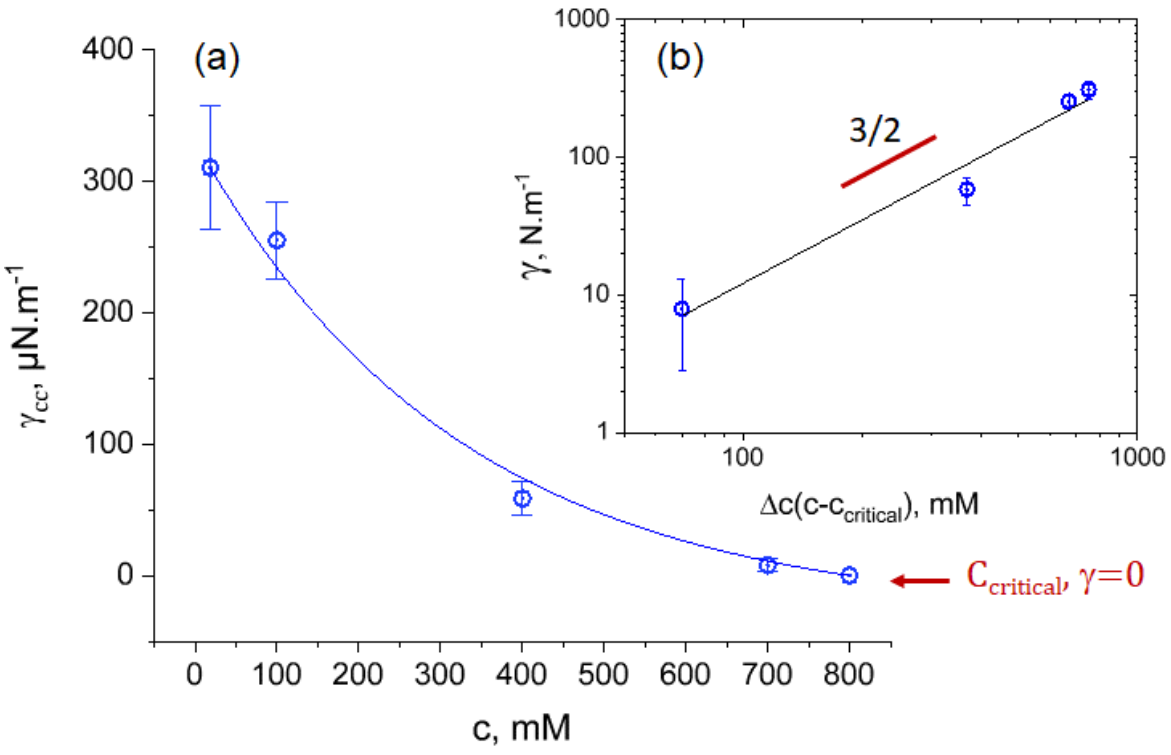

Figure 3-6. (a) Liquid-liquid interfacial tension $\gamma_{cc}(= {l_c}^2 \Delta\rho * g)$ between the supernatant and the coacervate phases as a function of the PE concentration. The blue solid line is a guide for the eyes. At critical (~800 mM), $\gamma_{cc} = 0$ and the medium is monophasic. (b) Log-Log representation of γ_{cc} as a function of $\Delta c = c - c_{critical}$. The black line is a linear fit with a slope of 3/2.

It is probably time to take a step back from these very surprising but very interesting results by exploring the literature. Self-suppression of coacervation was widely reported by by Overbeek et al.[7] and Veis et al.[8] for polyelectrolyte systems more than fifty years ago. But this phenomenon has not really been documented or investigated in depth in the literature since then, as most of the coacervation studies have been performed at a given (low) concentration. In the minds of these pioneers, self-suppression occurred when the precursor complexes (generated at charge stoichiometry, Z=1) overlapped at a given overlap concentration C*. At this particular concentration, the gain in entropy of mixing generally attributed to coacervation (small globally neutral precursor PECs mix in larger coacervate droplets) is thus strongly reduced or almost null, which will naturally prevent the system from coacerving for obvious reasons of non-minimization of the free energy of complexation. This explanation seems rather difficult to rationalize in our system.

Very recently, as we were writing these lines, a paper was published in macromolecules (November 15, 2021) by Zhang and Wang addressing the interfacial structure and tension of polyelectrolyte complex coacervates from a theoretical perspective [9]. They developed a model that shows, among other things, a decrease in interfacial tension with the concentration of the individual stock solutions for symmetric and asymmetric PE concentration (symmetric means here that polycations and polyanions have the same chain length, charge fraction, and concentration. As can be anticipated, the interfacial tension γ is dominated by the concentration profiles of the PE. They showed that γ is a function of the degree of phase separation S defined.

$$S \equiv \sqrt{\sum_{j=P_-,P_+,+,-} (\varphi^I - \varphi^{II})^2} \qquad (3.1)$$

Or in other words, the mismatch in the composition of the two phases, in agreement with our "density mismatch" observed in **Figure 3-3**. However, mechanistically, it is not clear what causes the decrease of γ $(\sim S^3)$ and, more importantly, why we observe a critical concentration where coacervation is self-suppressed.

In 2011, Spruijt *et al.* were the first to measure the interfacial tension of a symmetric coacervate using surface colloidal probe AFM measurements [10] . They showed that at a given (and low) PE concentration, γ decreases with increasing salt concentration φ_s as

$$\gamma \sim |\varphi_{s-critical} - \varphi_s|^{3/2} \qquad (3.2)$$

near the critical salt concentration ϕ_{s-c} where coacervation disappears. A critical concentration, thoroughly investigated in our group for the PDADMAC/PAA_{2k} system (desalting transition concentration) with a value around 0.3M (NaCl) in the case of 2k PAA chains [11]. This particular salt dependence was confirmed later by Priftis et al. (SFA measurements [12]) and Ali et al. (deformed droplet retraction method [13]). More recently Qin *et al.* have rationalized this scaling law by combining the Voorn–Overbeek theory (see chapter 1) with the Cahn–Hillard mathematical theory describing the process of phase separation (whereby the two components of a binary fluid separate spontaneously and form

pure domains in each component)[14]. The data from these different works are gathered in **Figure 3-7**.

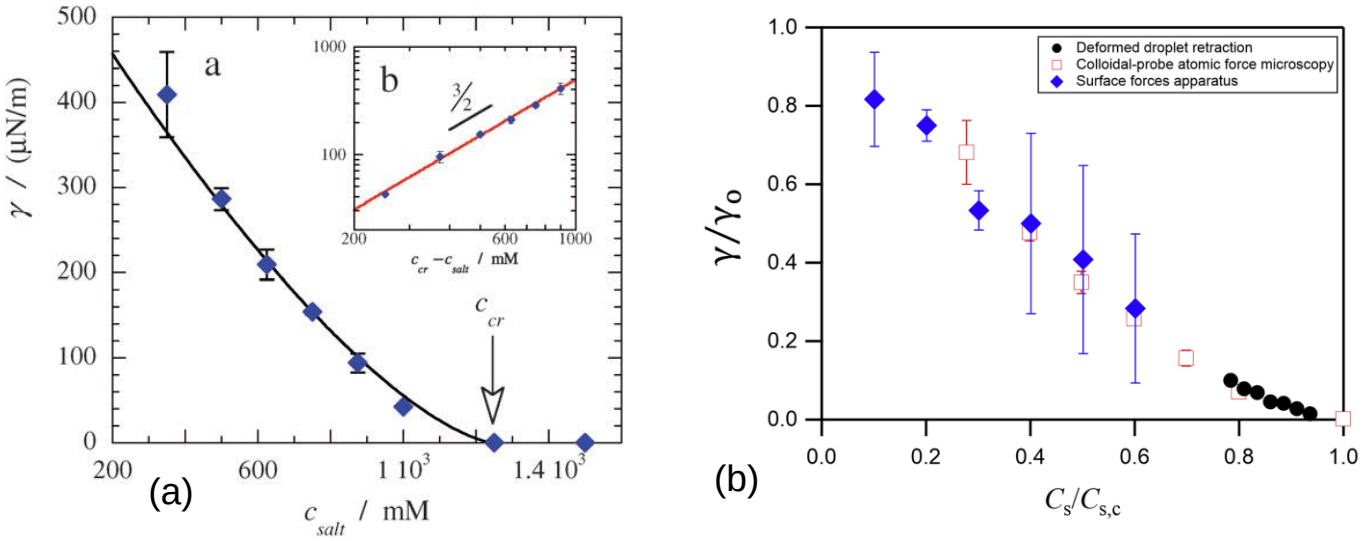

Figure 3-7. (a) Interfacial tension of complex coacervate phases γ as a function of salt concentration measured by colloidal probe AFM measurement [10]. The critical salt concentration, beyond which no capillary force could be measured, is indicated by the arrow. (b) Compilation of three different coacervate systems and interfacial tension probing techniques giving rise to the same salt dependency: Colloidal Probe-AFM (red square) from Spruijt *et al.(*Poly(trimethyl-aminoethyl methacrylate)/Poly(3-sulfopropyl methacrylate) [10]), Surface Force Apparatus (SFA - black diamond) from Priftis *et al. (*Poly(l-lysine hydrochloride)/ Poly(l-glutamic acid sodium salt)[12]), and Deformed drplet retraction (DDR - black sphere) from Ali et al. (potassium poly(styrene sulfonate)/Poly(diallydimethylammonium bromide)[13].

If we now plot our data from **Figure 3-6** (insert) on a double logarithmic scale as a function of $\Delta c = c - c_{SSCV}$ with C the PE concentration and C_{SSCV} the self-suppressed coacervation concentration, we find a linear variation with a slope of 3/2. The data of **Figure 3-7** and **Figure 3-6** then appear strikingly similar! In other words, the interfacial tension γ between the coacervate and supernatant phases does seem to vary in the same way when the salt concentration or the PE concentration is increased.

At this point, it is tempting to ask whether the ionic force generated by the free counterions can have a similar effect on the interfacial tension as the added salt ?

We know from Manning condensation theory that the concentration of free counterions in individual PE solutions increases linearly as $C_{counterions} = C_{PE}\, f_{eff}$, with f_{eff} the effective charged fraction of polymer units, at least for low concentration; a result that has been widely verified experimentally in the literature. In our system, the effective charge f_{eff} $(= 0.866\ \frac{a}{l_B})$ [15] is equal to 0.30 and 0.57 for (fully charged) PANa (a=0.25nm) and PDADMAC (a=0.47nm) respectively. In Chapter 2, we showed that the ionic strength generated by the free counterions was responsible for the decrease in surface tension with concentration. Similarly, it is therefore conceivable that such an increase in ionic strength is also responsible of the suppression of the coacervation. The interfacial tension decreases until there is no coacervation at about 800 mM with the presence of only one phase. At C_{SSCV}, one can estimate the ionic strength (*I*) of the mixture from the total concentration of free counter ions coming from PDADMAC and PANa:

$$I = (\tfrac{1}{2}) \sum C_i z_i^2 = \left(\tfrac{1}{2}\right) * (C_{PDAD}\, f_{eff} + \ C_{PANa} * \ f_{eff}) = (\tfrac{1}{2}) * (0.8 * 0.66 + 0.8 * 0.3) = 0.38\text{M}$$

A value not far away from the desalting transition concentration measured around 0.3M in our system[11]. However, De *et al.*[15] have shown recently that the extent of counterion condensation is greatly affected by the concentration and molecular weight of the polyelectrolyte, the concentration of the added electrolyte, and the temperature. The fractions of free counterions are found to increase as the PE concentration is increased likely due to an increase in the dielectric constant leading to a reduction in the Bjerrum length and then an increase in f_{eff}. Although the exact ionic strength present in our solution is difficult to estimate accurately, a direct measurement of the Na+ concentration would be interesting to perform in the future using an ion-selective electrode. Nevertheless, the ionic strength generated by the counterions could rationalize our observations on the variation of the interfacial energy up to a critical concentration at which coacervation is self-suppressed. Even if at this stage, we cannot exclude a contribution to the self-suppressed coacervation of an overlapping concentration of complexes, which remains difficult to define in our case.

As mentioned in the introduction, the very low interfacial tension of coacervates allows them to effectively encapsulate actives of interest, but also makes them very difficult to stabilize [16, 17]. From scaling laws arguments, the interfacial tension at a fluid-fluid interface is known to scale as $\gamma \sim k_B T/\xi^2$ where ξ is the interfacial thickness length scale [18, 19] which

can span tens of nm [20, 21]. As a result, the interfacial thickness between the coacervate phase and the surrounding medium can vary substantially with the concentration of stock solutions. A 4-fold change is foreseen in the PDADMAC/PANa system used here (**Figure 3-6.**).

One can therefore imagine that the difficulties encountered to stabilize coacervate droplets in an efficient and systematic way is partly due to a lack of knowledge of their essential characteristics: internal structure, interfacial energy and thickness. Finally, the fact that interfacial thicknesses can vary from a few tens to a hundred nm should lead us to carefully choose the type and size of stabilizing agents as well as their mechanism of action.

As already mentioned, our group in Bordeaux and those of J.-F. Berret, F Cousin and J. Fresnais in Paris have studied in depth the desalting transition of different PE/PE or PE/NPs systems. In these experiments, NaCl is added to the stock solutions to turn off the electrostatic interaction. The mixture is then diluted with or against DI water in order to decrease the ionic strength and to trigger again the complexation. [11, 22-28].

By analogy, we can formulate single-phase solution above C_{sscv} where the PEs no longer interact electrostatically and behave likely as neutral polymers as we have just seen. And then dilute it in a controlled manner to form increasingly dense coacervate phases. Indeed, it is likely that "dilution-induced coacervation" is mechanically similar to "self-suppressed coacervation" due to the equilibrium properties of the system.

3.3.1.2 Self-suppressed coacervation & reverse phase transition

Indeed, if we progressively dilute a monophasic transparent self-suppressed solution made at 1M below 0.8M, we obtain a turbid solution with the appearance of micron size coacervate droplets as can be seen in the optical macroscopy image shown in **Figure 3-8** suggesting that a reverse phase separation occurred.

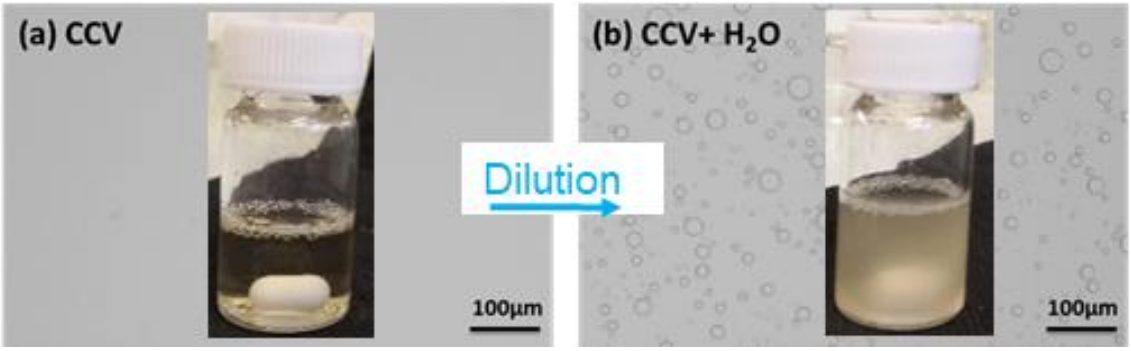

Figure 3-8. Optical microscopy images and photographs of self-suppressed PDADMAC/PANa 1 M solution (a) before and (b) after dilution below 0.8 M with DI water.

After a few days, macroscopic phase separation occurs showing the presence of a clear interface between the dense polymer-rich liquid coacervate and the polymer-poor supernatant phase, as shown in **Figure 3-9**. If we continue to dilute the previous solutions by adding DI water through the supernatant phase and let them stand for a few days to ensure equilibrium, we will then generate coacervate phases at different concentrations. We can notice that the level of the liquid-liquid interface actually decreases with concentration from 0.7 to 0.3M suggesting the formation of denser coacervate phases. An observation confirmed further down by TGA measurements.

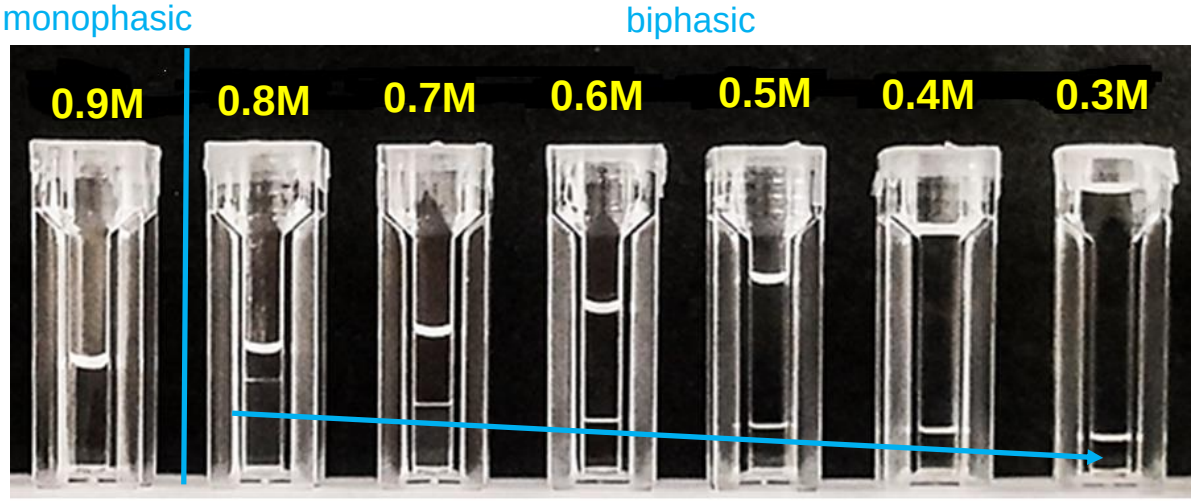

Figure 3-9. Optical photographs of reverse phase separation induced by dilution with DI water of a self-suppressed PDADMAC/ PANa solution prepared at 1M

Furthermore, by measuring the height ratio between the dense coacervate phase and the total solution in **Figure 3-9**, we can calculate the volume fraction of the coacervate and

then estimate the volume yield of the polymer-rich coacervate phase at different mixing concentrations. As the PE concentration increases, the volume fraction of CCV increases, resulting in an apparent increase in the yield of the coacervate phase production (**Figure 3-10**, red symbols).

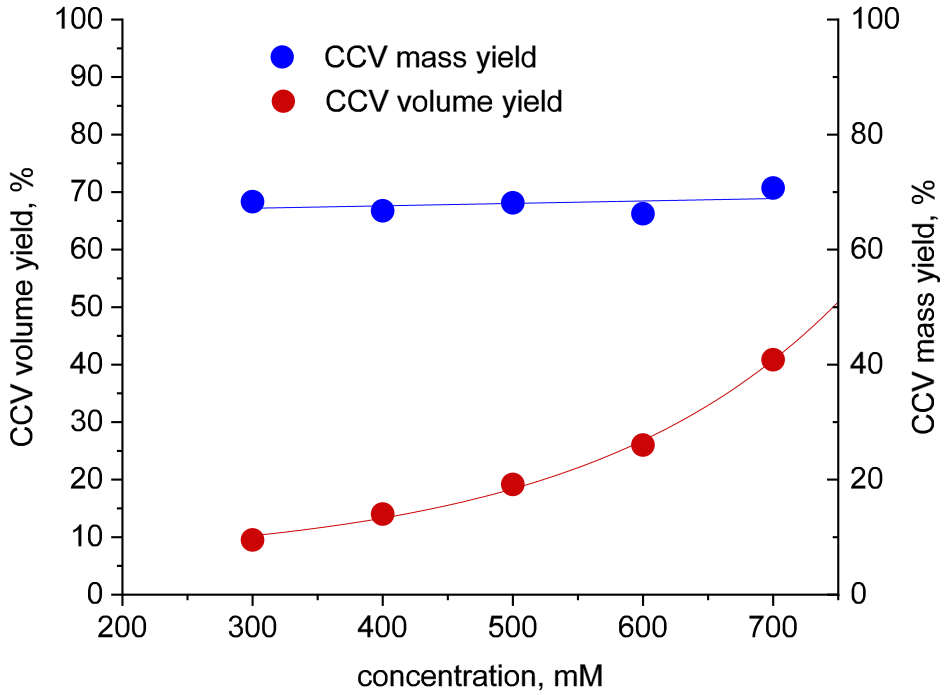

Figure 3-10. Volume and mass yield of the coacervated phase at different PE concentrations for the PDADMAC/PANa system. The phase separation is induced by dilution with DI water of a self-suppressed PDADMAC/ PANa solution prepared at 1 M.

What about the real polymer content inside the CCV phase? We can calculate the polymer mass yield defined as m_{CCV}/m_{total} where m_{CCV} is the mass in the CCV and m_{total} the total mass of PE initially introduced. m_{CCV} was calculated as the volume of the CCV phase multiplied by its density ? Strikingly, the polymer yield seems to be constant in each CCV phase, no polymer gain or loss! Only the internal structure of the CCV phase will change, as we will see below.

Thermogravimetric analyses (TGA) were then performed to further quantify the different solutions generated. They were first heated up to 80°C at 5°C /min with a final isotherm of 30 minutes to ensure all free water was evaporated. A final ramp at 5°C /min to 200°C was then performed to remove bound water this time. As expected, we can see in

Figure 3-11 that, the PEs content in the coacervate phase is much higher than in the supernatant at low concentrations. However, the polymer mass fraction clearly decreases with increasing concentration while that of the supernatant increases in line with the density measurements shown in **Figure 3-3**. The coacervate and supernatant phases become linearly lighter and denser respectively with the increase of the stock solution concentration. A result well in line with the density measurements shown in **Figure 3-3**.

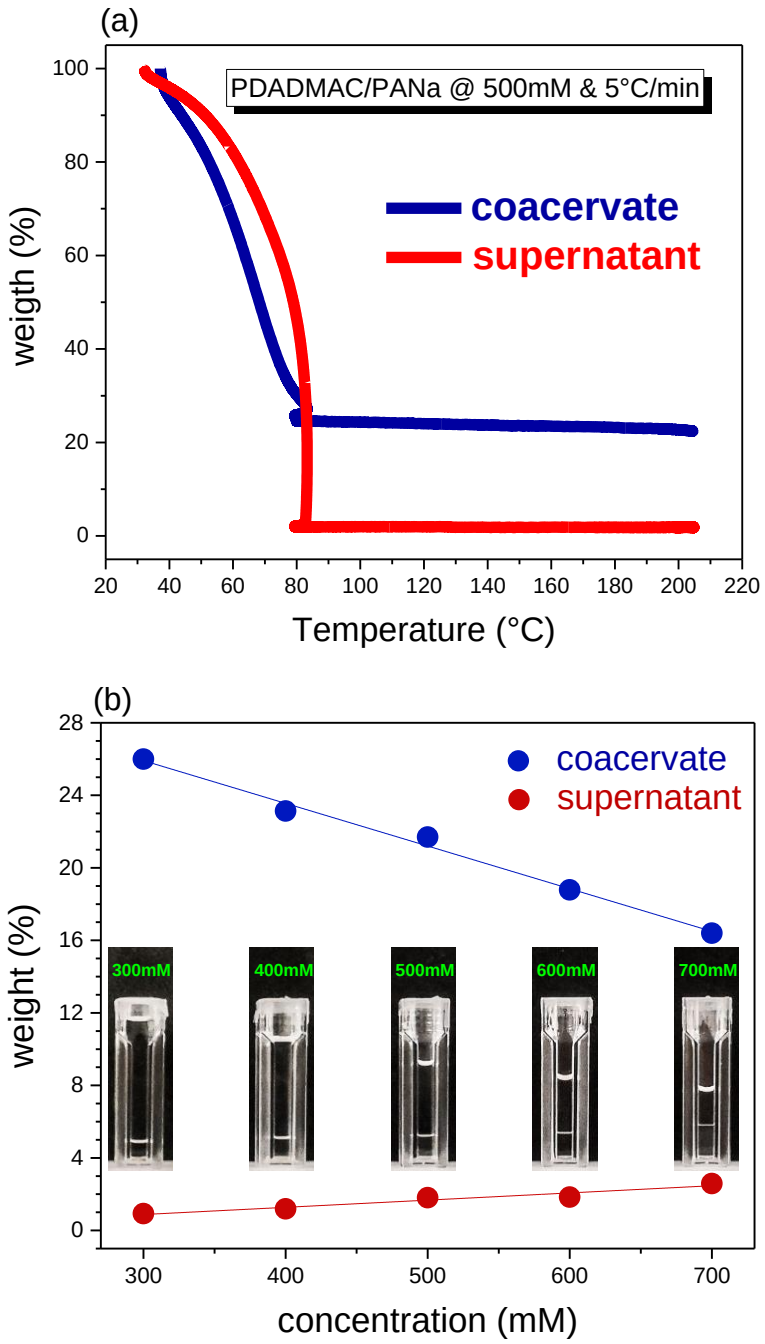

Figure 3-11. (a) Typical thermogravimetric analyses (TGA) experiment performed on a coacervate phase made from a 500mM PE solution. (b) Mass fraction of coacervate and supernatant phases

obtained from different concentrations of PDADMAC and PANa solutions. The solid lines correspond to a linear fit of the data.

The dilution of the coexisting phases will then reduce the ionic strength of the solution resulting from the free counter ions and consequently increase the intensity of the electrostatic complexation generating more and more dense coacervate phases, as the scheme showed in **Figure 3-12**. In other words, the counterions (Cl^- and Na^+) will tend to move away from the chains for osmotic reasons, then pushing the oppositely charged chains to interact and form small complexes close to neutrality that will eventually coacerve into larger droplets to increase the overall entropy (and minimize the free energy).

It would be very instructive in the future to dialyze the solution (at constant concentration then) instead of diluting it to distinguish between the contribution, if any, of the ionic strength and that of the hypothetical overlapping concentration on the self-suppression of coacervation.

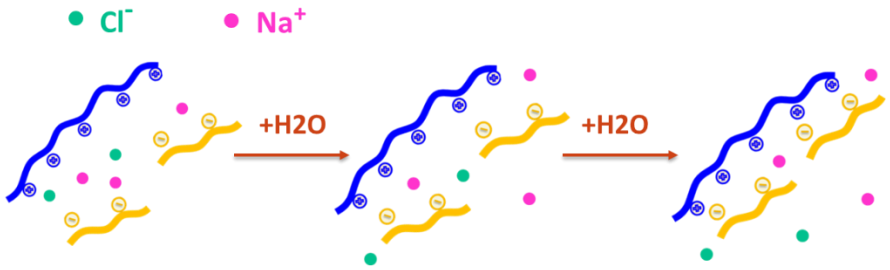

Figure 3-12. Schematic effect of dilution on dense coacervate phases: from the self-suppressed coacervate state (left) to the coacervate state (right)

To further investigate the local structure of the coacervate phase, dynamic light scattering (DLS) measurements were performed at 90° on the dense phase of the PDADMAC/PANa systems generated at different concentrations. For solutions of PE alone in the semi-dilute regime, it is known that the overlap between chains leads to the formation of a transient network having a characteristic correlation length ξ. Sections of a chain smaller than ξ will be fully stretched, but for distances larger than ξ, electrostatic interactions are screened out and therefore, the chains can be pictured as an ideal chain of segments with lengths ξ.[29]

From we can readily see two relaxation modes for concentrations below 900 mM. The fast mode corresponds to the relaxation of polymer segments of size ξ forming so-called blob subunits while the second mode, which is slower, is associated to large heterogeneities in the coacervate phase. The slow modes might reflect the presence of transient aggregates put forward by Muthukumar in the dynamics of solutions of charged macromolecules[30]. When the coacervate concentration increases larger (transient) aggregates expected to form through possibly dipole–dipole pairings as depicted in the insert of **Figure 3-13 a**.

Very clearly, the relaxation associated with blob diffusion is faster for lower PE concentrations, meaning that blobs are smaller at low concentrations (**Figure 3-13 a**). In fact this is the exact opposite of what we observe for concentrated solutions of neutral polymers in good solvent where the blob size decreases with the polymer concentration (C) as $\xi \sim C^{-0.70}$. [31]But, as explained previously, the increase in PE concentration readily opposes to the coacervation, denser coacervates being obtained at low PE concentrations.

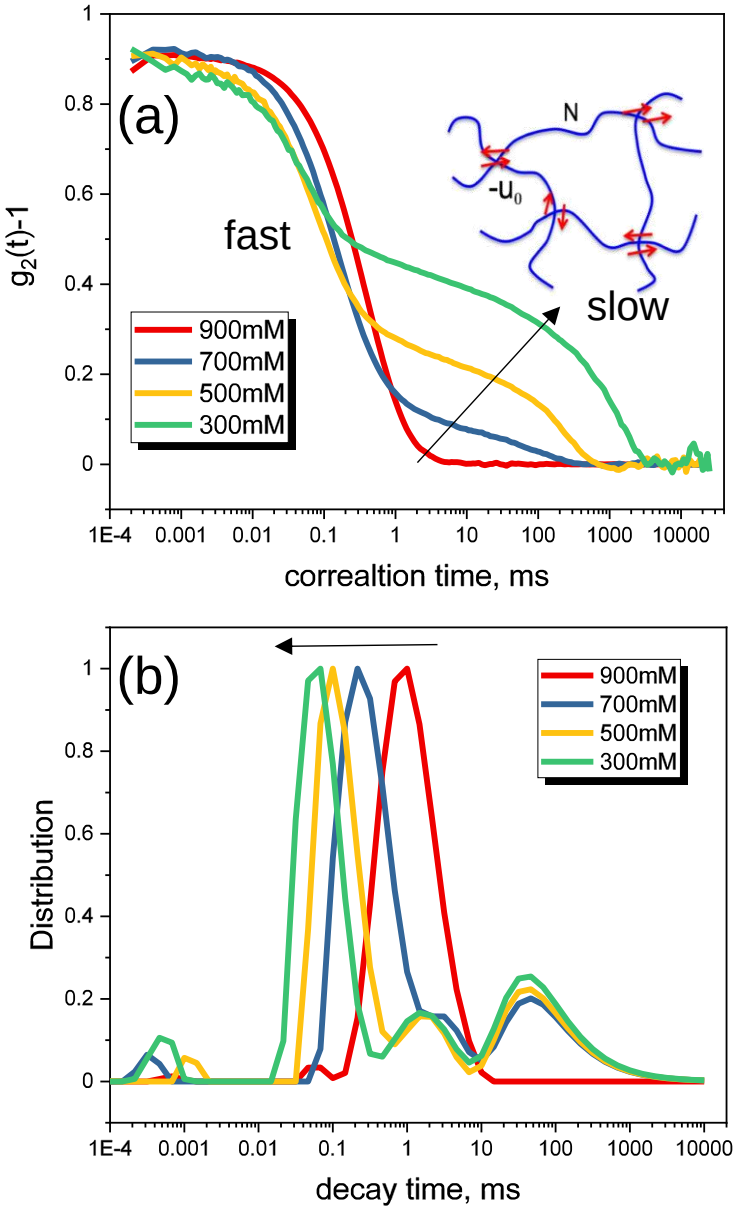

Figure 3-13. Intensity correlation functions and intensity-weighted distribution of decay times of coacervates (bottom phase) prepared at different PE concentrations (900 mM, 700 mM, 500 mM and 300 mM). DLS measurements were performed at 90° and 20°C. The coacervates were generated by dilution at different concentrations of the 900 mM stock solution.

In order to accurately determine the correlation length associated with the fast mode we measured the correlation functions (**Figure 3-14**) and distribution of decay times (**Figure 3-15**) over a wide-angle range from 30° to 150°. The trend is similar to that obtained at 90°C with decay times shifting to lower values and the appearance of an increasing slow mode as the concentration of the stock solutions decreases.

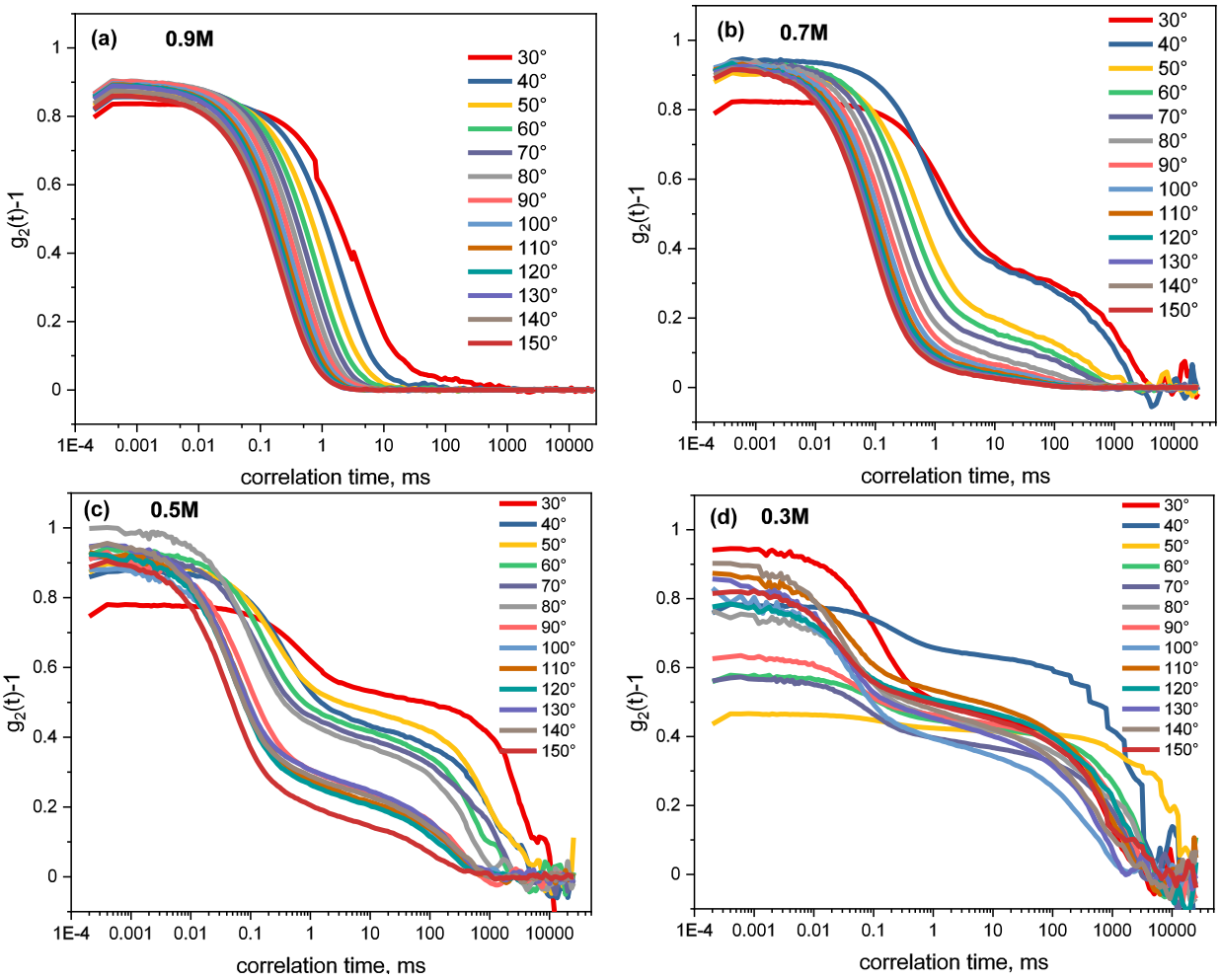

Figure 3-14. Intensity correlation functions at various angles of PDADMAC/PANa coacervates prepared at different PE concentrations. DLS measurements were performed at 20°C.

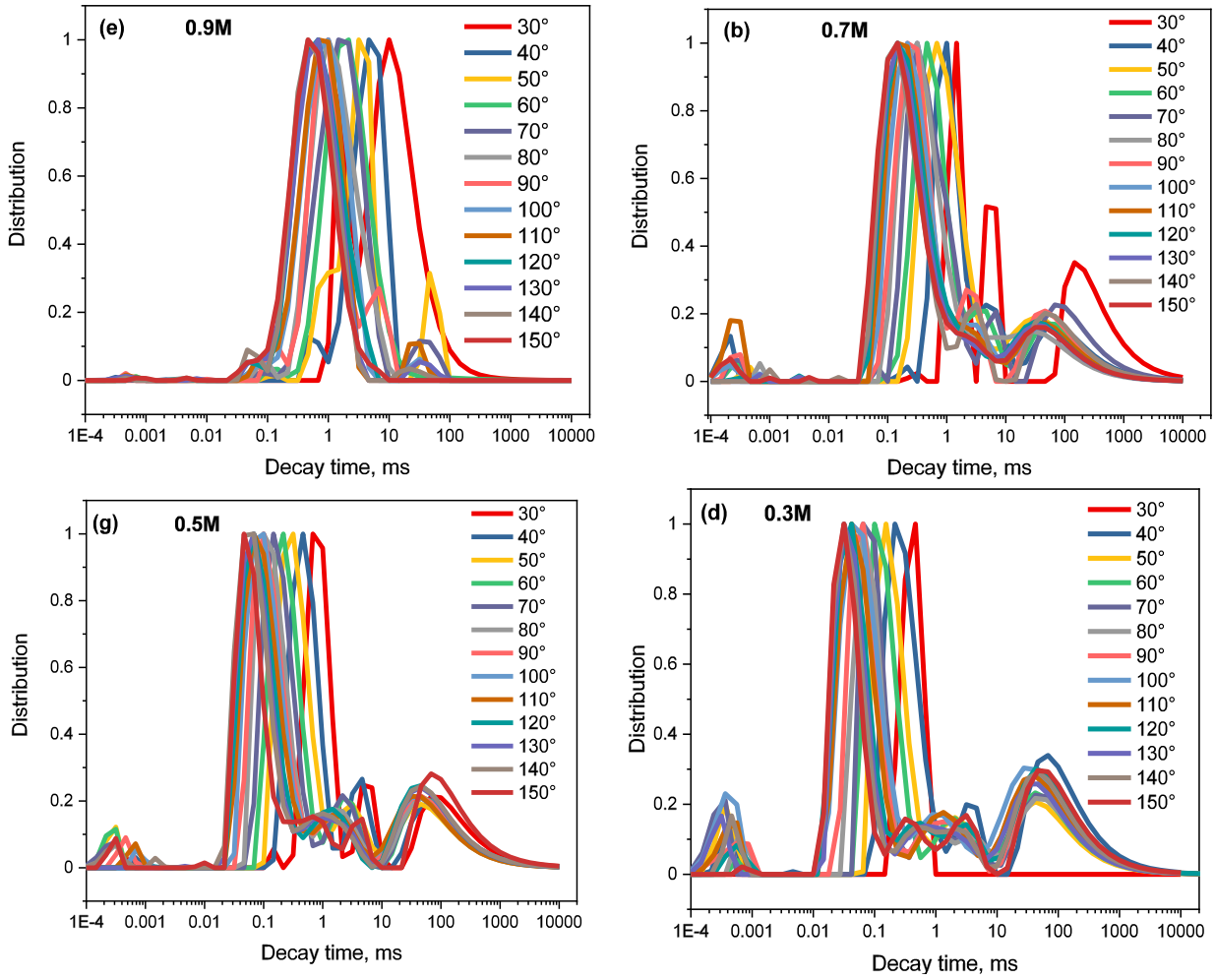

Figure 3-15. Intensity-weighted distribution of decay times obtained at different angles for coacervates (bottom phase) prepared at different PE concentrations. DLS measurements were performed at 20°C.

DLS observations detect the characteristic size of the concentration fluctuations i.e. the hydrodynamic correlation length ξ_H, which is numerically close to ξ, the correlation length of mesh size of the network. ξ_H is found from the Stokes Einstein relationship [32],

$$\xi_H = \frac{k_B T}{6\pi\eta D} \qquad (3.3)$$

where k_B is the Boltzmann constant, T the absolute temperature, η is viscosity of the solvent (D_2O) and D the mutual diffusion coefficient[33].

For a diffusive process, the decay rate ($\Gamma = 1/\tau$) is equal to

$$\Gamma = Dq^2 \qquad (3.4)$$

with q the wave vector defined as

$$q = \frac{4\pi n}{\lambda} sin\left(\frac{\theta}{2}\right) \qquad (3.5)$$

where θ represents the scattering angle, n represents the refractive index of the medium and λ represents the laser wavelength (λ = 632.8 nm).

We then plot the decay rate corresponding to the fast mode as a function of q^2 (**Figure 3-16**). The fact that the plots are linear emphasizes the diffusive behavior of the fast mode associated to blob diffusion. From the different slopes obtained from **Figure 3-16 a** we can determine the diffusion coefficients (D) of blobs as a function of the PE concentration as

$$\Gamma = Dq^2 \qquad (3.6)$$

As shown from the density and mass fraction measurements above, as the solution concentration increases, the coacervates generated are lighter with networks that therefore relax more slowly in agreement with smaller collective diffusion coefficients or larger correlation lengths ξ_H as shown in **Figure 3-16 b.**

Let us now plot a more physical representation i.e. the correlation length as a function of the coacervate volume fraction $\varphi_{coacervate}$ within the coacervate (and not the initial PE solution concentration). $\varphi_{coacervate}$ was determined by considering the mass fraction of polymer in the coacervate phase (TGA measurements, **Figure 3-11**) and by assuming a polymer density of 1. In a log-log representation, the variation of ξ_H is linear with an exponent ~ -3.2 (**Figure 3-17**).

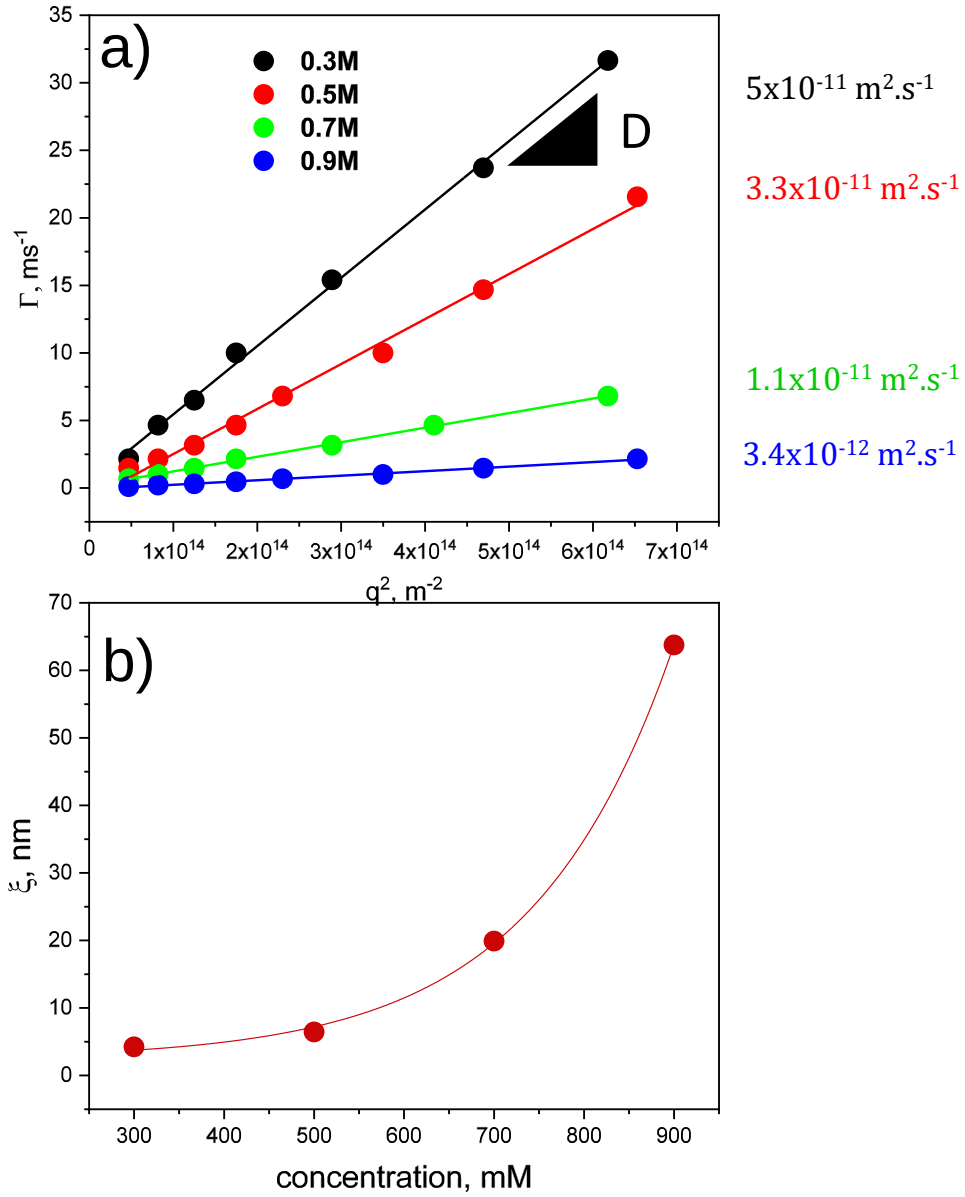

Figure 3-16. (a) Γ as a function of q^2 for the coacervate phases generated at four PE concentrations in the PDADMAC/PANa system. The solid lines are a linear fit of the data with the slope representing the diffusion coefficient D. **(b)** Hydrodynamic correlation length within the different coacervates as a function of the PE concentration. The solid red line is guide for the eyes.

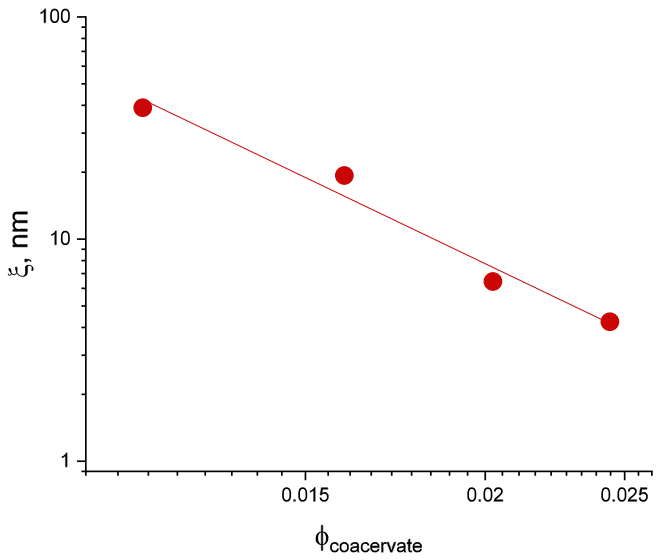

Figure 3-17. Correlation length ξ_H as a function of the coacervate volume fraction $\varphi_{coacervate}$ within the different coacervate phases (bottom phases).

In a semi-diluted polymer solution or physical polymer gel, the correlation length or correlation blob (within which there is a higher probability of finding a monomer of the same polymer chain rather than a monomer of another chain) would have scaled in a good solvent as

$$\xi_H \sim R_g \left(\frac{\varphi_p}{\varphi^*}\right)^{-0.75} \qquad (3.7)$$

In order then to evaluate more directly the local structure of the network, small angle neutron scattering measurements (SANS – D22 ILL) were performed on each coacervate & self-suppressed phase. Stock solutions were prepared in full D_2O as well and pD was adjusted with NaOD prior to complexation.

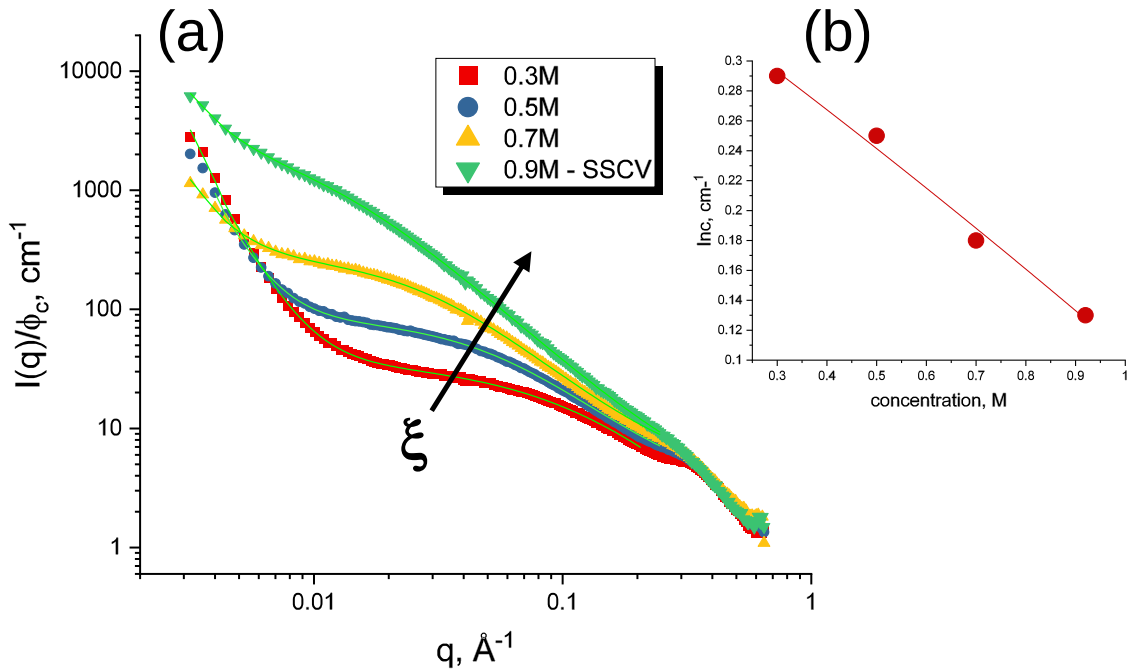

Figure 3-18. (a) Small angle neutron scatting (SANS) signature of the different coacervate phases measured at ILL on D22 in D_2O. The solid lines are an Ornstein–Zernike *(OZ)-Debye-Bueche (DB)* fit to the data (see below). The scattered intensity has been renormalized by the coacervate volume fraction **(b)** Incoherent intensity (background) taken at high q before applying any correction.

First of all, we can see from **Figure 3-18 b** that the incoherent scattering taken at high q (before any background subtraction) decreases linearly as the concentration of the stock solution increases. An effect due to the decreasing presence of hydrogen atoms (H) from both PEs and thus corresponds well to an increase in polymer content or density in the coacervate phase.

Moreover, from **Figure 3-18 a**, we can clearly see that the SANS signature varies within each phase suggesting that the local structure varies with concentration. A result that is not necessarily obvious to interpret without DLS results.

In the medium and high q region, one can easily imagine that the PE chains overlap in the complex coacervate phase, like neutral polymers in a semi-dilute solution. In this case, the semi-dilute polymer solution at equilibrium follows the Ornstein-Zernike (OZ) structure factor accounting for the concentration fluctuations at high q [34]

$$S_{OZ}(q) = \frac{S_{OZ}(0)}{1+(q\xi)^m} \qquad (3.8)$$

with S(0) the structure factor extrapolated to q=0 (and related to the entanglement density and longitudinal osmotic modulus of the network) and ξ the correlation length or mesh size of the entangled network. The exponent m characterizes the polymer/solvent interaction and thus the thermodynamics behind (m=2 for theta solvent or m=5/3 for good solvent).

In addition, an excess of diffusion at low q is always present in PE solutions. This upturn has been attributed to local inhomogeneities many times larger than the radius of gyration of PEs in the solutions[35]. We believe that these inhomogeneities actually originate from transient aggregates arising from the dipole-dipole interaction and highlighted by Muthukumar in the dynamics of charged macromolecule solutions [30]. These transient aggregates are probably responsible for the appearance of the slow relaxation modes observed earlier in our DLS data (see **Figure 3-13**).

It turns out that if the spatial scale of the concentration fluctuations due to the presence of these large transient inhomogeneities is large relative to the correlation length, then the two contributions can be added and treated separately [36].

The overall structure factor becomes

$$S_{total}(q) = S_{OZ}(q) + \frac{S_{DB}(0)}{1+(q^2\zeta^2)^2} \qquad (3.9)$$

where the second term is the Debye–Bueche (DB) structure factor $S_{DB}(q)$[37] which accounts for the scattering by an inhomogeneous solid. $S_{DB}(0)$ is the extrapolated structure factor at q=0 and ζ is the size of the inhomogeneities in the system. At low q, the DB contribution $S_{DB}(q)\sim 1/q^4$ dominates over that of the OZ while at high q where the DB scales as $S_{OZ}(q)\sim 1/q^2$ it is the opposite.

Indeed, **Figure 3-18 a** shows that the OZ-DB structure factor model accounts for the SANS data particularly well. From the fit we can see that the SANS correlation length ξ or the mesh size of the network increases with the PE concentration in agreement with DLS, density and polymer content data. The variation of the dynamic (DLS) and static (SANS) correlations

length agrees relatively well and scale with $\xi_H \sim (\varphi_c)^{-\beta}$ (β ~ 3.2 and 2.7 for DLS and SANS respectively) (**Figure 3-19**).

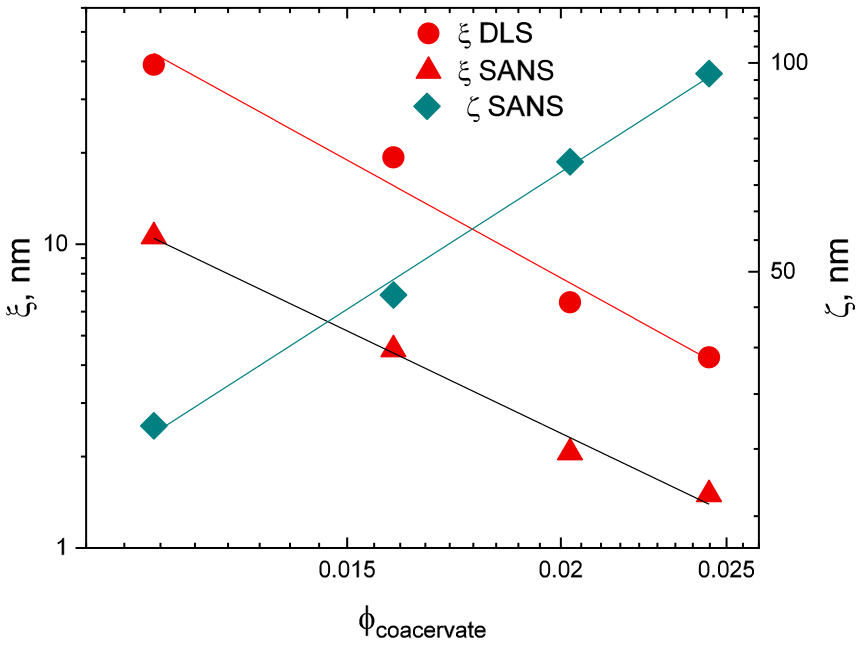

Figure 3-19. SANS and DLS correlation lengths ξ and SANS inhomogeneity sizes ζ as a function of the coacervate volume fraction $\varphi_{coacervate}$ within the coacervate phases (bottom phases) prepared at different PE concentrations.

At the same time, the size of the transient inhomogeneities ζ extracted from the OZ-DB fit decreases when the concentration of the stock solutions increases (**Figure 3-19**). A result that was somewhat expected since the size of the transient inhomogeneities should intuitively be a function of the overall polymer concentration in the coacervate phase. ξ decreases and ζ increases inside the coacervate and self-suppressed phases both with a power-law variation with the polymer volume fraction.

It should also be noted that the scattering intensity in the mid-q range decreases when the PE concentration decreases, as seen in **Figure 3-18 a.** In this q-range the scattering intensity can be related to the osmotic compressibility $\left(\frac{\partial \pi}{\partial \phi}\right)^{-1}$ which is obtained by extrapolating the scattered intensity at zero angle [38] :

$$I(q \to 0) = kT\phi^2 \left(\frac{\partial \pi}{\partial \phi}\right)^{-1} \qquad (3.10)$$

The osmotic pressure of a polyelectrolyte solution in the absence of added salt is the sum of two contributions due to polymer chains on one hand and the counterions on the other hand. In practice, the osmotic pressure is governed by the counterions. Indeed, for a PE of DP 1000 the osmotic pressure due to counterions is 1000 times higher than the osmotic pressure arising from the PE chains if one assumes that counterions are not condensed. The decrease of $\left(\frac{\partial \pi}{\partial c}\right)^{-1}$ with the decrease of the PE concentration is in accordance with the formation of a coacervate phase of higher polymer concentration. In order to differentiate the contribution due to PE chains and counterions, the spectra were normalized by the polymer volume fraction in the coacervate. In **Figure 3-18**, we see an increase of the renormalized scattered intensity when the coacervate becomes lighter suggesting a decrease in the osmotic pressure.

At this stage, this effect is not yet understood. However, it is conceivable that in such a dense coacervate phase, the high osmotic pressure (or low osmotic compressibility) is due to the small PANa (2k) chains and not necessarily to the counterions. Indeed it is unlikely that the densest coacervate, formed by the strongest interaction, would have many free counter ions. We can try to find out in the future by studying more precisely the counter ions partitioning into the supernatant and coacervate phases using a Na^+-selectrive electrode. [39]

Furthermore, if we consider very high q values (above 0.2 $Å^{-1}$), we observe a distinct correlation peak for each coacervate phase, which shifts (and flatten) towards lower q with increasing the PE concentration (i.e decreasing the polymer volume fraction in the coacervate phase) and, disappears in the self-suppressed monophasic phase (**Figure 3-20 a**).

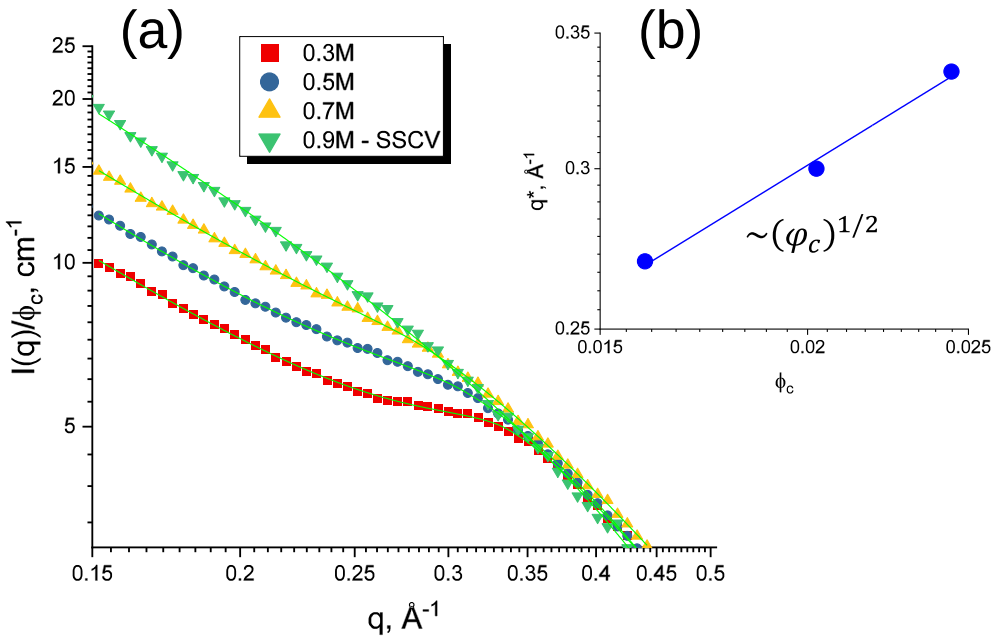

Figure 3-20. (a) High-q zoom of the SANS signature of the different coacervate and self-suppressed phases. The solid green lines are a fit to the data (see text). (b) correlation length peak q* as a function of the polymer volume fraction φ_p in the coacervate phase.

The scattering length density (SLD) of PDADMAC (~0.49.10^{-6} Å^{-2}) is smaller than PANa (1.8.10^{-6} Å^{-2}), we then mostly see PDADMAC chains by SANS in D_2O solvent (6.38.10^{-6} Å^{-2}). The observed peaks can then be assimilated to the polyelectrolyte peak seen for PDADMAC and PSSNa solutions at high concentration (>1M). [40] In these PE solutions, however, the polyelectrolyte peak shifts to lower q values with increasing concentration, with a flattening of the peak due to an increase in ionic strength, as clearly shown in **Figure 3-21** for our PDADMAC solutions.

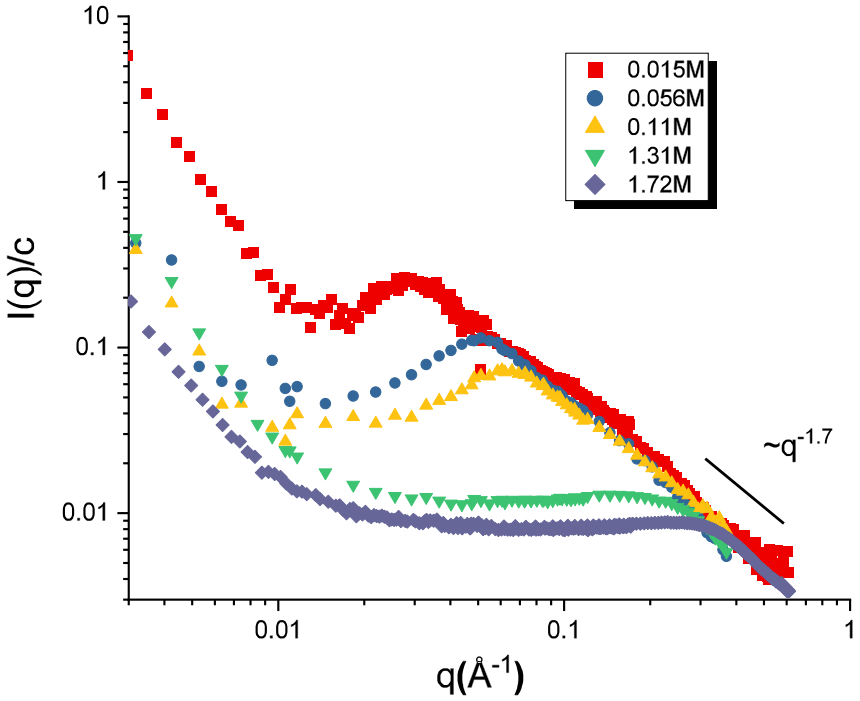

Figure 3-21. SANS signature of PDADMAC solutions at pH=10. Data were acquired on D22 (ILL) and PACE (LLB).

We then can fit the the SANS spectra of the different coacervate phases at high q (**Figure 3-20 a**) using the following equation[41]

$$S(q) = \frac{A}{q^n} + \frac{B}{(1 + (|q - q^*|\varsigma)^m)} + bkg \qquad (3.11)$$

The first term describes the intensity rise, and the second term characterizes the local solvation properties and interactions around the polyelectrolyte chains. ς is the correlation length for the local solvation structure, and $q^*$the peak position.

The correlation peak obtained at high q in the coacervate phase (**Figure 3-20 a**) is then a direct measure of the intensity of the electrostatic complexation between PDADMAC and PANa chains. In the densest phase, its intensity is the highest with a well-marked shape. As the density decreases while increasing the PE concentration, it shifts to smaller values of q

and disappears as does the complexation in the self-suppressed monophasic phase in which the ionic strength due to the both free counterions is the largest.

We can see that the correlation peak q* scales as $\sim(\varphi_c)^{1/2}$ in the coacervate phase (**Figure 3-20 b**). It is difficult to interpret this scaling law at this stage. For PDADMAC solutions, such scaling is found either in the case of semi-dilute solutions or in the highly concentrated regime consistent with nematic order [40]; although we cannot observe it at the µm scale using optical microscopy... Further studies are needed to better understand the local organization of the coacervate phase.

3.3.2 The effect of temperature

We have just seen that dilution (and possibly dialysis) of a 0.9M self-suppressed coacervate phase (SSCP) can generate a variety of coacervate phases with different density, mesh size and interfacial tension.

Very recent observations have put forward a lower critical solution temperature (LCST) behavior in polyelectrolyte complex coacervate phase [42, 43]. Does our self-suppressed coacervate phase also exhibit LCST behavior?

Figure 3-22 shows a clear, single-phase SSCV solution (0.9 M) that becomes immediately turbid when heated to 50°C (using a water bath and not an oven). After two days, it gradually separates macroscopically into a polymer-rich coacervate phase (bottom) and a polymer-poor supernatant phase (top) with the presence of a neat interface, similar to the complex coacervation obtained directly by mixing two PE stock solutions or by diluting an SSCV phase.

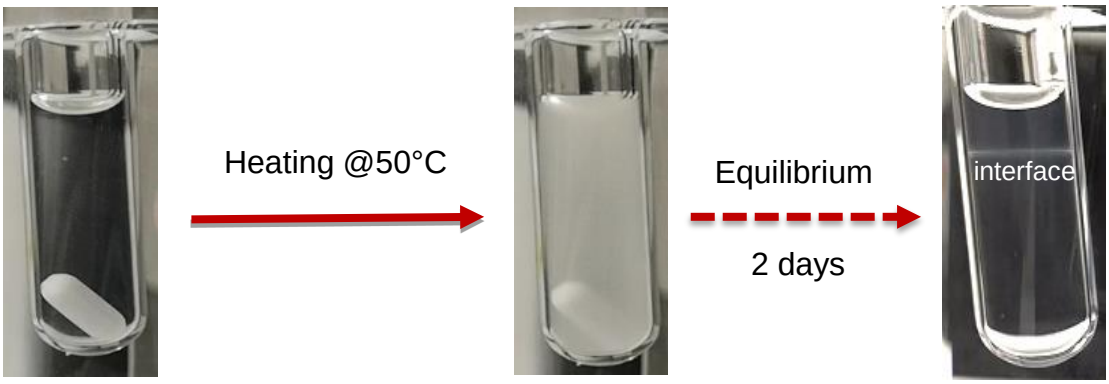

Figure 3-22. Lower critical solution temperature (LCST) behavior of a self-suppressed PDADMAC/PANa 0.9M coacervate phase after heating to 50°. Glass tubes were used for all heating experiments to avoid contamination or deformation.

The two-phase system is then left at room temperature (22°C) for two days. Interestingly, the system remains stable, i.e we can still observe the dense coacervate phase. If we heat it again at 38°C for 1 hour, the two phases become turbid again. If we continue to heat at 45°C for 1 days to reach equilibrium, a new two-phase system with a lower coacervate/supernatant interface will form as shown in **Figure 3-23**, suggesting that the new lower phase is denser.

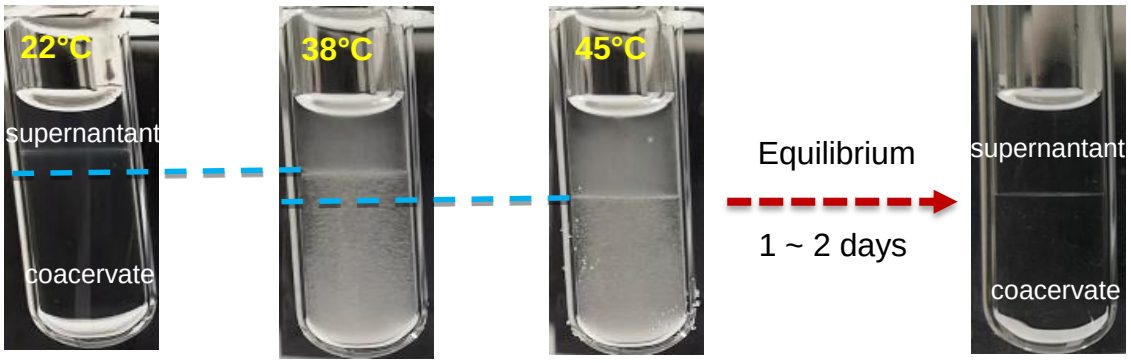

Figure 3-23. Effect of temperature on a coavervate and supernant phase of a PDADMAC/PANa system upon reheating the from 22°C to 38°C and then 45°C . The interface between the two phases is lowered by increasing temperature.

At a more local level, **Figure 3-24** shows optical microcopy images of a 0.9M self-suppressed coacervate phase heated to 35°C.

Initially, the clear coacervate phase becomes turbid with the appearance of numerous dense droplets of micrometer size. With time, these droplets coarsen by coalescence, forming

larger and larger droplets until a macro-phase separation occurs (1~2 days) with the appearance of two new transparent and homogeneous phases of coacervate and supernatant.

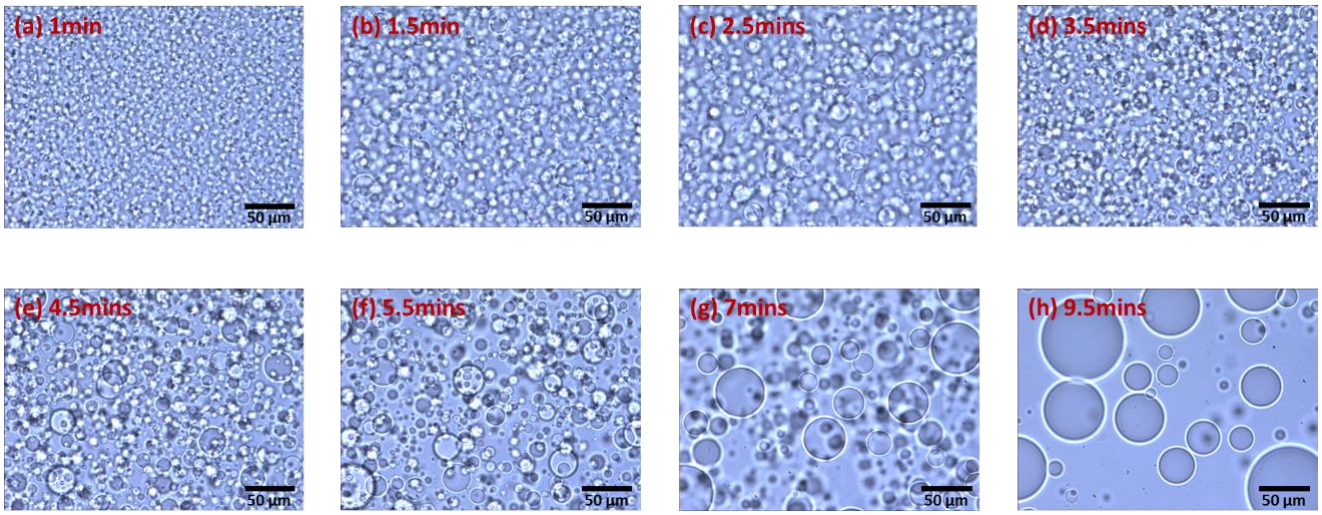

Figure 3-24. Dynamic changes observed in the 0.9M self-suppressed coacervate phase upon heating to 35°C monitored with an optical microscope. Pictures were taken at different times at 35°C.

On the other hand, if we cool the turbid coacervate phase from 35°C to 22°C, we obtain the opposite. The droplets will indeed become smaller and smaller until they disappear completely at the end as shown by the tracking of one of them circled in pink (**Figure 3-25**).

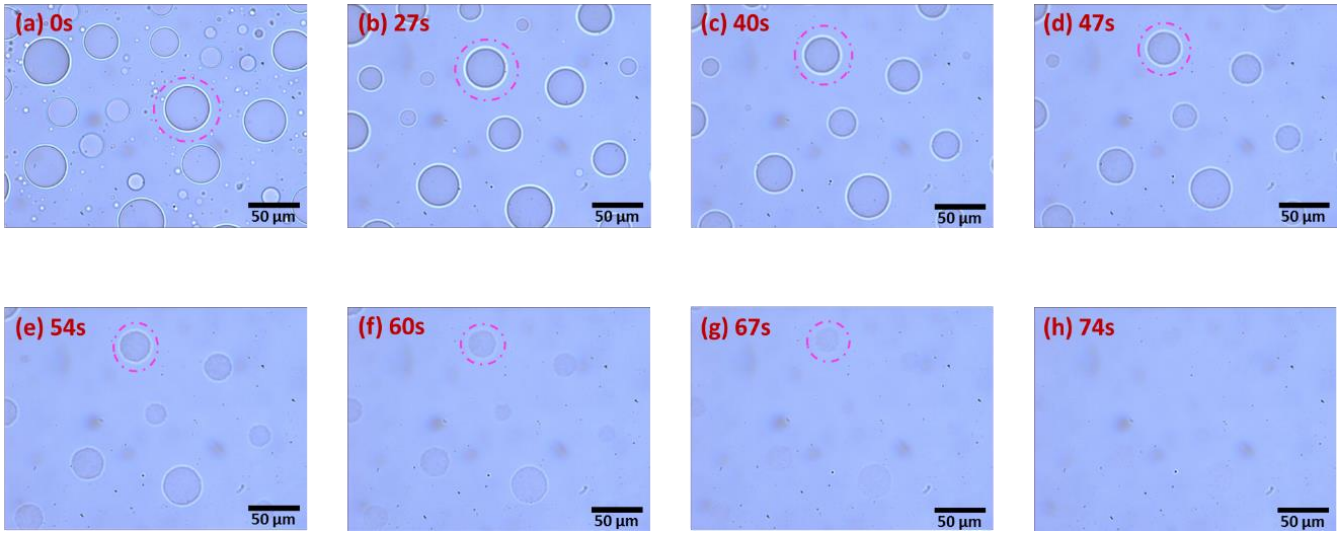

Figure 3-25. Dynamic changes observed in the 0.9M self-suppressed coacervate phase upon heating to 35°C and the cooling back at 22°C monitored with an optical microscope. Pictures were taken during the cooling step from 35°C to 22°C.

One can legitimately wonder if the new denser coacervate phases generated by an increase in temperature do not end up relaxing with time at RT in line with a complex coacervation known to be in equilibrium in contrast with PSSNa/PDADMAC type systems (see chapter 2) that are notoriously out of equilibrium.

Importantly, the fast and full reversibility observed in a few seconds at 35°C in **Figure 3-25** is not observed when samples are heated at higher temperature. For example, if we heat a coacervate/supernatant system at 45°C for 2 days (**Figure 3-23**), the new generated denser coacervate will take 2 months at RT to relax back its initial state with a concomitant rise of the coacervate/ supernatant interface (**Figure 3-26 a**).

The influence of temperature on the behavior of the self-suppressed state emphasizes a lightening/densification process of the "equilibrated phases". Indeed, the TGA measurements confirm this hypothesis as shown in **Figure 3-26 b**. We can clearly see an increase in density/polymer content during the heating phase at 45°C for 2 days for all the concentrations studied and a return to the initial density/polymer content when returning to room temperature for 2 months (with a symmetric effect for the supernatant)

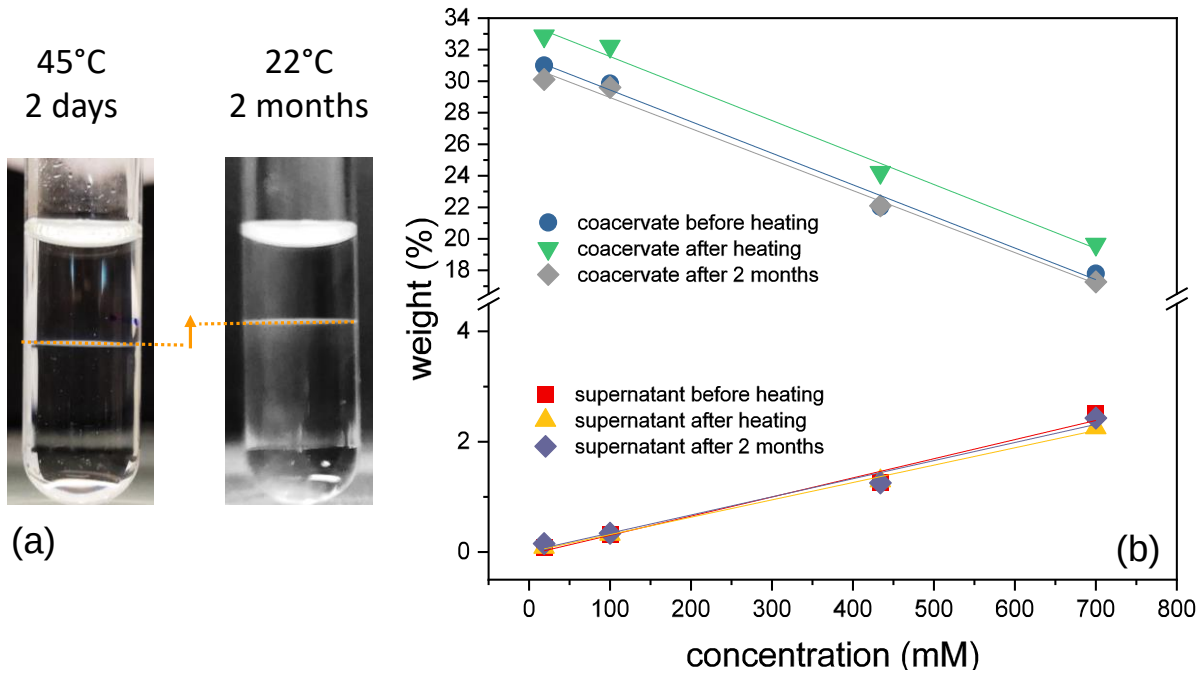

Figure 3-26. (a) Photograph showing the change in the interface position of a coacervate/supernatant system initially heated from 22°C to 45°C and then cooled to 22°C and allowed to stand for two months

and (b) Polymer weight fractions (TGA) obtained for coacervate phases generated at various concentrations that underwent the same heat treatment. The solid lines are a linear fit to the data.

As with the samples analyzed at RT (see above), DLS experiments were performed at various temperatures with the self-suppressed 0.9M coacervate solution and the 0.7M coacervate phase (obtained by diluting the previous phase) to monitor any changes on the network structure during heating (**Figure 3-27**).

In the case of the self-suppressed coacervate solution, we see the decay times shifting to lower values and the appearance of an increasing slow mode as the temperature is raised. A result equivalent to an increase in concentration as shown above in **Figure 3-13**. In the case of the coacervate phase at 0.7M, the trend is similar although less marked. The increase in temperature thus generates denser phases that possess shorter decay times, suggesting smaller lattice meshes that relax more rapidly.

At this point, we can safely say that an increase in temperature or a decrease in concentration goes in the same direction, i.e. towards an increase in the intensity of complexation resulting in a denser coacervate.

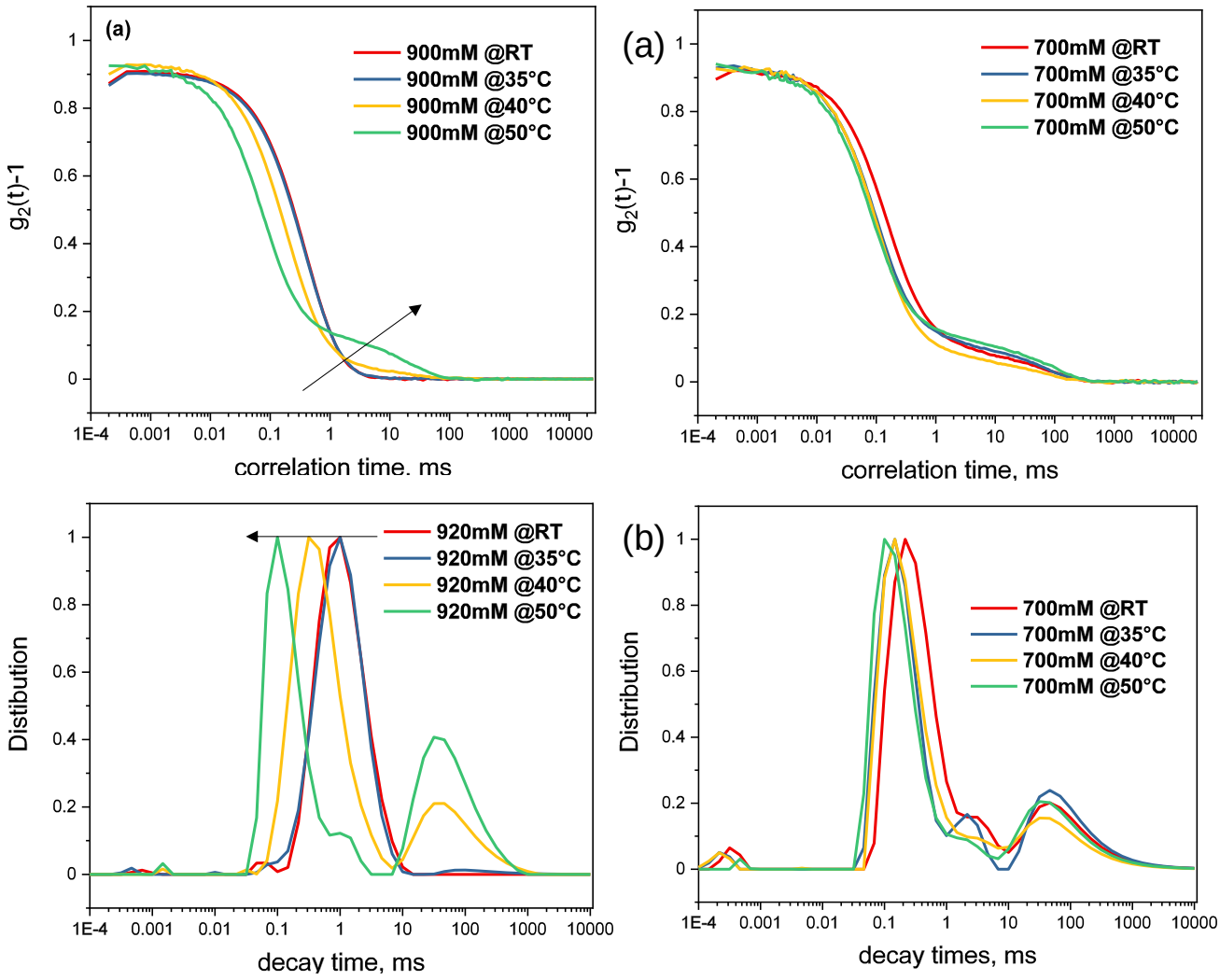

Figure 3-27. (a) Auto-correlation functions and (b) intensity-weighted distribution of relaxation times measured by DLS in D_2O at 90° as a function of temperature for the self-suppressed 0.9M solution and the 0.7M coacervate phase (obtained by dilution of the previous one) in the PDADMAC/PANa system.

We then performed static SANS measurements to probe the structure of the coacervate networks at different temperatures. The static measurements are very in good agreement with the dynamic data as can be seen in **Figure 3-28**. Increasing the temperature has a more pronounced effect on the self-supressed solution with a decreasing correlation length ξ (mesh size) accompanied by an increase in the size ζ of the transient inhomogeneities, both consistent with densification/concentration of the solution. The 0.7M coacervate solution undergoes a less marked effect in agreement with the DLS data where we nevertheless observe a decrease of ξ accompanied by an increase of ζ under the effect of temperature.

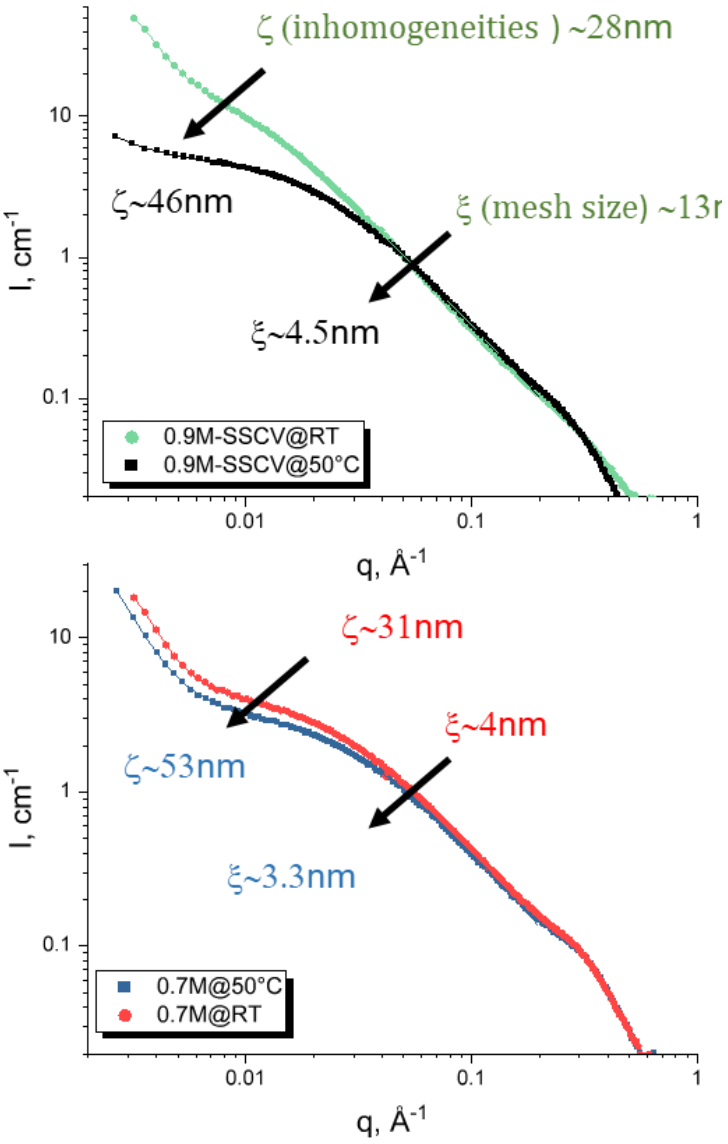

Figure 3-28. Small angle neutron scattering (SANS) analysis of the self-suppressed coacervate at 0.9 M and the coacervate at 0.7 M (obtained by diluting the former) at RT and 50°C. The solid lines represent the data adjustment by an Ornstein-Zernike (OZ) - Debye-Buche (DB) fit. The data were measured at ILL on D22 in D2O.

The increase in temperature then has a profound effect on the binary solution. The dielectric constant decreases and the Bjerrum length increases (see Chapter 1), resulting in stronger electrostatic and dipole-dipole interaction leading to additional complexatio. This gives rise to the appearance of a LCST-like behavior in the coacervate and self-supressed

phases. Denser complexes are then nucleated, generating some turbidity as in a direct mixing formulation. With time complexes reorganize into coacervate droplets that eventually coalesce to form a denser coacervate phase than that formed at RT (with a cocomitant lowering of the coacervate/supernatant interface). After more than two months or so, the system relaxes back to its original structure since the PADAMAC/PANa complexation occurs under equilibrium condition and then not prone to the impact of the formaulation pathway. (**Figure 3-29**).

This effect can perhaps be used advantageously to encapsulate/sequester active ingredients initially within stabilized droplets under the action of temperature. And then release the possible load after a few months, when the network relaxes back at room temperature. An idea that needs to be looked at closely in the future.

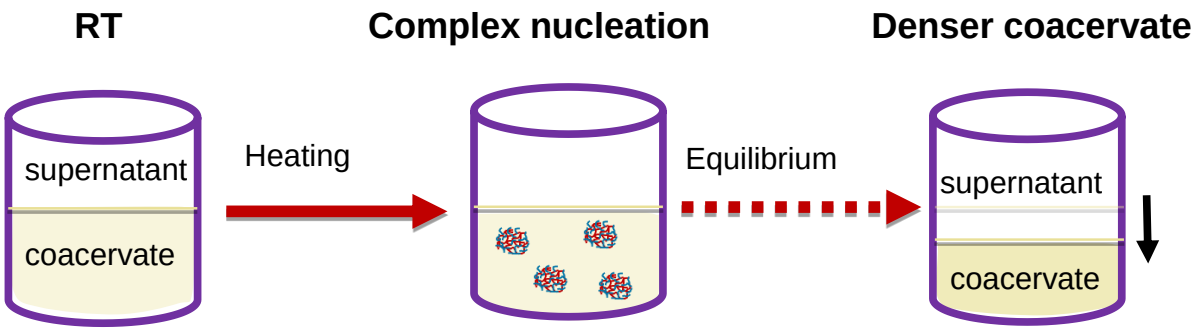

Figure 3-29. Schematic representation of the effect of increasing temperature on the lowering of the interface between the supernatant phase and the coacervate phase.

We have seen so far that an increase in temperature can generate multiple coacervate phases from a self-suppressed coacervate phaseAs coacervation is an equilibrium phenomenon, it must be independent of the formulation pathway followed. It must therefore be possible to densify a coacervate phase obtained directly by mixing two PE solutions of opposite charge.

Transmittance measurements (λ =400nm) were then performed as a function of temperature and time in quartz cells for coacervate phases prepared from 18.6 mM, 100 mM, 400 mM, and 700 mM salt-free PE solutions, respectively.

At low concentrations (18.6mM) a sharp drop in transmittance is observed slightly above room temperature, whereas it is necessary to reach 38°C to observe a similar drop in the case of more concentrated solutions (700mM) as seen in **Figure 3-30 a**. This suggests that more energy (kT) is required to nucleate complexes in the coacervate phase when the volume fraction of the polymer in the coacervate phase decreases (or the concentration of the PE solution increases). Note that the transmittance of the 700mM coacervate phase (green line) appears to re-increase rapidly after reaching its lowest value.

We therefore heated the four samples directly to 45°C. We observe the appearance of turbidity very quickly with a marked drop in transmittance at short times as can be seen in **Figure 3-30 b**. The transmittance then increases again with a rate that depends on the volume fraction of the polymer in the coacervate phases until it reaches the value of a transparent solution around 75-80%. This takes a few hours for low volume fractions of PE while it can take more than 2 days for higher fractions. The time required to obtain a new, denser coacervate phase (see below) is therefore a function of the volume fraction of the polymer and therefore the strength of the complexation existing within the initial coacervate phase. The stronger the complexation, the longer it will take to generate a new denser phase. The global phenomenon highlights a densification of the interactions by increasing the temperature due to the decrease of the dielectric constant (increase of the Bjerrum length). The densification is more pronounced when the Debye length is low (low PE concentration). This results in the formation of transient colloidal sub-structures (complexes) that scatter light (turbidity) before progressively relaxing into a isotropic (transparent) coacervate phase which is denser than the initial phase at room temperature.

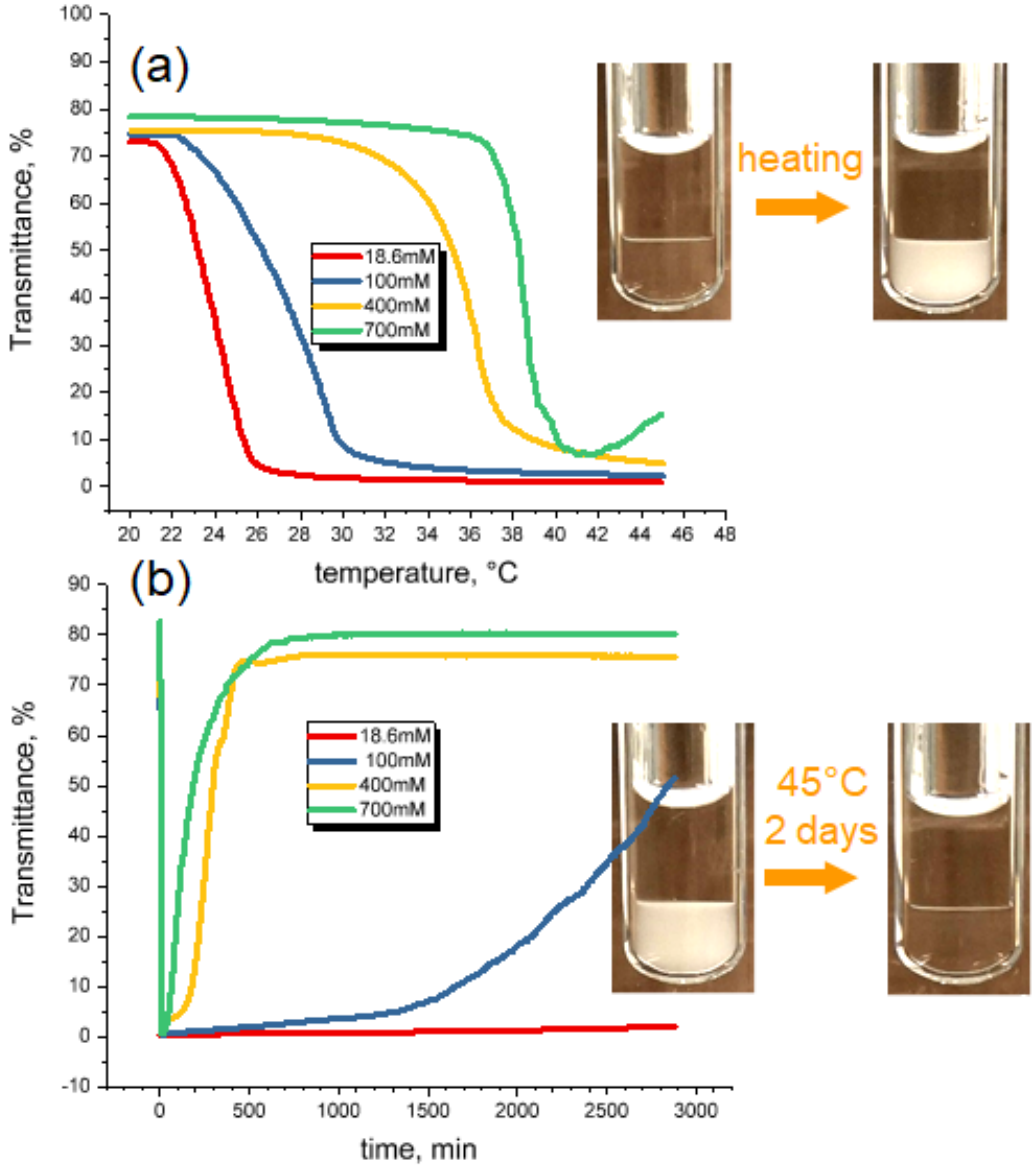

Figure 3-30. (a) Transmittance as a function of temperature achieved a 0.2°C/minute (b) and kinetic transmittance as a function of time measured at 45°C for PDADMAC/PANa coacervate phases prepared with 18.6mM, 100mM, 400mM and 700mM salt-free PE solutions.

Do we really generate a denser coacervate phase upon heating, consistent with the lowering of the coacervate/supernatant interface?

TGA experiments were then also performed on four coacervates generated at 22°C directly from different concentrations (18.6mM, 100mM, 434mM, 700mM) and then heated to 38°C and then to 45°C. From **Figure 3-31**, it can be clearly seen that the polymer content in

each new coacervate phase is indeed higher at 45°C than at RT and decreases linearly with the initial concentration of the PE stock solution. A result that corresponds well to the visible lowering of the supernatant/coacervat interface.

The polymer content in the supernatant increases linearly as expected, for both temperatures, but without significant difference, probably within the error bar of the measurement. The polymer content at the intermediate temperature of 38°C was not measured by TGA and only estimated (dashed blue lines).

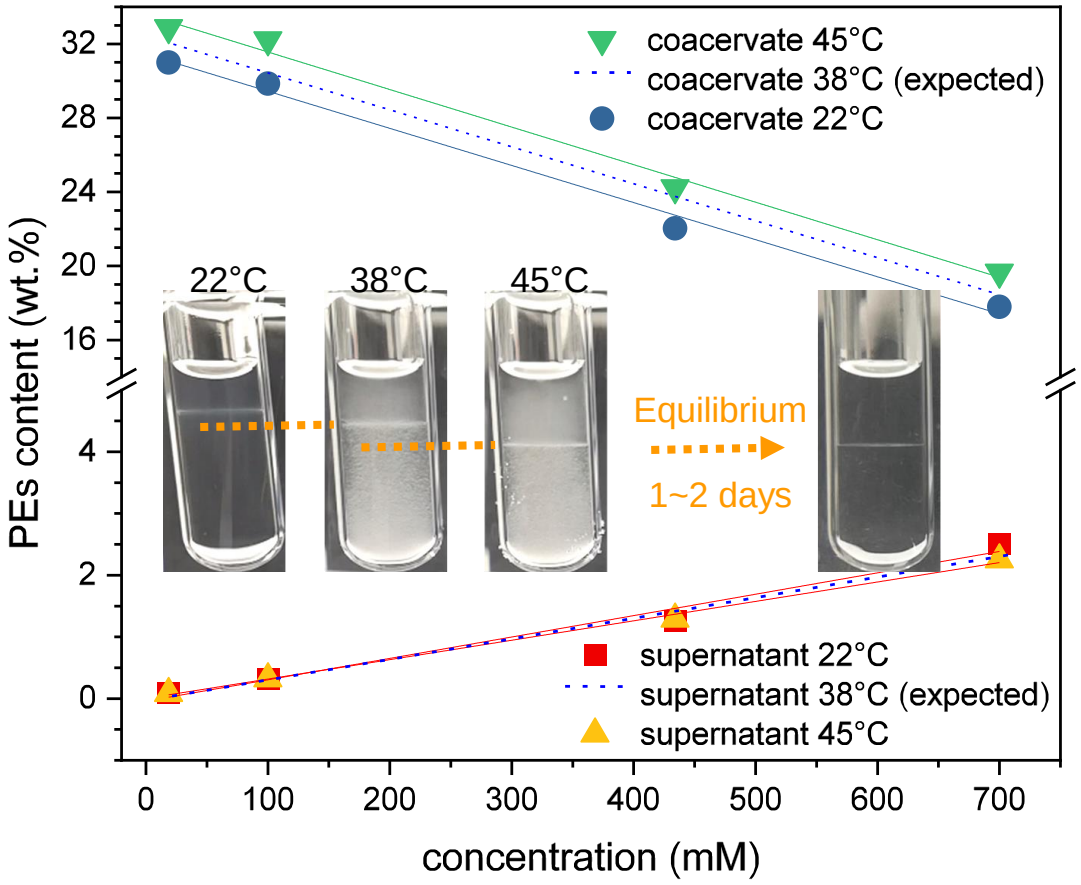

Figure 3-31. Thermogravimetric analysis (TGA) performed on different PDADMAC/PANa coacervates and supernatant phases generated at 22°C (RT) and 45°C, respectively. The solid lines are a linear fit to the data.

As the temperature increases, the dielectric constant decreases, which increases the interaction strenght between the charged PEs. The two oppositely charged chains then

become more intimately connected, releasing water molecules and counter ions, which leads to denser coacervate phases, as illustrated schematically in **Figure 3-32**.

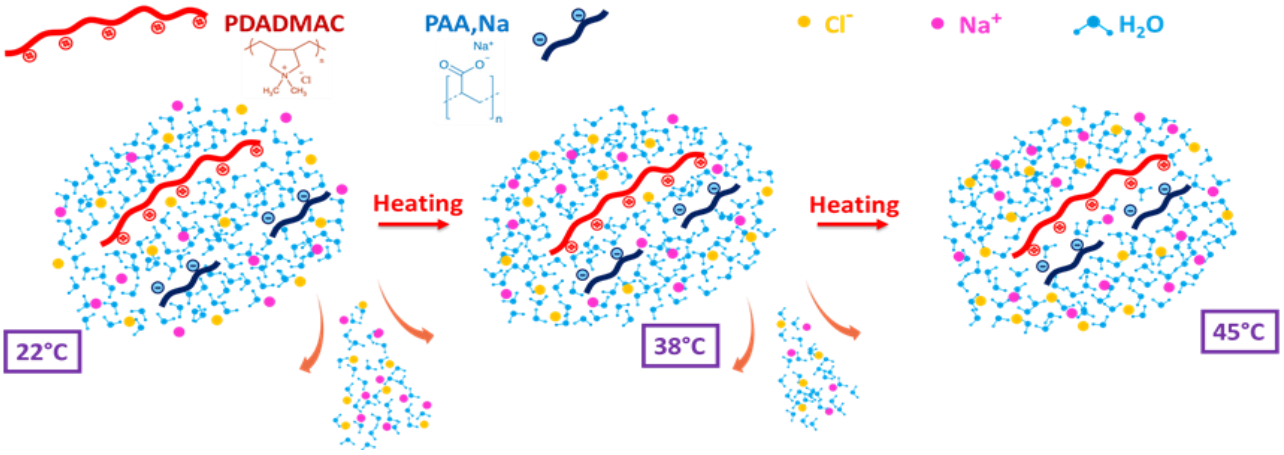

Figure 3-32. Schematic illustration of the complexation/association of oppositely charged PEs generated at different temperatures in the PDADMAC/PANa system.

3.3.3 The effect of ionic strength

The effect of salt addition on the behavior of a coacervate phase is well known and documented as we saw at the beginning this chapter (see **Figure 3-7**). The salt will screen and then weaken the strength of the electrostatic interaction between the oppositely charged PEs until a concentration where the complexation disappears (also called desalting transition).[10, 14, 44] However, structural evidence for this effect is not well documented in the literature. Here we present some key experiments that highlight the modulation of the complexation intensity within a coacervate phase with the addition of NaCl.

Figure 3-33 shows the effect of adding NaCl on the coacervate phase generated at 0.3M by directly mixing two oppositely charged PE solutions adjusted with different salt concentrations. We can clearly see that the increase of the ionic strength weakens the interaction and then makes the network swelling, leading consequently to the rise of the position of the coacervate/supernatant interface as shown in the following **Figure 3-33 a**. At 0.2M NaCL, the complexation disappears as well as the interface, thus generating a monophasic solution containing "neutral" PDADMAC and PANa chains without any interaction (the so-called *dormant solution*).

TGA experiments were also performed to quantify the impact of salt. We can see in **Figure 3-33 b** that the polymer content increases linearly as expected in the supernatant and consequently decreases linearly as well in the coacervate as the ionic strength increases. The two straight lines cross at about 0.2M NaCl in agreement with the monophasic state of the dormant solution. At this salt concentration, the overall material content including PDADMAC, PANa chains and NaCl ions is close to 18.5% (w/w) which is the expected value for a 0.3 M PE solution containing 0.2M NaCl.

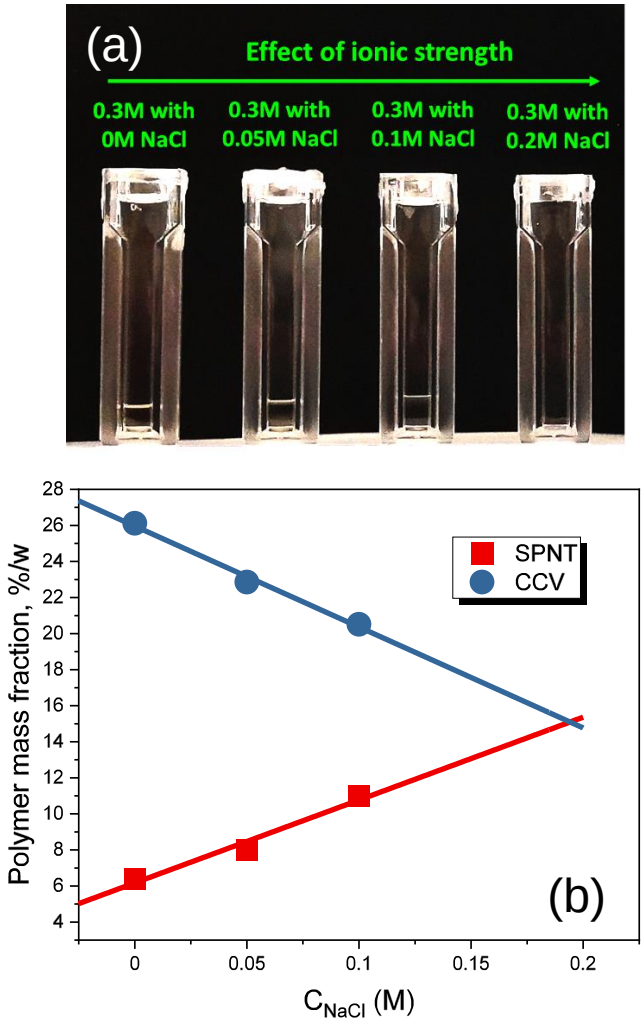

Figure 3-33. Pictures of solutions in cuvettes (a) and TGA measurements (b) of 0.3M PE solution with 0M, 0.05M, 0.1M and 0.2M NaCl, respectively. The solid lines are a linear fit to the data.

Furthermore, the addition of 0.05M NaCl to a 0.4M coacervate phase will induce the elevation of the coacervate/supernatant interface as expected, as shown in **Figure 3-34**.

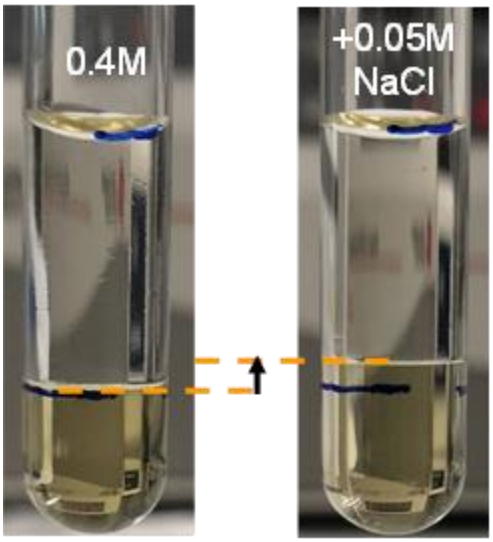

Figure 3-34. Rise of the coacervate/supernatant interface upon addition of 0.05M NaCl to a 0.4M PDADMAC/PANa coacervate system.

DLS experiments were also performed at 90° to determine structural changes in the network upon increasing the ionic strength (**Figure 3-35**), shows the impact of salt on a 0.3M coacervate solution at different NaCl concentrations (0.05M, 0.1M, 0.2M). As the ionic strength increases, the correlation and decay times shift to longer times , suggesting the de-densification of the PE network until it completely dissociates above 0.2M.

We can also note that the slow mode strongly present in the 0.3M coacervate solution starts to decrease with the addition of salt until it disappears completely above 0.2M where the chains do not interact anymore. The slow mode is probably due to transient aggregates due to dipole-dipole pairs put forward by Muthukumar recently[30] and represented in the insert of **Figure 3-13**. The progressive addition of salt will then screen the dipolar interactions thus reducing the contribution of the slow mode to the lattice dynamics.

We believe that the intensity up-turn observed at low q for SANS (or SAXS) for a polyelectrolyte solution (see **Figure 3-21**) and which disappears (along with the associated polyelectrolyte peak) when salt is added, reflect these transient aggregates in the solutions.

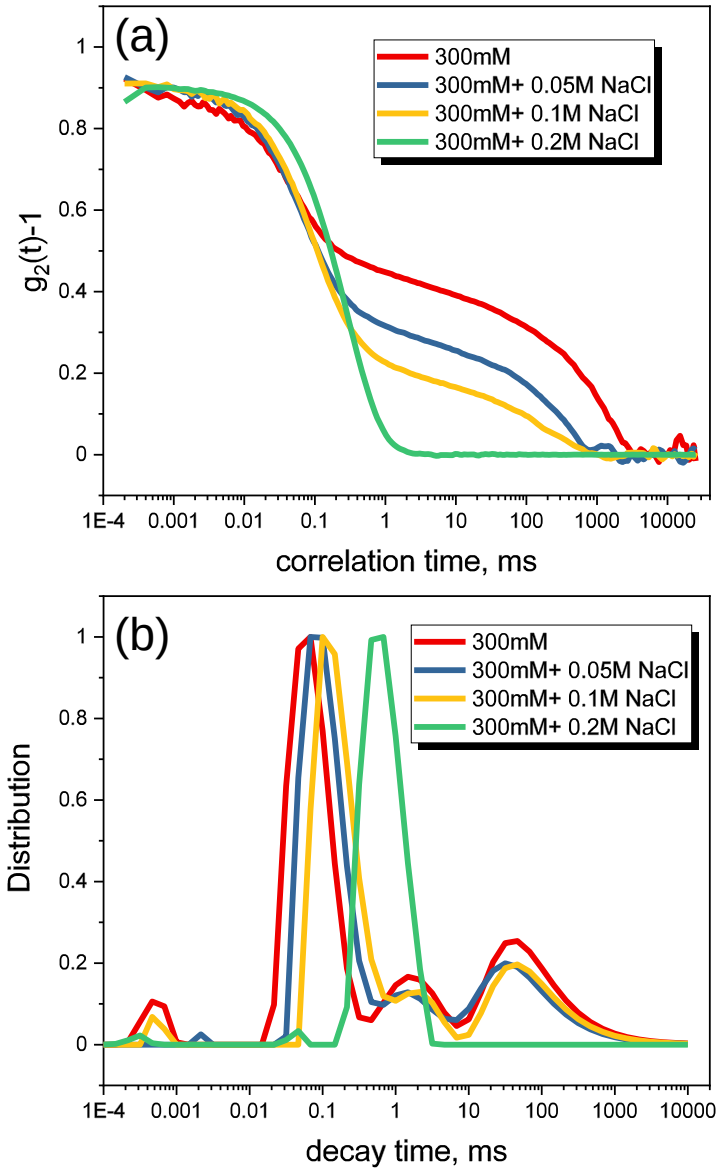

Figure 3-35. Intensity correlation functions (a) and intensity-weighted distribution of decay times (b) of a 0.3M PDADMAC/PANa coacervate phase at different NaCl concentration (0M, 0.05M, 0.1M, 0.2M). DLS measurements were performed in D_2O at 22°C with a 90° angle detection.

We then systematically measured the auto-correlation functions and decay times over a wide angle range from 30°C to 150°C (**Figure 3-36** and **Figure 3-37**). The trend is similar to that obtained at 90°C with decay times shifting to higher values and the gradual disappearance of the slow mode as the ionic strength increases. Above 0.2M NaCl, the autocorrelation function is monomodal and shifts to a lower correlation time with q.

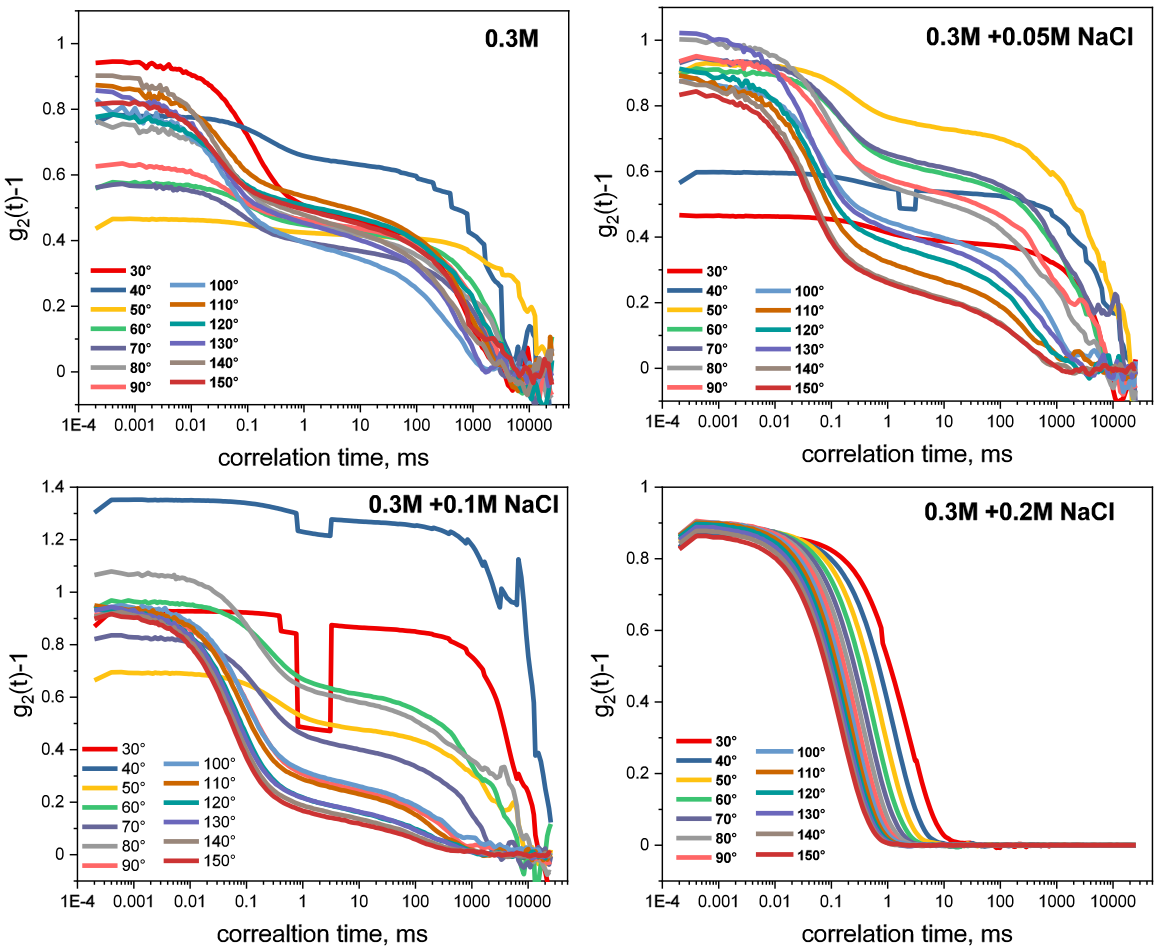

Figure 3-36. Intensity autocorrelation functions measured by DLS at different angles and NaCl concentrations within a 0.3M PADADMAC/PANa coacervate phase.

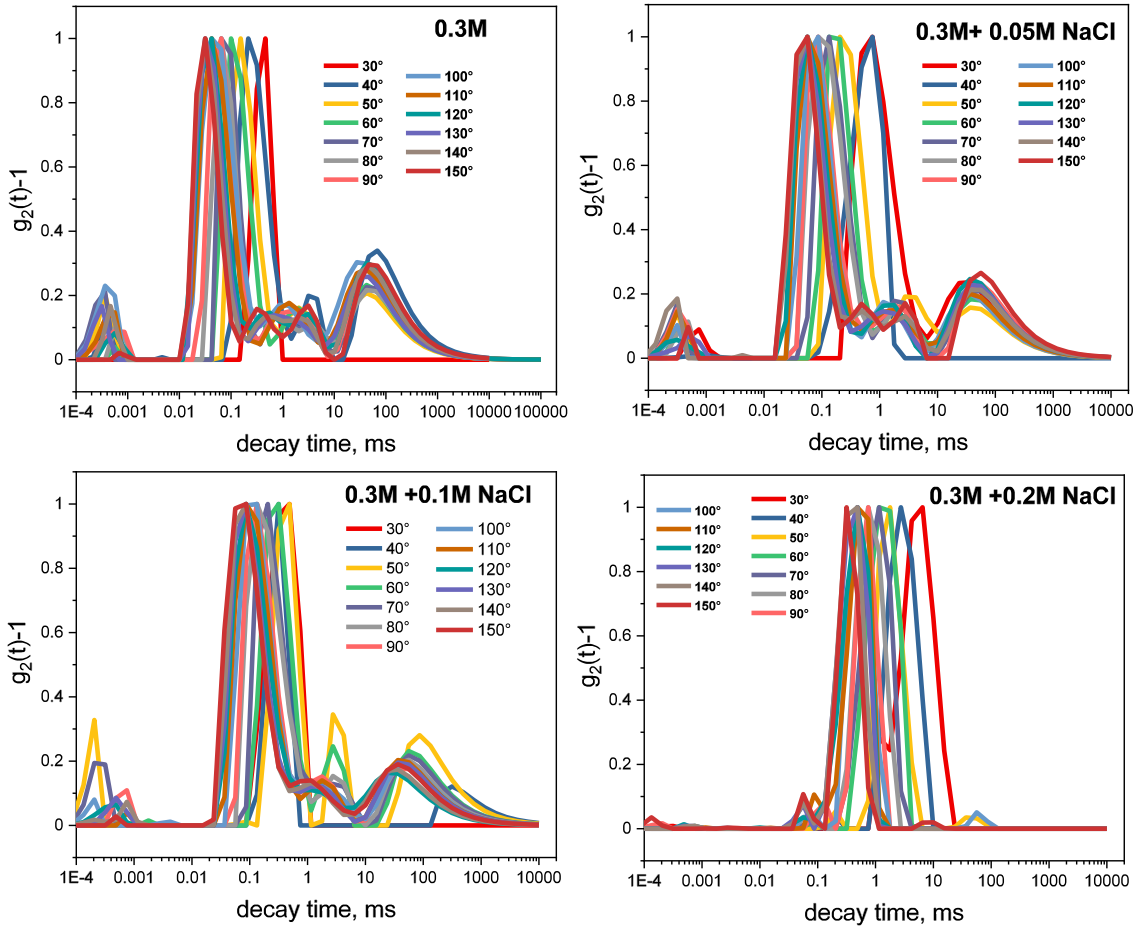

Figure 3-37. Intensity-weighted distribution of decay times at different angles and NaCl concentrations within a 0.3M PADADMAC/PANa coacervate phase.

By plotting plot $\Gamma(=\frac{1}{\tau})$ as a function of q^2 with the mean decay times τ taken from the main peak values of the fast modes, we were able to extract the mean diffusion coefficient D as a function of the ionic strength from the different slopes obtained from **Figure 3-38**. As anticipated, the diffusion coefficient decreases with increasing the ionic strength, which is consistent with increasing the network mesh size or the hydrodynamic correlation length $\xi_H(=\frac{k_B T}{6\pi\eta D})$ (**Figure 3-39 a**). The polymer mass fraction decreases as expected with [NaCl] but it does so in a linearly fashion, which is not yet understood at this stage.

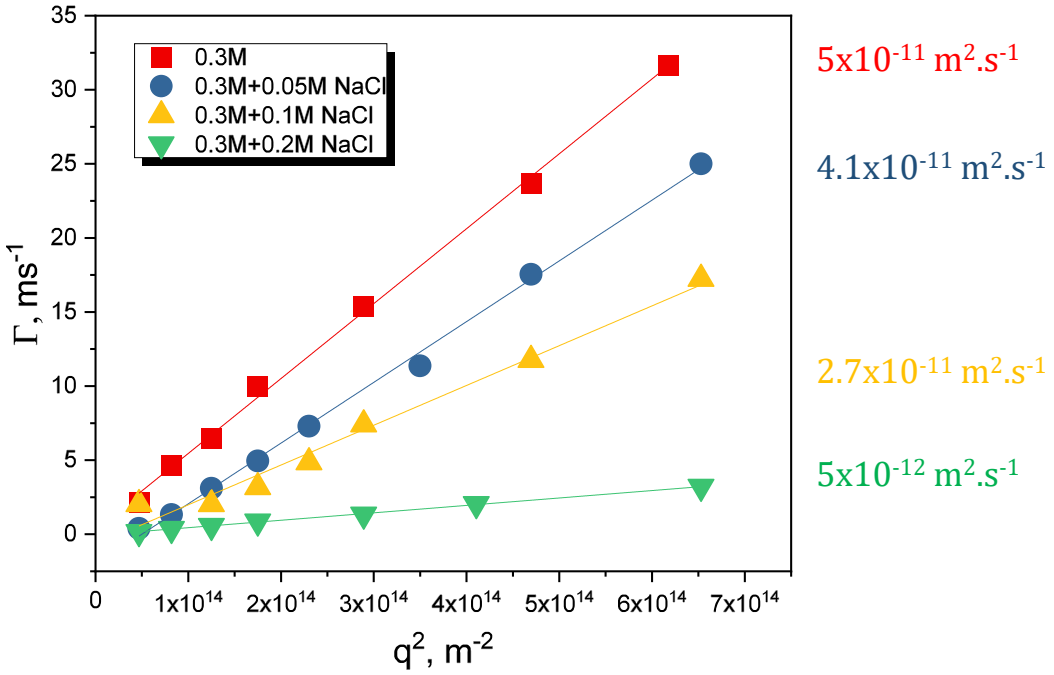

Figure 3-38. $\Gamma(=1/\tau)$ as a function of q^2 for a 0.3M PDADMAC/PANa coacervate phase generated at different NaCl concentrations. The solid lines are a linear fit of the data with the slope representing the diffusion coefficient D.

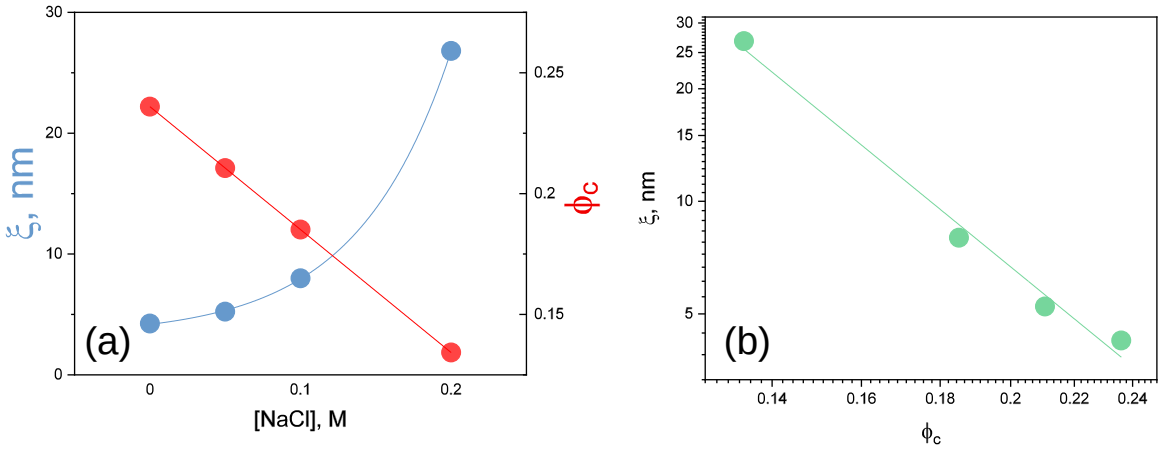

Figure 3-39. (a) Correlation length ξ_H and coacervate volume fraction φ_c within the different coacervate phases as a function of NaCl concentration. (b) Correlation length ξ_H as a function of φ_cThe red and green lines are a linear fit of the data. The blue line is a guide for the eyes.

Most interestingly, ξ_H increases as ${\varphi_c}^{-3.3}$ (**Figure 3-39 a**) upon addition of salt in a manner very similar to the variation of the coacervate volume fraction φ_c with the

concentration of the PE solutions used to generate the coacervate (see **Figure 3-17**) where $\xi_H \sim \varphi_c^{-3.2}$.

A similarity that strongly suggests that the concentration of PE and the added salt have roughly the same effect: i.e., they will both reduce the intensity of complexation, resulting in a reduction of the polymer fraction in the coacervate and the interfacial tension between the coacervate/supernatant until a single-phase system is obtained where the chains no longer interact.

Finally, the static SANS signatures of the salt effect on the local network structure re also presented in **Figure 3-40** where the arrow point to higher NaCl concentration.

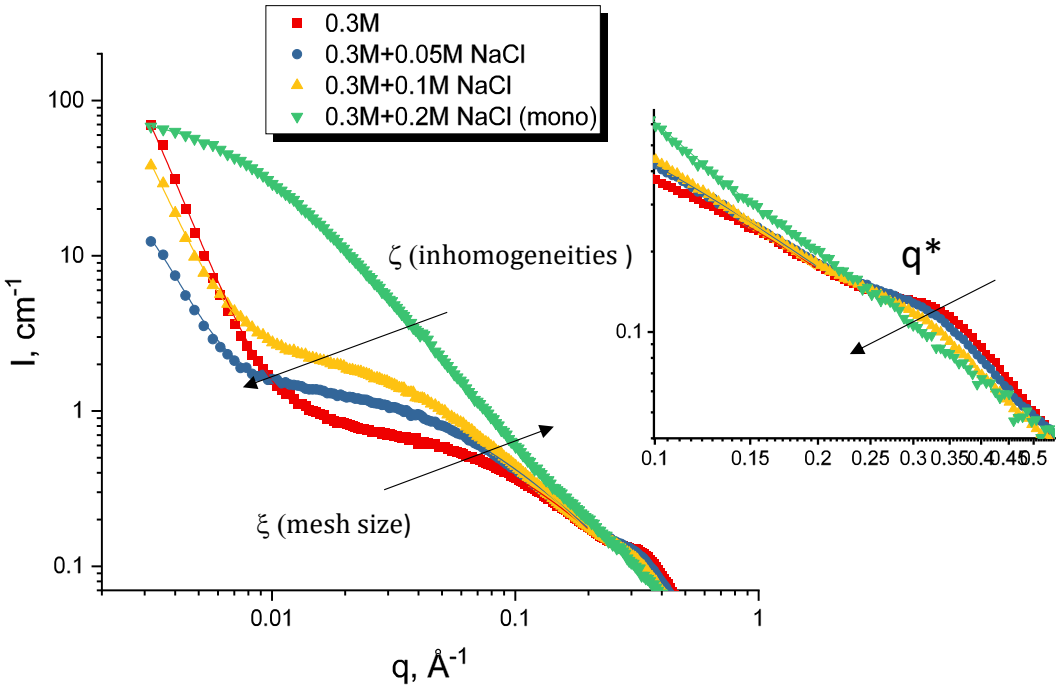

Figure 3-40. Small angle neutron scatting (SANS) signature of the 0.3M PDADMAC/PANa coacervate phases as a function of the added NaCl concentration. Measurements were performed at ILL on D22 in D_2O. The solid lines are an Ornstein–Zernike *(OZ)-Debye-Buche (DB)* fit to the data. The insert is a high-q zoom (>0.2 $Å^{-1}$) of the different formulations where the correlation peak (q*) are more easily seen.

As expected, the static correlation length ξ and the size of the transient aggregates ζ increase and decrease respectively with the ionic strength very well in line with dynamic data. Moreover, we can clearly see on the insert of **Figure 3-40** that the correlation peak (q*) seen at high q tends to move towards low q values with the increase of the complexation strength. It then disappears in the single-phase region where the chains do not interact anymore. Note that the upturn at low q disappears in this single phase (DB fit gives zero) in complete agreement with DLS where the slow mode is effectively absent when 0.2M NaCl is added.

Finally, the correlation lengths ξ_H and ξ determined by dynamic and static scattering techniques vary similarly with the coacervate volume fraction in the coacervate phase obtained at various salt concentrations. We found $\varphi_c{}^{-n}$ with an exponent n ~ 3.2-3.6 which emphasizes once again the soundness and complementarity of the two approaches (**Figure 3-41**).

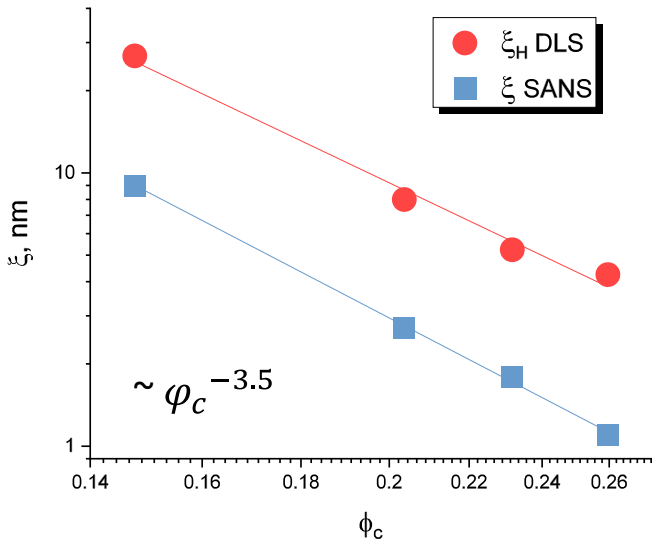

Figure 3-41. SANS and DLS correlation lengths ξ as a function of the polymer mass fraction φ_m.The solid lines are a power law fit to the data.

3.3.4 The effect of a co-solvent: the binary water/ethanol system

So far, we have studied the impact of concentration, temperature and ionic strength on the internal structure of complex coacervates made from aqueous solutions of oppositely charged PEs.

Can the complexation also be modulated using a co-solvent such as ethanol? **Figure 3-42** shows the impact of ethanol addition on a coacervate prepared at 0.4M. The height of the coacervate/supernatant interface clearly decreases linearly suggesting a densification of the coacervate phase (**Figure 3-44**) following a decrease of the dielectric constant of the system with the addition of ethanol which increases the complexion strength.

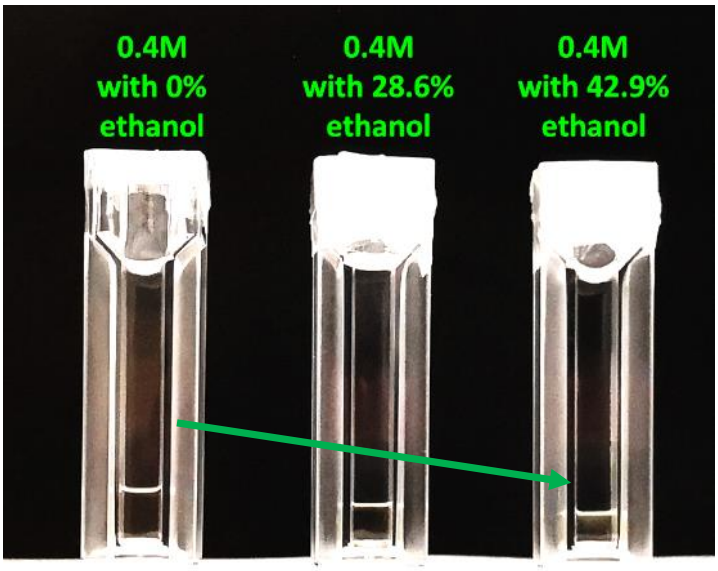

Figure 3-42. Lowering of the coacervate/supernatant interface of a PDADMAC/PANa 0.4M coacervate as function of the ethanol volume fraction (0%, 28.6% and 42.9%, respectively). Ethanol is added in the PE solutions prior to their mixing.

We then systematically explored the impact of ethanol on coacervate phases prepared at different concentrations from co-dilution with ethanol and water of a 0.7M coacervate phase (**Figure 3-43**). We recall that dilution with water alone leads to denser coacervates (and consequently less dense supernatants) as shown in the green curve in **Figure 3-44**.

Figure 3-43 shows that dilution of a 0.7M coacervate phase with an increasing fraction of ethanol will lower the coacervate/supernatant interface more significantly than dilution with a constant ethanol fraction.

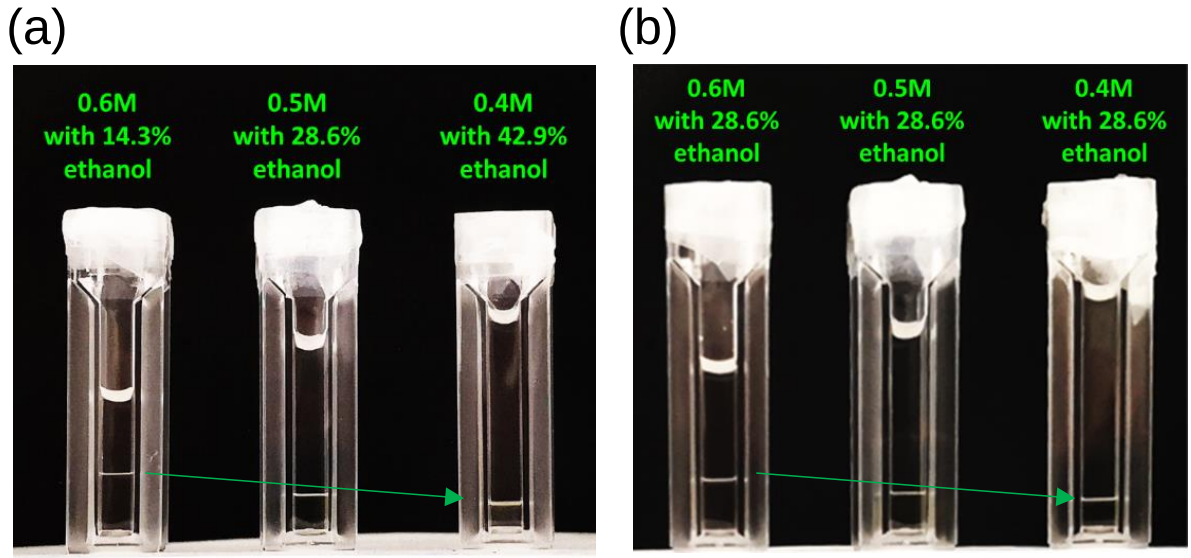

Figure 3-43. Lowering of the coacervate/supernatant interface by co-dilution of a 0.7M PDADMAC/PANa coacervate phase (a) with increasing volume fraction in ethanol of 14.3%, 28.6%, and 42.9%) (b) with water holding the volume fraction of ethanol constant (28.6%).

In the TGA measurements **(Figure 3-44**), we can clearly see that a direct dilution with an increasing ethanol volume fraction (from 0 to 42.9%) increases more significantly the polymer mass fraction (orange data) than a dilution made at constant ethanol volume fraction (28.6% - blue data). The dilution with pure water has a weaker effect on the densification of the coacervate phase as expected (green curve).

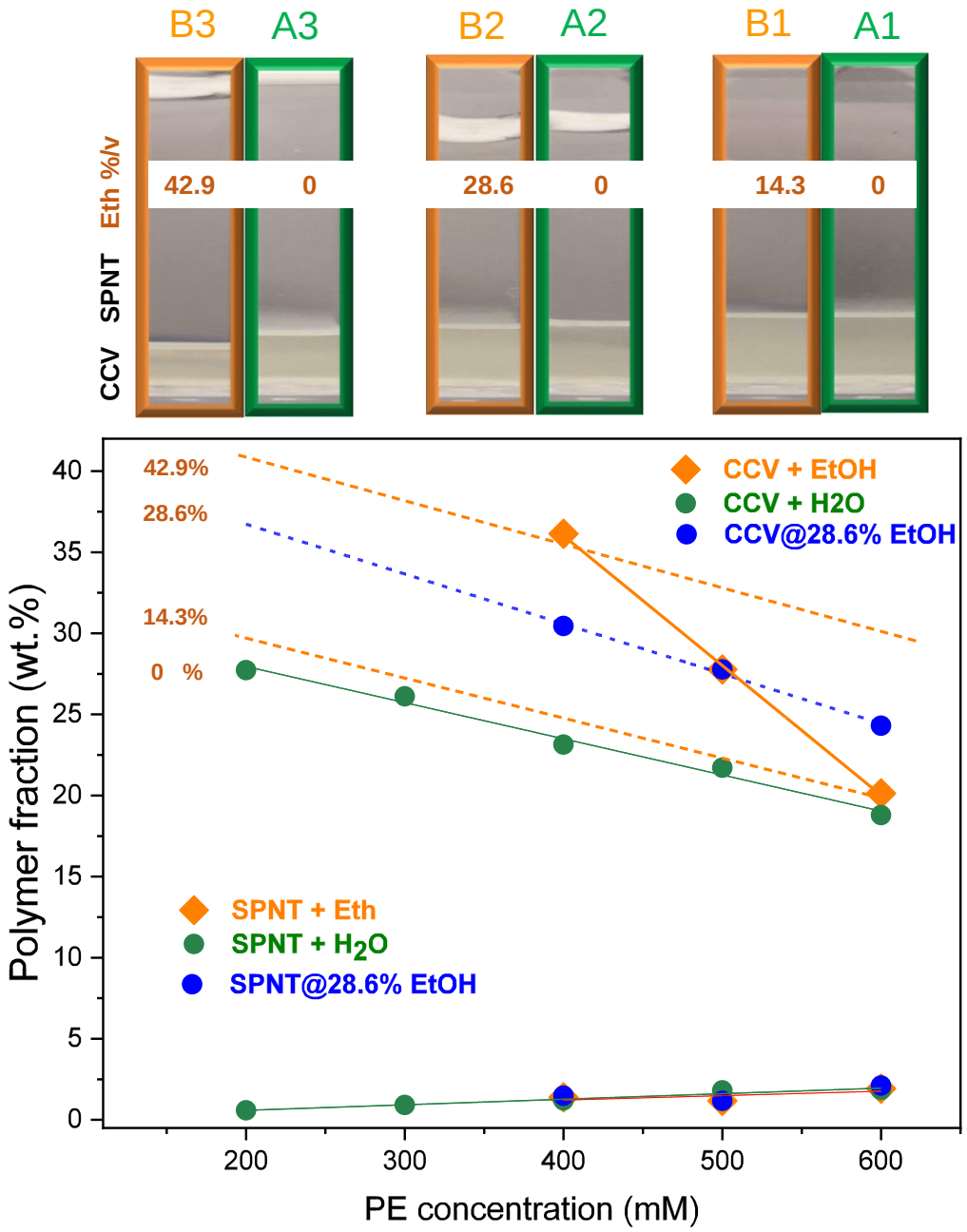

Figure 3-44. TGA measurements performed on different coacervate/supernatant systems obtained by diluting a PDADMAC/PANa 0.7M coacervate system with either pure water or a binary water/ethanol mixture at different ethanol volume fractions. A1, A2 and A3 represent the coacervate phase obtained by dilution with water only. B1, B2 and B3 represent the coacervate phase obtained by co-dilution with ethanol and water to obtain final volume fractions in ethanol of 14.3%, 28.6% and 42.9%, respectively. The solid lines are a linear fit to the data

SANS experiments were also performed on a 0.5M coacervate system generated from a 1M self-suppressed by co-dilution with different volumes of ethanol and water to get final volume fraction in ethanol of 20%, 30% and 50%. **Figure 3-45** shows the variation of the local structure of the coacervate phase with the ethanol fraction.

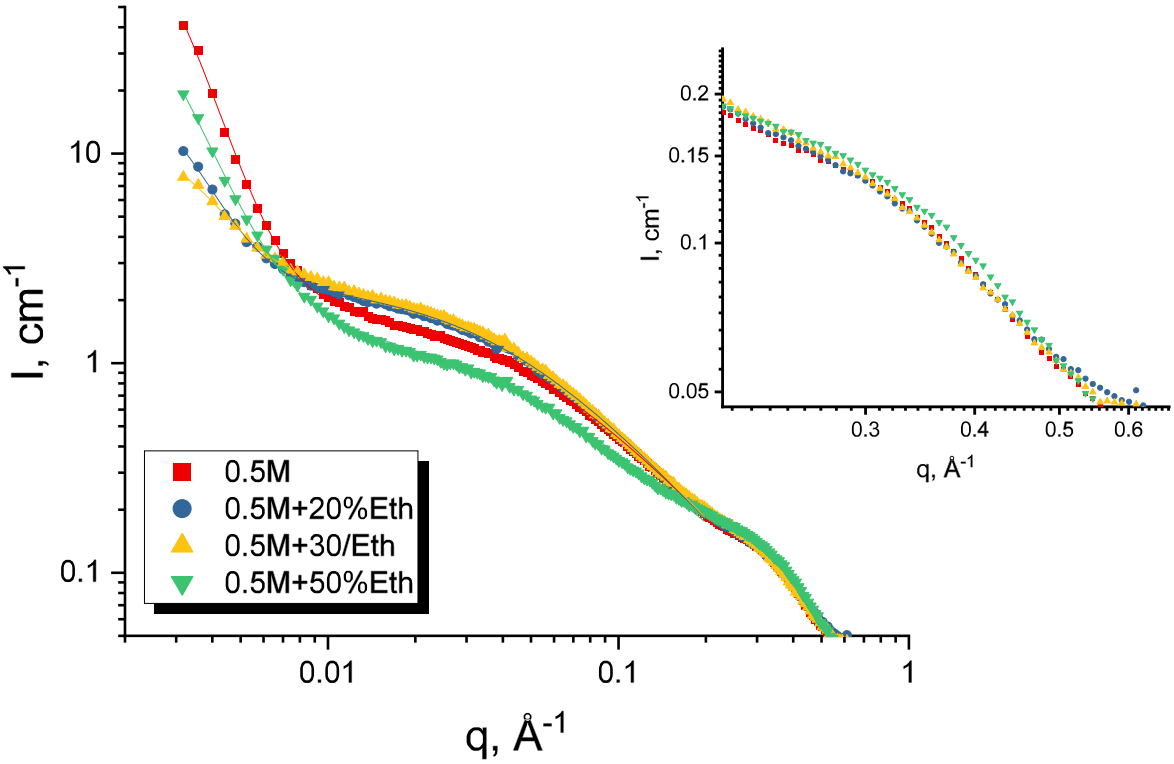

Figure 3-45. Small angle neutron scatting (SANS) signature of the 0.5M PDADMAC/PANa coacervate phases as a function of the ethanol fraction. Measurements were performed at ILL on D22 in D_2O and EtOD. The solid lines are an Ornstein–Zernike *(OZ)-Debye-Buche (DB)* fit to the data. The insert is a high-q zoom (>0.2 $Å^{-1}$) of the different formulation where the correlation peak (q*) is more easily seen.

Surprisingly, the SANS signature does not show a monotonic variation with ethanol volume fraction with a somewhat unexpected trend. Indeed, as the fraction increases from 0 to 30%, the correlation length ξ increases from 1.9 nm (0%) to 3 nm (30%) with the subsequent size of the heterogeneities ζ (low q upturn) decreasing. This is a counter-intuitive effect for such samples which, according to TGA measurements, become increasingly dense when the ethanol content increases. For an ethanol content of 50%, the trend reverses and one observes an increase in ξ (and a decrease of ζ). No clear explanation has been found at this

stage regarding this particular behaviour but possibly it may relate to the reduced solubility of PEs in hydroalcoholic solution.

One can legitimately wonder if the measurements were correct, if the samples were well prepared and if they were well relaxed before the SANS measurements. Preliminary data obtained in a previous D22 session 3 months earlier on 0.6M coacervates with 20% and 40% ethanol gave similar results...

If we dilute with 95%/v ethanol, the lowering of the dielectric constant will increase the intensity of complexation to such an extent that the PDADMAC/PANa system will no longer form a coacervate phase by a liquid-liquid transition but a precipitate by a liquid-solid transition as in the strongly interacting PDADMAC/PSSNa system, shown in **Figure 3-46**. Therefore one can observe a continuous transition from a self-suppressed single-phase liquid solution prepared at 1M to coacervate phases obtained with 50 and 80% ethanol to finally obtain a solid precipitate with the addition of 95%/v ethanol.

This result is equivalent to the polyelectrolyte/coacervate complex continuum put forward by Schlenoff and co-workers who tuned the complexation strength in the PSSNa/PDADMAC system by adding salt (KBr) (and thus increasing the ionic strength) to transform a solid precipitate where the chains interact strongly into a coacervate phase with weaker interactions and finally to a dormant solution where no interaction exist anymore.[45] The increase in ionic strength is replaced in our case by an increase/decrease of the dielectric constant by using water/ethanol binary solutions.

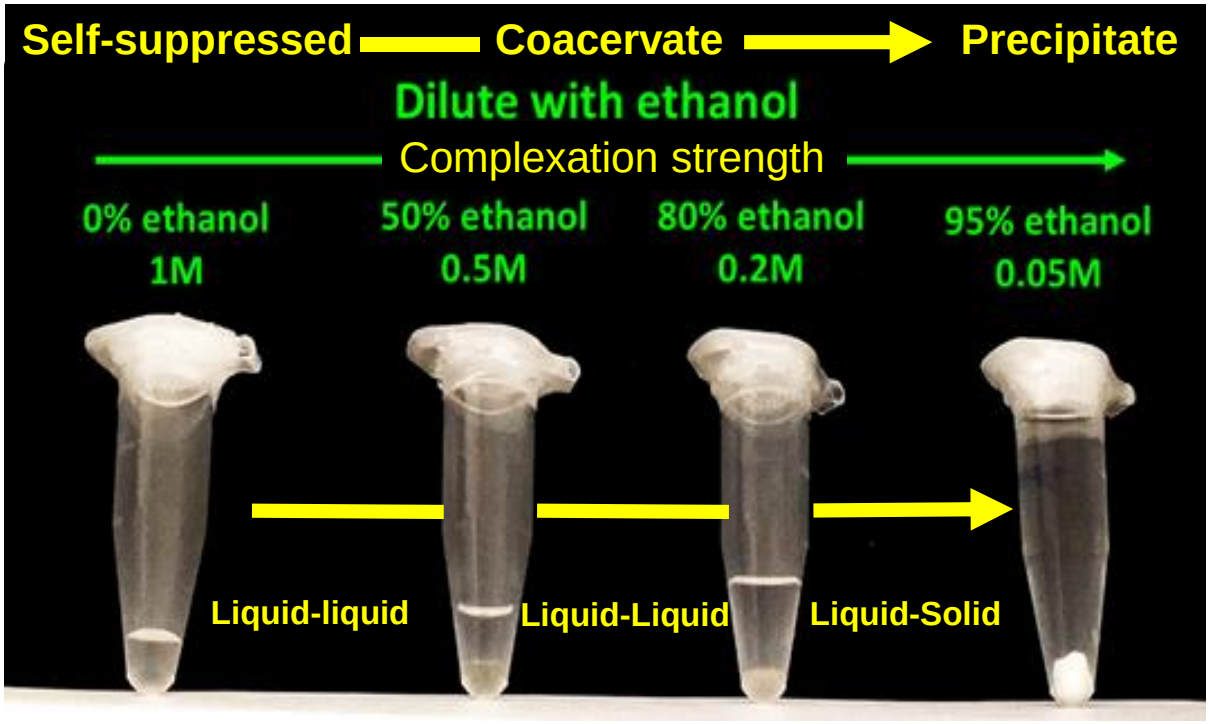

Figure 3-46. From a liquid coacervate to a solid precipitate by dilution of a self-suppressed 1M PDADMAC/ PANa solution with ethanol (0%, 50%, 80% and 95%). The PE concentration decreases accordingly.

3.4 Conclusions

In this chapter, we have comprehensively and systematically investigated the effect of concentration, temperature, ionic strength, and co-solvent (ethanol) concentration on the complex coacervation strength and local structure of oppositely charged PEs at charge stoichiometry in a PDADMAC/PANa system through different and complementary techniques (interfacial tension, TGA, DLS, SANS, optical microscopy). In short, we have seen these different parameter can tune the complexation strength occurring between PDADMAC and PANa chains leading to a denser or lighter coacervate or self-suppressed single-phase coacervate.

At high concentration of PE (>0.8M), we generate a self-suppressed single-phase coacervate phase (SSCV) where the chains no longer interact. This effect is thought to be primarily due to the free counterions present in the solution, which completely screen the electrostatic interaction. Interestingly, if we dilute these SSCVs with pure water, we form a two-phase system with a polymer-rich coacervate phase coexisting with a polymer-poor supernatant phase. The density or polymer content of this coacervate phase will increase with dilution. The dilution will indeed decrease the ionic strength increasing the intensity of the electrostatic complexation, densifying the polymer network with a mesh size (correlation length) that will decrease accordingly. Since the PANa/PDADMAC complexation occurs under equilibrium condition, it must therefore be pathway-independent. Indeed, by directly mixing PE solutions with increasing concentration, one also obtains less and less dense phases until the appearance of the single-phase SSCV above 0.8M.

In addition to the decrease of the mesh size, the interfacial tension between the two phases decreases with the polymer content in the dense phase until a point where the interfacial tension cancels at the onset of the transition to a SSCV. This phenomenon has strong similarities with the decrease of the interfacial tension observed in a given coacervate by increasing the ionic strength (NaCl) which also screens the complexation until obtaining a so-called dormant solution where the chains do not interact either.

We can also form a coacervate phase from a self-suppressed coacervate phase (e.g., at 0.9M) by increasing the temperature (50°C) owing to a critical solution temperature behavior

(LCST) that will eventually form a two-phase system with a sharp coacervate/supernatant interface. We can also densify an already generated coacervate phase (by either mixing two oppositely PE solutions directly or by diluting a SSCV solution) by heating the system with the subsequent lowering of the coacervate/supernatant interface. If we wait long enough (>two months) at room temperature or cool it, such system will go back to its original state with a rising back of the interface indicating that the coacervate phase has relaxed into a looser state 'de-densification'') due to a weaker complexation strength.

The density and mesh size of a coacervate phase can also be reduced by adding salt to increase the ionic strength. An effect that is visibly equivalent to generating a coacervate from increasingly concentrated stock solutions.

Finally, as we saw above, we can densify the coacervate phase by diluting it with water. We can also amplify this effect by diluting the coacervate with a water/ethanol mixture which will cause a decrease in the dielectric constant and lead to even greater complexation. For a volume fraction of ethanol of 95%/v we obtain a solid precipitate instead of a liquid coacervate.

Figure 3-47 summarizes the main results and presents the reversible change that a coacervate or self-suppressed phase can undergo under the action of concentration, temperature, ionic force and ethanol content.

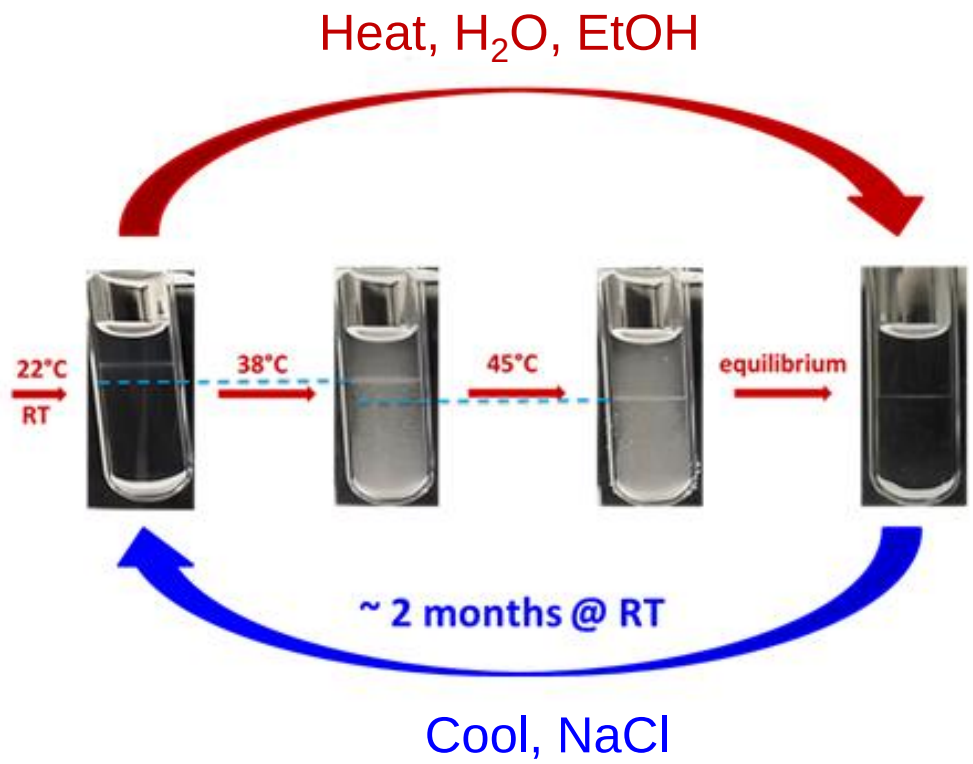

Figure 3-47. Schematic illustration of the impact of the different parameters (concentration, temperature, ionic strength and ethanol content) on coacervate and self-suppressed phases in a PDADMAC/PANa system.

References

[1] Koga, S., et al., *Peptide–nucleotide microdroplets as a step towards a membrane-free protocell model.* Nature Chemistry, 2011. **3**(9): p. 720-724.

[2] Buddingh', B.C. and J.C.M. van Hest, *Artificial Cells: Synthetic Compartments with Life-like Functionality and Adaptivity.* Accounts of Chemical Research, 2017. **50**(4): p. 769-777.

[3] Keating, C.D., *Aqueous Phase Separation as a Possible Route to Compartmentalization of Biological Molecules.* Accounts of Chemical Research, 2012. **45**(12): p. 2114-2124.

[4] Martin, N., et al., *Photoswitchable Phase Separation and Oligonucleotide Trafficking in DNA Coacervate Microdroplets.* Angewandte Chemie International Edition, 2019. **58**(41): p. 14594-14598.

[5] Liu, X., et al., *Early stage kinetics of polyelectrolyte complex coacervation monitored through stopped-flow light scattering.* Soft Matter, 2016. **12**(44): p. 9030-9038.

[6] Nekrasova, T.N., et al., *Potentiometric titration of polyacrylic acid, polymethacrylic acid and poly-l-glutamic acid.* Polymer Science U.S.S.R., 1965. **7**(5): p. 1008-1018.

[7] Michaeli, I., J.T.G. Overbeek, and M.J. Voorn, *Phase separation of polyelectrolyte solutions.* Journal of Polymer Science, 1957. **23**(103): p. 443-450.

[8] Veis, A., E. Bodor, and S. Mussell, *Molecular weight fractionation and the self-suppression of complex coacervation.* Biopolymers, 1967. **5**(1): p. 37-59.

[9] Zhang, P. and Z.-G. Wang, *Interfacial Structure and Tension of Polyelectrolyte Complex Coacervates.* Macromolecules, 2021. **54**(23): p. 10994-11007.

[10] Spruijt, E., et al., *Interfacial tension between a complex coacervate phase and its coexisting aqueous phase.* Soft Matter, 2010. **6**(1): p. 172-178.

[11] Giermanska, J., et al., *Influence of the formulation pathway on the growth of polyelectrolyte multilayer films.* Colloids and Surfaces A: Physicochemical and Engineering Aspects, 2016. **509**: p. 666-674.

[12] Priftis, D., R. Farina, and M. Tirrell, *Interfacial Energy of Polypeptide Complex Coacervates Measured via Capillary Adhesion.* Langmuir, 2012. **28**(23): p. 8721-8729.

[13] Ali, S. and V.M. Prabhu, *Characterization of the Ultralow Interfacial Tension in Liquid–Liquid Phase Separated Polyelectrolyte Complex Coacervates by the Deformed Drop Retraction Method.* Macromolecules, 2019. **52**(19): p. 7495-7502.

[14] Qin, J., et al., *Interfacial Tension of Polyelectrolyte Complex Coacervate Phases.* ACS Macro Letters, 2014. **3**(6): p. 565-568.

[15] De, R., D. Ray, and B. Das, *Influence of temperature, added electrolyte, and polymer molecular weight on the counterion-condensation phenomenon in aqueous solution of sodium polystyrenesulfonate: a scaling theory approach.* RSC Advances, 2015. **5**(68): p. 54890-54898.

[16] Esquena, J., *Water-in-water (W/W) emulsions.* Current Opinion in Colloid & Interface Science, 2016. **25**: p. 109-119.

[17] Douliez, J.-P., et al., *Preparation of Swellable Hydrogel-Containing Colloidosomes from Aqueous Two-Phase Pickering Emulsion Droplets.* Angewandte Chemie International Edition, 2018. **57**(26): p. 7780-7784.

[18] de Hoog, E.H.A. and H.N.W. Lekkerkerker, *Measurement of the Interfacial Tension of a Phase-Separated Colloid−Polymer Suspension.* The Journal of Physical Chemistry B, 1999. **103**(25): p. 5274-5279.

[19] Gennes, P.-G., *Scaling Concepts in Polymer Physics* 1979: Cornell Univ. Press.
[20] Vis, M., et al., *Water-in-Water Emulsions Stabilized by Nanoplates.* ACS Macro Letters, 2015. **4**(9): p. 965-968.
[21] Scholten, E., L.M.C. Sagis, and E. van der Linden, *Bending Rigidity of Interfaces in Aqueous Phase-Separated Biopolymer Mixtures.* The Journal of Physical Chemistry B, 2004. **108**(32): p. 12164-12169.
[22] Qi, L., et al., *Influence of the Formulation Process in Electrostatic Assembly of Nanoparticles and Macromolecules in Aqueous Solution: The Interaction Pathway.* The Journal of Physical Chemistry C, 2010. **114**(39): p. 16373-16381.
[23] Qi, L., et al., *Influence of the Formulation Process in Electrostatic Assembly of Nanoparticles and Macromolecules in Aqueous Solution: The Mixing Pathway.* The Journal of Physical Chemistry C, 2010. **114**(30): p. 12870-12877.
[24] Vitorazi, L., et al., *Evidence of a two-step process and pathway dependency in the thermodynamics of poly(diallyldimethylammonium chloride)/poly(sodium acrylate) complexation.* Soft Matter, 2014. **10**(47): p. 9496-9505.
[25] Mehan, S., et al., *The desalting/salting pathway: a route to form metastable aggregates with tuneable morphologies and lifetimes.* Soft Matter, 2021. **17**(37): p. 8496-8505.
[26] Yan, M., et al., *Magnetic Nanowires Generated via the Waterborne Desalting Transition Pathway.* ACS Applied Materials & Interfaces, 2011. **3**(4): p. 1049-1054.
[27] Demirelli, M., et al., *Influence of polycation/cation competition on the aggregation threshold of magnetic nanoparticles.* Colloids and Surfaces A: Physicochemical and Engineering Aspects, 2021. **612**: p. 125876.
[28] Fresnais, J., C. Lavelle, and J.F. Berret, *Nanoparticle Aggregation Controlled by Desalting Kinetics.* The Journal of Physical Chemistry C, 2009. **113**(37): p. 16371-16379.
[29] Mandel, M., *Application of dynamic light scattering to polyelectrolytes in solution*, in *Dynamic light scattering : the method and some applications*, W. Brown, Editor. 1993, Oxford University Press, 1993.: New-York.
[30] Muthukumar, M., *Ordinary–extraordinary transition in dynamics of solutions of charged macromolecules.* Proceedings of the National Academy of Sciences, 2016. **113**(45): p. 12627-12632.
[31] Jian, T., et al., *Coupling of concentration fluctuations to viscoelasticity in highly concentrated polymer solutions.* Colloid and Polymer Science, 1996. **274**(11): p. 1033-1043.
[32] Rochas, C. and E. Geissler, *Measurement of Dynamic Light Scattering Intensity in Gels.* Macromolecules, 2014. **47**(22): p. 8012-8017.
[33] Tanaka, T., L.O. Hocker, and G.B. Benedek, *Spectrum of light scattered from a viscoelastic gel.* The Journal of Chemical Physics, 1973. **59**(9): p. 5151-5159.
[34] Spruijt, E., et al., *Structure and dynamics of polyelectrolyte complex coacervates studied by scattering of neutrons, X-rays, and light.* Macromolecules, 2013. **46**(11): p. 4596-4605.
[35] Koberstein, J.T., C. Picot, and H. Benoit, *Light and neutron scattering studies of excess low-angle scattering in moderately concentrated polystyrene solutions.* Polymer, 1985. **26**(5): p. 673-681.
[36] Sharma, J., et al., *Small-Angle Neutron Scattering Studies of Chemically Cross-Linked Gelatin Solutions and Gels.* Macromolecules, 2001. **34**(15): p. 5215-5220.

[37] Debye, P. and A.M. Bueche, *Scattering by an Inhomogeneous Solid.* Journal of Applied Physics, 1949. **20**(6): p. 518-525.
[38] Nierlich, M., et al., *Small angle neutron scattering by semi-dilute solutions of polyelectrolyte.* J. Phys. France, 1979. **40**(7): p. 701-704.
[39] Zhang, P., et al., *Salt Partitioning in Complex Coacervation of Symmetric Polyelectrolytes.* Macromolecules, 2018. **51**(15): p. 5586-5593.
[40] Lorchat, P., et al., *New regime in polyelectrolyte solutions.* EPL, 2014. **106**(2): p. 28003.
[41] Hammouda, B., F. Horkay, and M.L. Becker, *Clustering and Solvation in Poly(acrylic acid) Polyelectrolyte Solutions.* Macromolecules, 2005. **38**(5): p. 2019-2021.
[42] Ali, S., M. Bleuel, and V.M. Prabhu, *Lower Critical Solution Temperature in Polyelectrolyte Complex Coacervates.* ACS Macro Letters, 2019. **8**(3): p. 289-293.
[43] Adhikari, S., V.M. Prabhu, and M. Muthukumar, *Lower Critical Solution Temperature Behavior in Polyelectrolyte Complex Coacervates.* Macromolecules, 2019. **52**(18): p. 6998-7004.
[44] Chollakup, R., et al., *Polyelectrolyte Molecular Weight and Salt Effects on the Phase Behavior and Coacervation of Aqueous Solutions of Poly(acrylic acid) Sodium Salt and Poly(allylamine) Hydrochloride.* Macromolecules, 2013. **46**(6): p. 2376-2390.
[45] Wang, Q. and J.B. Schlenoff, *The Polyelectrolyte Complex/Coacervate Continuum.* Macromolecules, 2014. **47**(9): p. 3108-3116.

General conclusion

In this thesis work, the formation, structure and properties of polyelectrolyte complexes (PECs) assembled from oppositely charged polyelectrolytes (PEs) were studied in two model systems with very different complexation strength: (i) the strongly and weakly interacting poly(diallyldimethylammonium chloride) (PDADMAC)/sodium poly(4-styrenesulfonate) (PSSNa) system and (ii) the PDADMAC/poly(sodium acrylic acid salt) (PANa) system respectively in aqueous solution. At charge stoichiometry, PECs can indeed exist in very different physical forms, such as a solid-like precipitate obtained through a liquid-solid phase separation in the PDADMAC/PSS system or as a liquid-like coacervate through a liquid-liquid phase separation in the PDADMAC/PANa system. This distinct complexation behavior is due to the strength of the electrostatic interaction unfolding between oppositely charged PEs.

We have highlighted in a first step that simple surface tension measurements can be a very sensitive tool to characterize, discriminate and better understand the formation mechanism of the different structures encountered during the formation of PECs by systematically studying the surface activity of the two PEC suspensions as a function of the molar charge ratio Z (= [-]/[+]) at a given low stock solution concentration (18.6mM). In particular, the PEC surface tension decreased for both systems as the system approaches charge stoichiometry (Z=1) whenever the complexation occurs in the presence of excess PDADMAC (Z < 1) or excess polyanion (Z > 1) consistent with an increased level of charge neutralization of PEs forming increasingly hydrophobic and neutral surface-active species. The behavior at stoichiometry (Z=1) was also particularly informative about the physical nature of the complexes. Besides, the high sensitivity of surface tension measurements, which can detect the presence of trace amounts of aggregates and other precursors in the supernatant allowed the very accurate determination of the exact charge stoichiometry of the complexes. Finally, the very low water/water interfacial tension (~300 µN/m) that develops between the dilute and denser coacervate phases in the PDADAMAC/PANa system was measured using the generalized Young-Laplace method to complete the full characterization of both systems.

In a second step, the influence of the complexation strength on the local structure of the polymer-rich coacervate phase generated in the PDADMAC/PANa system was studied using different and complementary techniques such as TGA, DLS, SANS and interfacial tension measurements. In particular, we have shown that the complexation strength can be tuned by varying the concentration of the PE solutions, temperature, ionic strength or co-solvent (ethanol) content, with a direct effect on the polymer volume fraction, network mesh size and interfacial tension.

At high concentration of the PE stock solution (>0.8M), we have highlighted the presence of a so-called self-suppressed coacervate phase (SSCV) where the PE chains no longer interact electrostatically. This effect is partially due to a very high ionic strength generated by the free counterions present in the solution that can completely screen the electrostatic interaction. Interestingly, if we dilute these SSCVs with pure water, we form a two-phase system with a polymer-rich coacervate phase coexisting with a polymer-poor supernatant phase. Counter-intuitively, the density (or polymer content) will then increase with dilution as a result of a decrease in ionic strength and network mesh size due to a higher complexation strength. If we mix directly PE solutions with increasing concentration, we indeed obtain less and less dense phases until the appearance of the single SSCV phase above 0.8M. Complexation is then pathway independent, suggesting that coacervation does indeed occur under equilibrium conditions as described for most coacervate systems.

We have shown furthermore that the coacervate/supernatant interfacial energy exhibits a critical behavior. Indeed, it decreases when the complexation strength is weakened and finally cancels at the onset of the SSCV phase above 0.8M. A critical behavior that shares similarities with the decrease of the polymer volume fraction observed in a given coacervate phase by increasing the ionic strength (NaCl) until a "dormant solution" is obtained where the chains do not interact either.

This study also highlighted the marked lower critical solution temperatures (LCST) behavior of the PEs in both the coacervate and SSCV phases. The SSCV phase can indeed undergo coacervation when the temperature is elevated (50°C), generating a higher complexation strength that will eventually form a biphasic system with a clear coacervate/supernatant interface. Similarly, heating a coacervate phase (already prepared

by direct mixing or dilution) will results in a lowering of the coacervate/supernatant interface due to a densification of the network (smaller mesh size) as well. If we wait long enough at room temperature (>two months) or cool it, the new coacervate phase will go back to its original state with a rising of the interface suggesting that it has relaxed into a looser state due to a weaker complexation strength. An effect that corresponds well to a pathway-independent coacervation that occurs under equilibrium conditions.

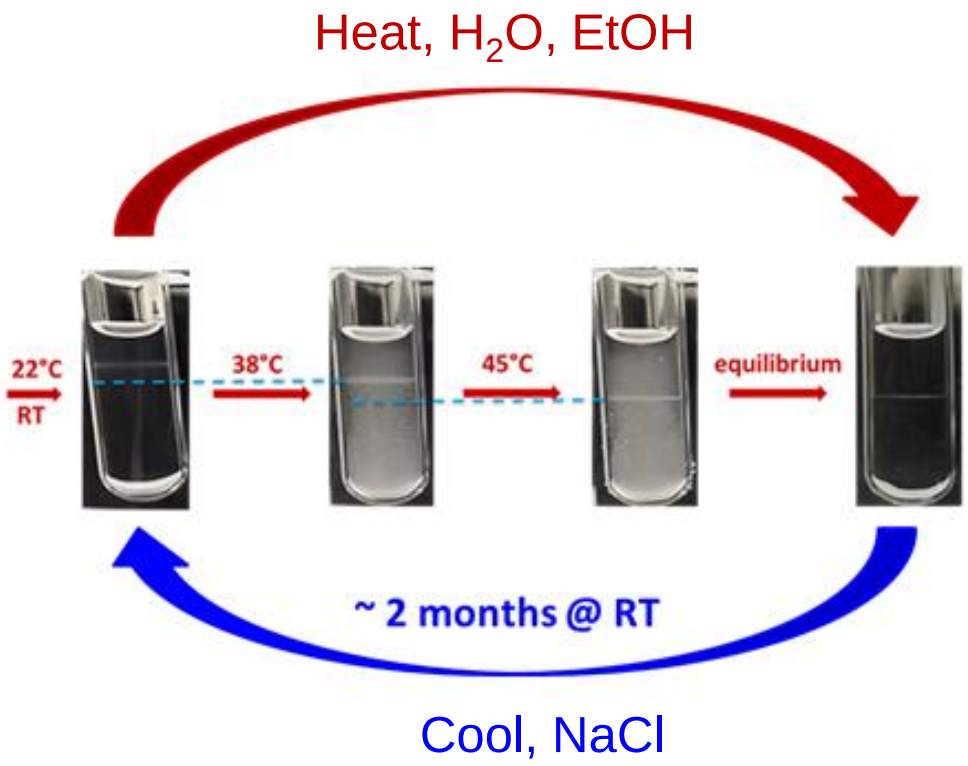

The influence on the complexation strength can be greatly amplified by diluting the coacervate with a water/ethanol mixture (or mixing directly two binary solutions). This will result in the concomitant decrease of the dielectric constant of the solution and an increase of the Flory interaction parameter leading to even greater complexation. The density (and the polymer volume fraction) of such generated coacervate phase increases then with the ethanol content. Above a certain ethanol fraction (95%/v), the liquid-liquid phase separation observed so far is replaced by a liquid-solid transition generating a precipitated solid as in the strongly interacting PDADMAC/PSSNa. This emphasizes once again the key importance of the interaction strength on the formation mechanisms and structural features of PECs.

There are of course many perspectives to this work in the short and mid-term. The complete determination of the phase diagram of the PDADMAC/PANa pair would be important to synthesize the global behaviour of the system. It would be also important to correlate our structural results with rheological measurements performed on the different phases generated. These measurements that we could not integrate in time in the manuscript are currently in progress.

A very important point remains to be elucidated or at least better understood. Where do the counterions go after the coacervation? This question is not really answered in the literature, even if the hypothesis of an equipartition between the coacervate and supernatant phases is often invoked. We have therefore started delicate measurements in the supernatant phase of our systems using a Na^+-selective electrode. Preliminary experiments suggest that counterions are more expelled from the coacervate phase as the strength of the interaction increases.

As mentioned earlier, the very low interfacial tension of coacervates allows them to efficiently encapsulate/sequester actives of interest (proteins, enzymes, nucleic acids …), but also makes them very difficult to stabilize. A difficulty that may be due in part to the variable and unknown width of the interphase between the coacervate droplets and the continuous phase? We have shown that the liquid-liquid interfacial tension between the coacervate and supernatant varies with the PE concentration of the solutions. And thus, that the interfacial thickness ξ can vary also over distances up to several tens of nm as $\gamma \sim k_B T/\xi^2$ from scaling arguments. As a result, the interfacial thickness between the coacervate phase and the surrounding medium can vary substantially with the PE concentration. More precisely, a 4-fold change is foreseen in our PDADMAC/PSSNa system. It is therefore very interesting to correlate interfacial tension and thickness in order to study the stabilization of coacervate droplets with the help of nanoparticles, latex, lipid or block copolymers for example... The densification of the coacervate phase ''on demand'' by a simple dilution or an increase in temperature could also offer a way to encapsulate, to concentrate active substances before releasing them and/or to stabilize the droplets

In any case, many questions remain on the properties of the coacervate phase and more generally on the liquid-liquid phase separation in polymeric systems, which have

experienced a renewed interest generated by the recent discovery of the presence of membrane-less organelles in living cells that have been identified as immiscible liquid phases forming a so-called coacervate phase. Membraneless organelles contain high concentrations of one or more proteins and/or nucleic acids and are thought to be preferential microenvironments for certain biochemical reactions or the sequestration of toxic substances. The physical chemistry behind the assembly and properties of these compartments is expected to be similar to some extent to that of synthetic coacervates. In this sense, the study carried out during this research work can bring a significant advance in the understanding of these systems.